Department of Mechanical Engineering
University of Strathclyde
James Weir Building,
Montrose Street,
Glasgow,G1 XXJ,
Scotland, U.K.

M.Sc. Thesis

Investigation of Performance Characteristics of a Novel VAWT

Neeraj Mittal
M.Sc.(Energy Systems and The Environment)
September 2001

Declaration of Author's Rights

Abstract

Most of the horizontal axis wind turbines currently available on the market have their cut-off speeds ranging from 20 to 25 m/s making them unsuitable for cyclone and storm prone areas. Delta Wind Turbines Ltd. claimed to have developed a novel vertical axis wind turbine (VAWT), which would be fully functional at wind speeds throughout the Beaufort scale and generating sufficient power output despite being mounted at ground level. This thesis was aimed at determining the performance characteristics of this novel VAWT. For this purpose, the full-scale prototype was subjected to field testing at Fionnphort on the Island of Mull, Scotland under the supervision of the Scottish Energy Environment Foundation.

All instruments, which were deployed for field-testing, were calibrated and verified for accuracy of measurements at University laboratories before hand. The test set up carried out the field testing of the novel VAWT successfully and provided useful data for the development of its performance characteristics. The performance curves were drawn for two different resistive loads connected across the directly coupled alternator. The peak value of coefficient of performance was found to be 0.19 at tip speed ratio of 0.59 in the case of an external load of 104 ohms, which is lower than those of most of the horizontal axis wind turbines currently available on the market. Further it was observed that the novel VAWT was a low speed machine with high shaft torque which is attributable to its high solidity ratio. The low rotor speed makes it unsuitable for generation of electricity unless coupled with a gearbox. However it can be advantageously deployed for mechanical applications such as for pumping of water in remote areas. Since this was the first prototype of the novel VAWT to be subjected to full scale field testing, the report concludes that the field test results should be viewed as the beginning of a new chapter in wind turbine technology rather than giving an absolute measure of success or failure. The report ends with certain suggestions for improving the performance of the novel VAWT.

Acknowledgements

I feel indebted to my supervisor, Dr. A. D. Grant, for his help and advice and also for his patience in the face of my constant questioning throughout the project. I would also like to express my gratitude to Mr. Cameron Johnstone, technical director of Scottish Energy Environment Foundation, for his encouragement and support, which was a constant source of inspiration and a major guiding force in the completion of this project. Like a Santa Claus, he provided me everything whatever I needed for carrying out the work. My special thanks are also due to Mr. Mr. Chris L. Baigent of Delta Wind Turbines Ltd. and Mr. David for co-ordinating the field activities and downloading of data from data logger on regular basis. Last but not the least I owe a lot of thanks to the technicians of University labs especially Mr. Eric Duncan, Mr. Alistair J. Duff, Mr. Patrick McGinnes, Mr. Roderigh Galbraith, Mr. Jim Doherty and Ms. Aileen Petrie for their valuable contribution in this endeavour. I must admit that I would have not emerged winner in my race against time in this project without their help. I record my special appreciation for cool-headed Mr. Alistair J. Duff who never missed a heart beat nor allowed his blood pressure to rise beyond 120/80 even under the most tight work schedule. He did his job with the rhythmic regularity of an I.C. engine.

17th September 2001 Neeraj Mittal

Glasgow

About the Author

The author is a mechanical engineer with a project management experience of over 14 years in the construction of power plants. The present thesis is submitted towards partial fulfilment of the requirements for the award of degree of M.Sc. in Energy Systems and the Environment by the University of Strathclyde, Glasgow, Scotland, U.K. For any clarification in respect of the present work, the author may be contacted at the email address 'ccmnm@yahoo.com' or phone no. 0091115740309.

NOMENCLATURE

Symbol	Explanation
ρ	: Air density
ω	: Angular speed
μ	: Hysteresis coefficient
τ	: Shaft torque
λ	: Tip speed ratio
θ	: Wind direction, in degrees, from north direction
η_{com}	: Composite efficiency of the alternator and rectifier
η_{motor}	: Motor efficiency
ρ_o	: Dry air density at sea level (750 mm of Hg column pressure) and 15 ^{0}C
A	: Swept area of rotor
B	: Magnetic flux per pole of alternator
C_P	: Coefficient of performance of wind turbine
D	: Diameter of wind rotor
E	: E.m.f. induced in stator windings of an alternator
F	: Force
f	: Frequency of alternating current
H	: Height of wind rotor
I_a	: Current flowing through armature winding of motor/ alternator
I_f	: Current flowing through field winding of motor/alternator
n	: Number of coils per phase in stator windings of alternator
N	: Rotational speed in revolutions per minute
$\dot{m}$	: Mass flow rate of wind
P	: Absolute pressure
p	: Number of poles in alternator
P_{ca}	: Copper losses in armature winding of alternator
P_{cf}	: Copper losses in field winding of alternator

P_{el} : Electrical power dissipated in load resistors

P_{Hg} : Atmospheric pressure measured in mm of mercury column

P_{in} : Shaft power input to alternator

P_{out} : Electrical power output of alternator with rectifier

P_{input} : Electrical power input to motor

P_{output} : Shaft power output of motor

P_{st} : Airflow static pressure recorded by pilot static tube in wind tunnel

$P_{turbine}$: Power extracted by a wind turbine from freely flowing wind

$P_{Std\text{-}turbine}$: Power output of a wind turbine at standard air density (ρ_o) of 1.225 kg/m^3

P_{wind} : Power contained in a freely flowing wind stream

R : Gas constant for dry air

r : Radius of wind rotor

R_a : Resistance of armature winding of motor/alternator

R_f : Resistance of field winding of motor/alternator

S : Rotor Solidity

T : Temperature

t : Thickness of lamination of iron core of alternator/motor

V : Speed of a freely flowing wind stream

V_a : Voltage applied across armature winding of motor

V_{act} : Actual wind speed recorded by pilot static tube in wind tunnel

V_c : Volume of iron core of alternator

V_{corr} : Correction in wind speed recorded by wind anemometer due to ratemeter and rotor non-linearity

V_f : Voltage applied across field winding of motor

V_{out} : Voltage output of potentiometer of wind vane

V_{ref} : Reference voltage applied across potentiometer terminals of wind vane

V_{speed} : Voltage output of DC generator tachometer coupled with DC shunt motor

X_l : Armature leakage reactance

X_s : Armature synchronous reactance

List of Illustrations

Chapter 4

Chapter 5

Chapter 6

Chapter 7

Chapter 8

References

1. Eggleston Eric, *What Are Vertical-Axis Wind Turbines (VAWTs)?,* American Wind Energy Association, Washington DC, U.S.A., 2001.
2. Ghosh K., Dixit P.M., Singh R., Murthy C.V.R., Das P.K., Selvaraj K., Shevadeb A.V. and Singh J., *Design of a 10 kW Wind Turbine for Cyclone Prone Areas*, Indian Institute of Technology, Kanpur, 1991.
3. *The Delta Wind Turbine Prospectus*, Delta Wind Turbines Ltd., Glasgow, 2001.
4. Grant A. D., *Delta Wind Turbines – report on recent wind tunnel testing,* 1998.
5. Nath N., *Preface in Windmills and Mill Writhing*, Cambridge, 1975
6. *Past, Present and Future of Wind Energy in Europe*, University of Bath, U.K,1995
7. *Vertical Axis Wind Turbines: The History of DOE Program*, U.S. Department of Energy, Sandia National Laboratories, U.S.A., 1998.
8. *LIOR Wind Energy CD-ROM, Renewable Energy Series*, LIOR International NV, Belgium, 1998.
9. Eldridge Frank R., *Wind Machines, 2nd Edition*, Van Nostrand Reinhold Company, New York, U.S.A., 1980.
10. Shepherd Dennis G., *Wind Power*, Handbook of Energy Technology and Economics edited by Robert A. Meyers.
11. Doerner H.H., *Efficiency and Economic Comparison of Different WEC-(Wind Energy Converter) Rotor Systems*, International Conference on Appropriate Technologies for Semiarid Areas: Wind and Solar Energy for Water Supply, Berlin, 1975.
12. Sivasegram S., *Power augmentation in wind rotors: a review*, Wind Engineering, vol.10, 1986.

CONTENTS

Appendices

Chapter 1: Introduction

1.1.0 Motivation:

1.1.1 Today the wind turbine industry is dominated by horizontal axis wind turbines (HAWTs). The vertical axis wind turbines (VAWTs) seem to be virtually non-existent. In fact the only VAWT, which has ever been manufactured commercially at any volume, is the Darrieus machine but its manufacturer, Flo Wind, United States went bankrupt in 1997[1]. There were other small manufacturers of cylcoturbine, another variant of VAWT but these too did not perform well in the commercial wind turbine market. A lot of research work had been carried out on VAWTs, mainly Darrieus types, in the late 1970s, 1980s and early 1990s in the U.K., United States, Canada and Australia. But in terms of efficiency, the results were not very promising and inferior to HAWTs. VAWTs were, therefore, abandoned.

1.1.2 The last decade of the twentieth century witnessed a phenomenal growth of HAWTs both in terms of number and size throughout the world. The continuous research and design efforts led to the development of HAWTs in the MW range - 1MW, 1.3 MW, 1.5 MW, 2 MW and now 3 MW machines are appearing. Undoubtedly the HAWTs have proved a big commercial success. Their future appears to be bright with increasing worldwide emphasis on development of renewable energies.

1.1.3 Despite their wide use, a major disadvantage associated with the HAWTs is that these must be shut down when the wind speed exceeds a particular value known as cut-off speed. The shutting down is required from the point of view of safety of the wind turbine structures, mainly blades. For most of the HAWTs currently available on the market, the cut-off speed ranges from 20 to 25 m/s. These

machines are designed to survive in wind speeds up to 60 m/s but only under shut down conditions. This limitation of the HAWTs makes them unsuitable for cyclone and storm prone areas.

1.1.4 One is amazed by the energy contained in wind gusts. The efforts required to push the doors or windows in home against the wind thrust under stormy conditions makes one speculate if a machine could be devised to convert the energy contained in these wind gusts into useful energy. Obviously the answer does not lie in HAWTs which look for shelter for themselves to escape the wrath of the wind gusts just like human beings. This has led to the renewal of interest of researchers in VAWTs, which may bridge the gap created by HAWTs. Efforts are on to develop a wind turbine for cyclone prone areas. A 10 kW turbine was developed for such a purpose[2] but did not meet much success later.

1.1.5 Delta Wind Turbines Ltd. (DWT) claim to have developed a novel VAWT which will be fully functional at wind speeds throughout the Beaufort scale, making most of the opportunity for effective conversion of available wind energy at both high and low wind speeds[3] . The turbine can be mounted at ground level or any flat surface and is therefore said to be deployable in a wide variety of situations. Another core feature of this novel turbine according to DWT is that, despite ground shear affects on wind (the slowing down of wind speed and turbulence effects near ground due to rough terrain), it will generate significant power output when mounted at ground level. A series of wind tunnel tests were carried out on the model turbine in 1988 at the University of Strathclyde. At that time it was commented that it would be reasonable to expect the power coefficient for a larger developed prototype to be around 0.2 which is comparable with values for conventional small wind turbines currently on the market[4]. DWT have, now, developed a full size prototype and erected it at Fionnphort on the Isle of Mull. DWT have also got the novel VAWT patented in Great Britain in August 1998.

1.1.6 The novel VAWT developed by DWT, if found to be working in accordance with the claims of the inventor, may make a successful entry in the market for small wind turbines. It can be deployed for small communities and domestic users, especially located in the remote areas experiencing frequent storms and cyclones leading to frequent power failures. In fact, there would be virtually no competition from any HAWT for this specific application. With this interest in mind, this project was pursued under the supervision of the Scottish Energy Environment Foundation (SEEF), a conglomerate of universities (Strathclyde, Edinburgh), industries (British Energy, Scottish Power, Hydro Electric) and the Scottish Executive.

1.2.0 Project Aims:

1.2.1 The overall aim of the project was to determine the performance characteristics of the novel VAWT invented and patented by DWT. For this purpose the prototype was subjected to field testing at Fionnphort at Isle of Mull, Scotland.

1.3.0 Project Deliverables:

1.3.1 The deliverable from the project is the present report comprising field test results, data analysis and performance characteristics of the novel VAWT developed by DWT. The project report also includes a literature review on VAWTs, technical documentation of the novel VAWT and calibration/ verification procedures and results of instruments deployed for field-testing. Besides, certain improvement areas and recommendations for future work are mentioned in the last section of the report. Further the field-test results, data analysis and conclusions drawn in the present report will also be used by the SEEF in their concluding report on the novel VAWT.

1.4.0 Project Planning and Scheduling:

1.4.1 Broadly, the project involved the following activities:

- literature review of VAWTs;
- selection, calibration and verification of field instruments;
- deployment of field test set-up;
- documentation of the novel VAWT;
- compilation and analysis of field test data;
- development of performance characteristics of the novel VAWT;
- identification of improvement areas and
- preparation, submission and approval of thesis

1.4.2 The total project duration was 18 weeks and the bar chart used for the project scheduling was the following:

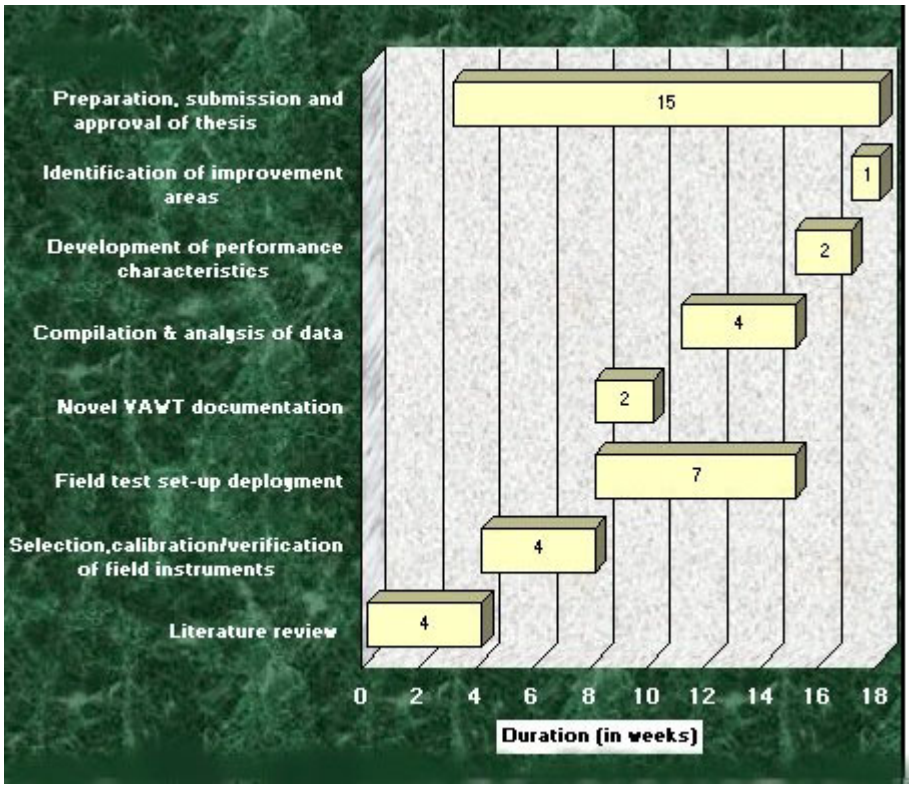

Chapter 2: Vertical Axis Wind Turbines

General

This chapter provides an overview of vertical axis wind turbines (VAWTs). The chapter is divided into three sections. The first section describes the history of the wind turbines with particular emphasis on VAWTs and important events relating to them. The next section discusses the various types of VAWTs along with their operating principles, relative merits and demerits. The last section is focussed over the ongoing dispute of VAWTs versus HAWTs, where the advantages and disadvantages of VAWTs in comparison with HAWTs are brought out.

2.1.0 History:

2.1.1 Man has always been fascinated by the energy in the wind, perhaps because it is there free, just to be used or so he believes. For centuries, wind energy has been used for many applications such as grinding corn, sailing ships, pumping water and lately for generating electricity. The history of wind mills is lengthy and dates back to about 500 BC when the use of wind mills for pumping water had been documented in a Hindu epic called 'Kautilya Arthasastra'[5].

2.1.2 Around 200 BC Persia developed a simple vertical axis panemone (figure 2.1) for grinding grains[6,7]. The rotor was made from bundles of reeds tied to frame, which rotated by the thrust of wind as wind blew. Originally, the millstones were placed above the rotor blades. Later on, the design was modified and the millstones were situated under the rotor. Perhaps it was learnt that the wind speed increases with height and the modified design would be more efficient and convenient for the miller as well![6]

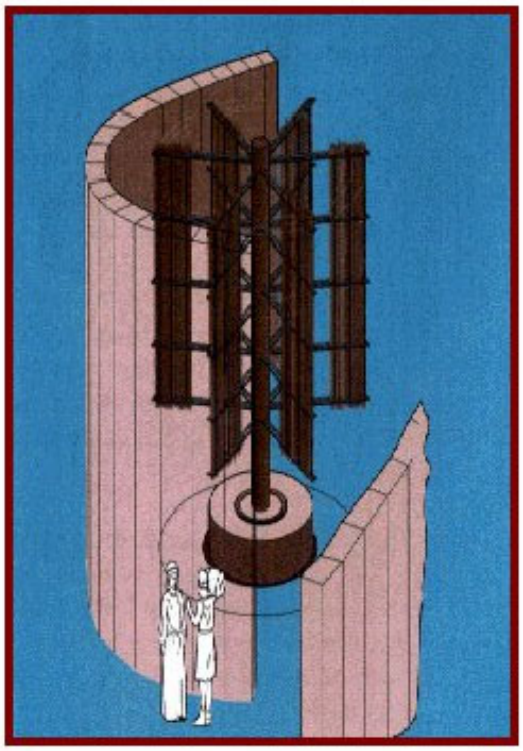

Figure 2.1

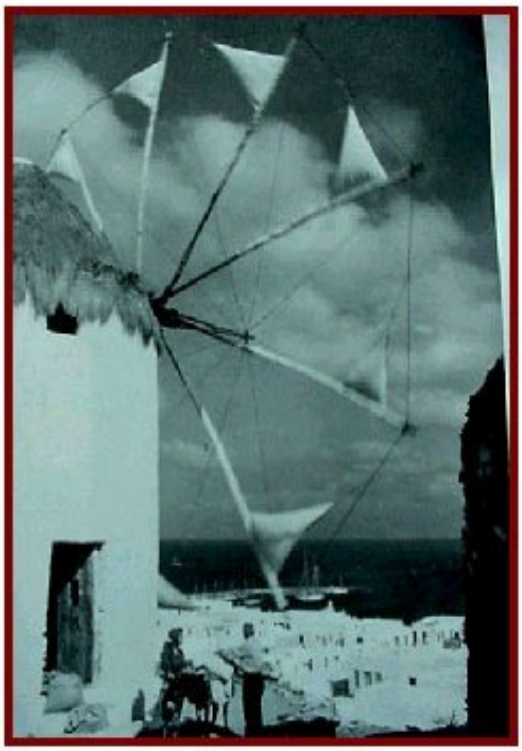

Figure 2.2

2.1.3 By 1100 AD, the windmills were in extensive use in the Middle East. Horizontal axis windmills, consisting of up to 10 wooden booms, rigged with jib sails, were developed. One such windmill is shown in figure 2.2. In Europe, the use of windmills was introduced around 1300 AD. At that time, the windmills were used mainly for cereal grinding. Interestingly, the vertical axis windmills were considered more efficient than their horizontal counterparts, which were in the primitive stages of development at that time. By 1400 AD, the Dutch had developed improved design of horizontal machines and beyond this point, the horizontal windmills overtook the vertical design. A traditional four bladed Dutch mill is shown in figure 2.3[8].

Figure 2.3

2.1.4 There was not much advancement in technology until the late 19th century when the wind turbines were developed for the first time for generation of electricity. In 1891, Paul la Cour developed the first wind turbine for generation of electricity in Denmark (figure 2.4)[8].

Figure 2.4

2.1.5 Between 1890 and 1980, there have been periods of growing and declining interest in wind turbines. For example, in Denmark, by the end of 19th century, there were about 2500 industrial windmills in operation, supplying a total of about 30 MW power, which was nearly 25% of the total power available to Danish industry at that time. However by the 1930s, the number has gone down to about 1000, perhaps because at that time the fossil fuel based power became cheap enough to force wind power out of the market. The outbreak of World War II and the consequent shortage of fuel drew attention of industrialists towards wind turbines and new types of large-scale wind machines were developed for generating electricity. The number of these machines increased from 16 in 1940 to 88 in 1944 in Denmark. After the World War II, there was period of slump again and their number dropped down to 57 by the end of 1947[9].

2.1.6 The Arab oil embargo in 1973 forced the developed countries to take a sobering look at their reliance on foreign fuel sources for their energy demands. Once again there was a renewed interest in development of alternative resources of energy and wind turbines were looked upon favourably. National Research Council, Canada; Sandia National Laboratories, U.S.A and many research institutions in the U.K. started experimenting with Darrieus vertical axis wind turbines with new vigour. However as stated earlier in chapter 1, the results were not very promising and hence VAWTs could hardly move from researchers' test bed to market.

2.1.7 An interesting event in the history of VAWTs, which again highlights the growing and declining periods of interest in wind turbines in 19th century, is the re-invention of Darrieus wind turbine. French inventor George Jean Marie Darrieus got his invention, Darrieus VAWT, patented in France in 1925 and subsequently in the United States in 1931. His invention drew hardly any

attention at that time until in late 1960s, two Canadian researchers re-invented his concept without knowing about Darrieus patent[7].

2.1.8 The depleting reserves of fossil fuels and the alarming signals of global warming due to ever-increasing percentage of greenhouse gases by fossil fuel burning for energy have once again revived the interest of world community in renewable energy resources. The phenomenal rise in wind turbines in the last decade is its proof. But the fall out of the United States in ratification of 'Kyoto Protocol' for reduction of greenhouse gases by advanced countries may have serious implications on the future of wind turbines. 'Where does the World move from here?' will be an interesting issue to watch in the coming months.

2.2.0 Types of Vertical Axis Wind Turbines:

A vertical axis wind turbine, by definition, has its axis of rotation perpendicular to both the earth surface and the wind stream. On the other hand, the axis of rotation of a horizontal axis wind turbine is parallel to the direction of wind stream. Typical schemes of a HAWT and VAWT are shown in figure 2-5.

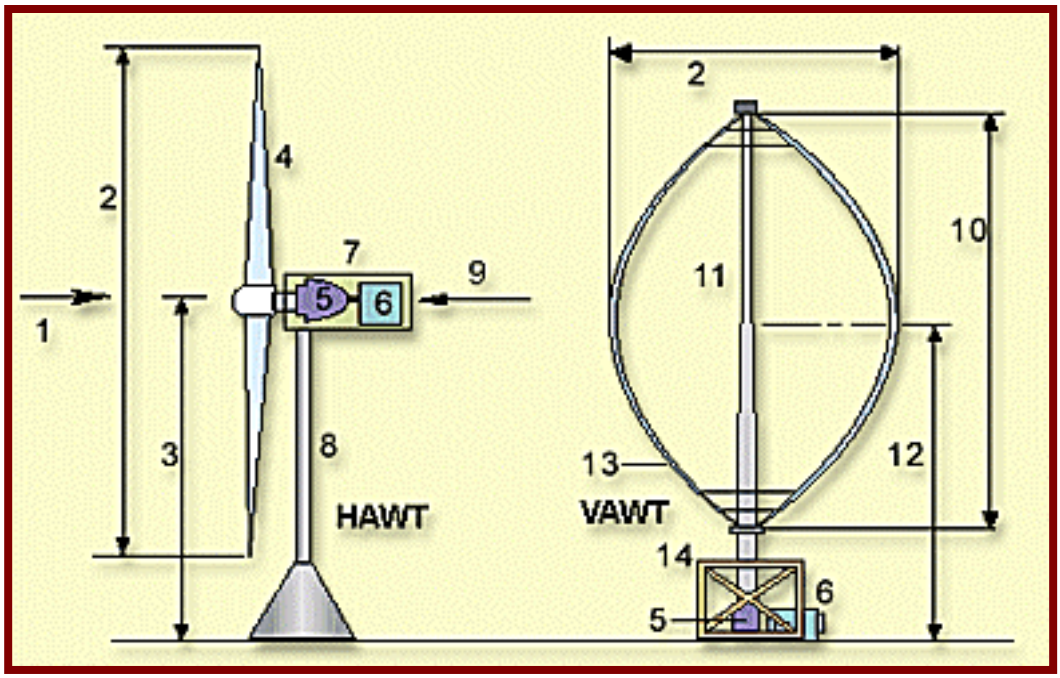

1. Wind direction for an upwind HAWT 2.Rotor Diameter 3.Hub height
4.Rotor blade 5.Gear box 6.Generator 7.Nacelle
8.Tower for HAWT 9.Wind direction for a downwind rotor
10. Rotor height 11.Tower for VAWT 12.Equator height
13.Fixed-pitch rotor blade 14. Rotor Base

Figure 2.5

Broadly, the VAWTs can be classified into two categories - drag based design and lift based design.

2.2.1 Savonius: Drag Based VAWT:

2.2.1.1 Drag based design works on the principle of a paddle propelling a boat through water. If there is no slip between the paddle and water, the maximum speed attained will be same as the tangential speed of the paddle. Similarly in a drag based VAWT, the speed at the tip of the blade can seldom exceed the speed of

the wind. In short terms, the drag can also be described as the pressure or the thrust on the blades created by the wind as it passes through it.

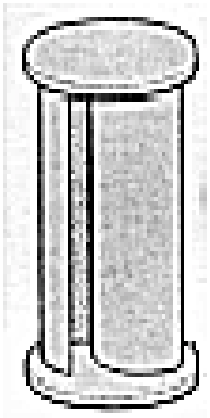

Figure 2.6

2.2.1.2 Various types of drag based VAWTs have been developed in the past which use plates, cups, buckets, oil drums, etc. as the drag device. The Savonius rotor is a S-shaped cross section rotor (figure 2.6), which is predominantly drag based but also uses a certain amount of aerodynamic lift. It was developed in Finland. Drag based VAWTs have relatively higher starting torque and less rotational speed than their lift based counterparts. Further their power output to weight ratio is also less. Because of the low speed, these are generally considered unsuitable for producing electricity although it is possible to do so by using proper gear trains. Drag based wind mills are useful for other applications such as grinding grain, pumping water, etc. A major advantage associated with the drag based VAWTs is that these are self starting unlike of purely lift based VAWTs.

2.2.2 Darrieus: Lift Based VAWT:

2.2.2.1 Lift based designs work on the aerodynamic theory of aeroplanes. The blades of the rotor are designed airfoil in cross section so that the wind has to cover a

longer distance on one side than the other one (see figure 2.7). As a result, the wind speed is relatively higher on one side. Applying Bernoulli's equation, it can be found that this differential speed creates differential pressure, which is used to pull the rotor blade around as the wind passes through.

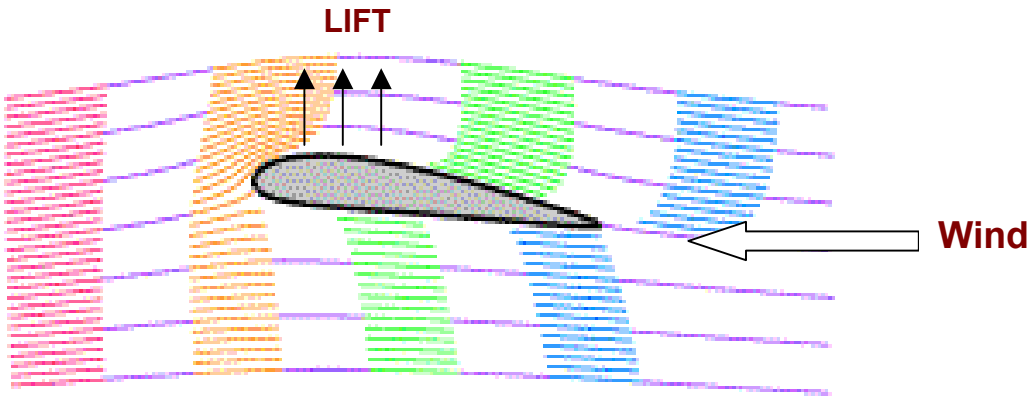

Figure 2.7

Darrieus VAWT is primarily a lift-based design. The machine is characterised by its C-shaped rotor (figure 2.8) which makes it look like an eggbeater. It is normally built with two or three rotor blades. It has low starting torque but high rotational speed making it suitable for coupling with an electrical synchronous generator. For a given rotor size, weight and cost, its power output is higher than any drag based VAWT. Darrieus VAWT suffers from the disadvantage that it is not self-starting.

Figure 2.8

In grid connected applications, this drawback can be overcome as initially the coupled generator can act as motor drawing current from the grid and once the machine has reached its pick up speed (the peripheral speed at the tip of the blade becoming equal to the wind speed), the motor can reverse its role to generator feeding power in the grid. In stand-alone applications, Darrieus rotor can be combined with a Savonius rotor of suitable size to give it starting torque.

2.2.2.2 In the late 1970s and 1990s, Darrieus rotor had been a fancy for the researchers and was considered a potential threat to its rival, HAWT. In 1980s these were produced in hundreds by Flowind, a U.S.A based manufacturer and employed in California for generation of electricity. The largest prototype was located in Quebec, Canada. It had a diameter of 100 m and a rated power output of 4.2 MW, which was more than seven times of the largest HAWT available at that time. But now it has been brought down as VAWTs are no more considered reliable and efficient. But the race between VAWTs and HAWTs is still on.

2.2.3 Other Lift based VAWTs:

2.2.3.1 A variant of Darrieus VAWT is Giromill (figure 2.9)[9], which has straight vertical blades. Cycloturbine is another type of VAWT using a wind vane to mechanically orient a blade pitch change mechanism (figure 2.10)[9]. Other types of VAWTs use ducts and/or vortex generator towers, augmented by shrouds or diffusers to deflect the horizontal wind stream to a vertical direction and increase its speed.

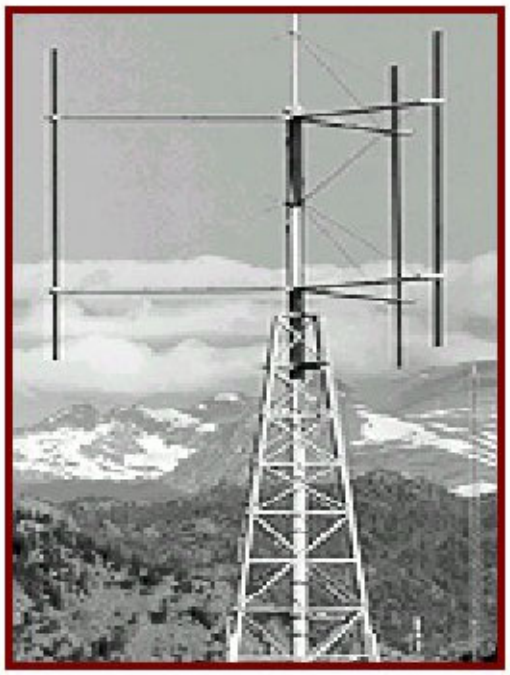

Figure 2.9

Figure 2.10

2.3.0 VAWTs versus HAWTs:

This dispute is certainly as old as the invention of the wind energy converters. Different experts seem to carry varied opinion on this subject. A good comparison has been made on the two types of turbines by Dennis G. Shepherd in his article *"Wind Power"*[10]. The relative advantages and disadvantages of VAWT vis-a-vis HAWT are given hereunder:

2.3.1 Advantages of VAWT over HAWT:

a) Traditionally a VAWT is an omni-directional machine. It means that it is not required to be turned into the wind as the later changes its direction. Thus complex yaw mechanism as being used in conventional upwind HAWT is not required in VAWT.

b) A VAWT is placed on the ground unlike of a HAWT being mounted on a high tower. Therefore the heavy gear box, generator and control mechanism may be situated at ground permitting easier erection and accessibility for maintenance.

c) For a comparable power output, the overall height of HAWT (including tower height) is much more than that of Darrieus VAWT resulting in more pronounced visual impact on the surroundings. In this way, the VAWTs can be considered more friendly to environment than their counterparts.

d) The blades of a VAWT are not subjected to fatigue stresses due to vertical wind velocity gradient and gravitational forces during rotation. In case of HAWT, the blades pass through a vertical wind gradient with the wind speed increasing upwards from the ground level. Further the loading due to gravitational force also changes as the blades go upward and come downward. Accordingly both the blades and blade roots are subject to low cyclic fatigue and unless designed for extreme conditions, may be subjected to potential fatigue failure. The fatigue loading also has a bearing on the cost and longevity. The blades of VAWT are less expensive and last longer than their counterparts for HAWT.

e) A VAWT is designed in such a way that centrifugal loads are balanced by pre tension forces in the blades, thus avoiding bending moments; thus the turbine shaft carries axial and torsion loads only. In a HAWT, the rotor blades are additionally subject to cantilever loads resulting in bending moments at blade roots.

2.3.2 Drawbacks of VAWT:

a) VAWTs are generally not self-starting. The Savonious rotor is an exception but it has fairly low efficiency.

b) Since VAWTs are mounted close to ground, they are subject to less wind speed and more turbulence. Hence for the same rotor size (swept area) and weight, the power output of VAWT is less than that of a comparable HAWT.

c) Guy cables are required to hold VAWT. These Guy cables interfere with the secondary use of footprint. For example, it becomes practically impossible to use the land for farming.

d) The entire weight of a VAWT rests on the lower main bearing requiring it to be very robust and reliable in operation. However in case of malfunctioning, the whole machine is required to be brought down for replacement of the bearing.

e) In a VAWT, the torque and the power output fluctuates in a cyclic manner during each revolution as the blades move into and out of the wind whereas in HAWT, the torque and power output is fairly steady.

f) Because of the cyclic variations in torque, the VAWT has many natural frequencies of vibration which must be avoided and crossed over fast by the control mechanism otherwise resonance may result in serious vibrations damaging the rotor. A well-designed HAWT has no such vibration problems.

2.3.3 Efficiencies and Economics:

H.H. Doerner made a comparison of efficiencies and economics of the following rotors on equitable basis[11]:

a) Two bladed HAWT
b) Two bladed Darrieus VAWT
c) S-shaped Savonius rotor
d) Shrouded Propeller (aerogenerator)

The figure 2.11 shows the biggest possible swept area for each type of rotor, which can be built up with a certain area of same material (3.2 m^2). Further using the general values of C_P, coefficient of performance (For definition, please refer to paragraph 3.2.0 of chapter 3) for these rotors, the power output was computed for each rotor for a wind speed of 5.6 m/s.

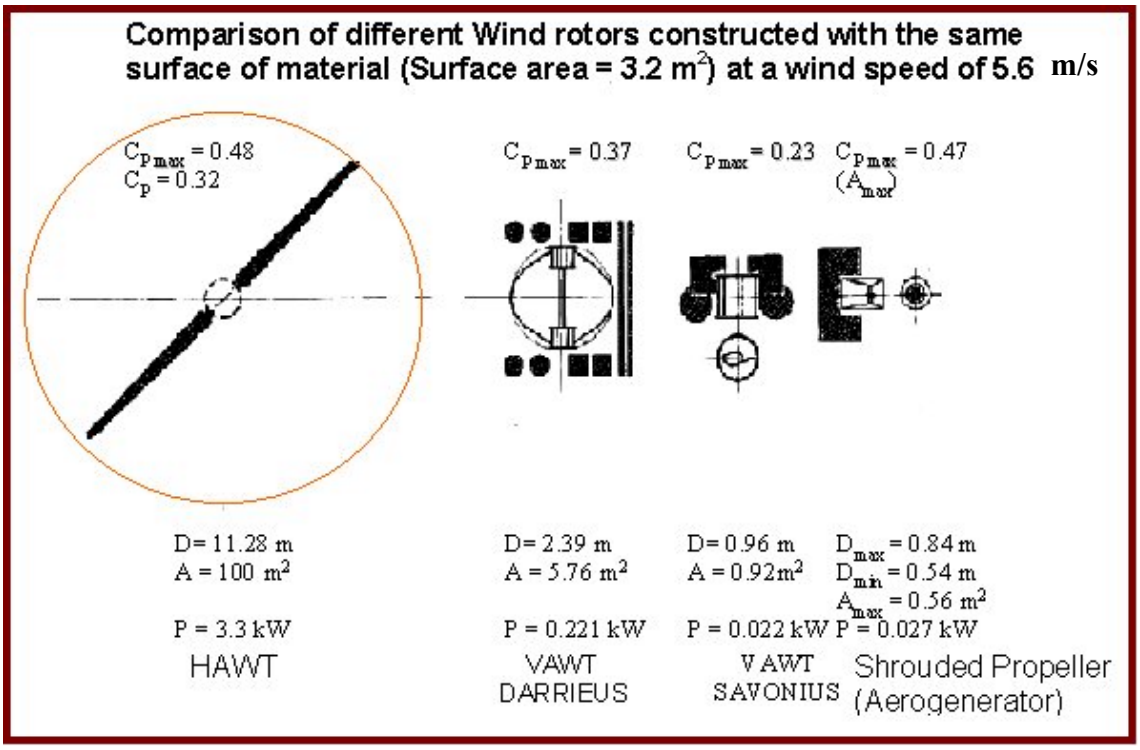

Figure 2.11

The power output of HAWT, being maximum establishes its superiority over other rotors. However, it is important to note that the comparison involves the following simplifications:

- Only the aerodynamic parts (rotors) of the different systems have been taken into account and

- The calculation of swept area is based purely on the area of the material used without looking to the structure, the strength, the stiffness, the forces, blades rigidity, bending moment, etc.

Hence the results can just give an indication on relative performance of rotors rather than the absolute comparison. Further, if commercial success is viewed as another criteria for establishing the superiority, the VAWTs definitely lag much behind HAWTs.

Chapter 3: Conceptual Background

General

This chapter deals with some fundamental concepts and terminology used in context of wind turbines and their testing which will aid in better understanding of subsequent sections of the thesis.

3.1.0 Wind Power:

3.1.1 The power contained in a freely flowing wind stream of cross sectional area A (figure 3.1) can be expressed as

Power = (Volumetric flow rate) x (Kinetic energy per unit volume)

$P_{wind} = (A\ V) \times (0.5\ \rho\ V^2)$

$= 0.5\ \rho\ A\ V^3$ (3-1)

$= 0.5\ \dot{m}\ V^2$

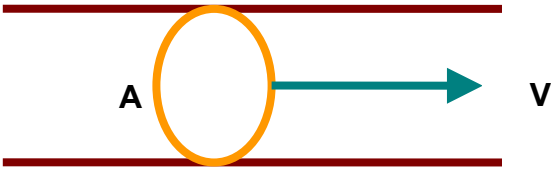

Figure 3.1

Where V is the wind speed

ρ is the air density

$\dot{m}$ is the mass flow rate of wind

Assuming air to be a stable mixture of perfect gases, the air density ρ can be derived from Perfect gas equation as under:

$PV = m\ R\ T$

$$m / V = P/RT$$

$$\rho = P/ RT \quad (3\text{-}2)$$

Where P is the absolute pressure in N/m^2

T is the absolute temperature in K and

R is the gas constant for dry air = 287.1 J/kg K

Strictly speaking, R should be gas constant for moist air, which will vary depending upon the moisture content of the air. Since the moisture content present in the air is very small (usually varying between 0.0003 to 0.003 kg/kg of dry air depending upon temperature and pressure), the use of gas constant for dry air introduces negligible error in calculations and is a standard practice for computation of air density.

3.2.0 Coefficient of Performance:

3.2.1 Coefficient of Performance is defined as the ratio of power extracted by a wind turbine to the total power available in the cross sectional area of the wind stream subtended by the wind turbine. It is generally denoted by C_P and mathematically, expressed as under:

$$C_P = P_{turbine} / P_{wind}$$

Therefore, power extracted by a wind turbine can be expressed as

$$P_{turbine} = 0.5\ C_P\ \rho\ A\ V^3 \quad (3\text{-}3)$$

Where A is the swept area of the rotor and

V is the speed of freely flowing wind stream.

Coefficient of Performance is a measure of turbine efficiency and is generally used to compare the performance of various rotors.

3.2.2 Betz limit: Theoretical value of C_p for extracting maximum power from wind

Consider a wind rotor to be placed in the path of free flowing wind stream at wind speed V_o as shown in figure 3.2. As the wind passes across the rotor, it extracts a fraction of the energy from the wind so that its speed at the exit from the rotor reduces to V_2. The power extracted by the rotor from the wind is given by the following expression:

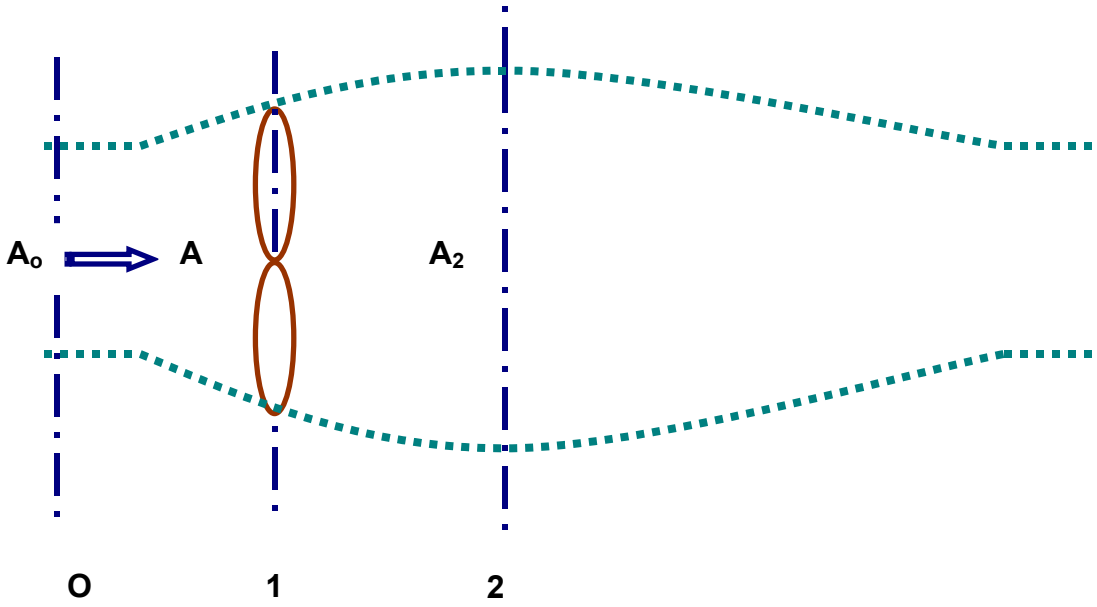

Figure 3.2

$$P_{turbine} = 0.5 \dot{m} V_o^2 - 0.5 \dot{m} V_2^2$$

$$= 0.5 \dot{m} (V_o^2 - V_2^2) \quad (3\text{-}4)$$

Let F be the mean thrust acting on the rotor due to wind.

By Newton's second law of motion, it can be written as

$$F = \text{Rate of change of momentum}$$

$$F = \dot{m} (V_o - V_2) \quad (3\text{-}5)$$

If V is the wind speed at the rotor, the power extracted by the rotor can also be written as

$$P_{turbine} = FV$$

$$V = P_{turbine} / F$$

Substituting $P_{turbine}$ and F from equations (3 - 4) and (3-5) respectively, we get

$$V = 0.5 (V_o + V_2) \quad (3\text{-}6)$$

Also by conservation of mass, we have

$$\dot{m} = \rho A_o V_o = \rho A V = \rho A_2 V_2$$

Substituting $\dot{m} = \rho A V$ in equation (3-4), we get

$$P_{turbine} = 0.5 \rho A V (V_o^2 - V_2^2)$$

Substituting V from equation (3-6) above, we get

$$P_{turbine} = 0.25 \rho A (V_o + V_2) (V_o^2 - V_2^2)$$

$$= 0.25 \rho A (V_o + V_2) (V_o + V_2) (V_o - V_2)$$

$$= 0.25 \rho A (V_o + V_2)^2 (V_o - V_2)$$

$$P_{turbine} = 0.25\ \rho\ A\ V_o^3 \left(1 + \frac{V_2}{V_o} \right)^2 \left(1 - \frac{V_2}{V_o}\right)$$

Denoting the ratio of exit wind speed to initial wind speed by b i.e. $b = V_2 / V_o$, we get

$$P_{turbine} = 0.25\ \rho\ A\ V_0^3 (1 + b)^2 (1 - b) \qquad (3\text{-}7)$$

By definition of coefficient of performance, we have

$$P_{turbine} = 0.5\ C_P\ \rho\ A\ V_0^3 \qquad (3\text{-}8)$$

From equations (3-7) and (3-8), we get

$$C_P = 0.5\ (1 + b)^2 (1 - b)$$

Let us now determine the velocity ratio b, which will yield the maximum value of C_P.

By using $\frac{d C_P}{d b} = 0$, we get

$$(1+ b)\ (1-b) - 0.5\ (1+b)^2 = 0$$

$$(1+ b)\ (1 - b - 0.5 - 0.5b) = 0$$

$$b = -1 \quad \text{or} \quad b = 1/3$$

$$\frac{d^2 C_P}{d b^2} = -2b - 1 - b = -3b - 1$$

$$\left.\frac{d^2 C_P}{db^2}\right|_{b=1/3} = -2 < 0$$

Therefore C_P is maximum at b = 1/3 and the maximum value is given by

$$C_{P\,max} = 0.5\,(1 + 0.33)^2\,(1 - 0.33)$$

$$= 0.593$$

This is known as Betz limit after the name of the person who first derived it. Its significance lies in the fact that it puts a limit on the fraction of the wind energy, which can be extracted by any wind turbine.

3.3.0 Tip Speed Ratio:

It is defined as the ratio of tangential or peripheral linear speed at the tip of the blade to the free flowing wind speed. It is usually denoted by λ and is mathematically expressed as under:

$$\lambda = \omega r / V \qquad (3\text{-}9)$$

Where ω is the angular speed of the rotor;

r is the radius of rotor and

V is the speed of free flowing wind stream

The variation of coefficient of performance, C_P with tip speed ratio λ for various types of typical rotors is shown in figure 3.3[8]. By wind tunnel experiments, it has been found that a two bladed HAWT of good aerodynamic design can achieve C_P of 0.48 at tip speed ratio of around 9-11. Likewise a Darrieus rotor has been found to attain a C_P of nearly 0.39 at tip speed ratio of around 5.

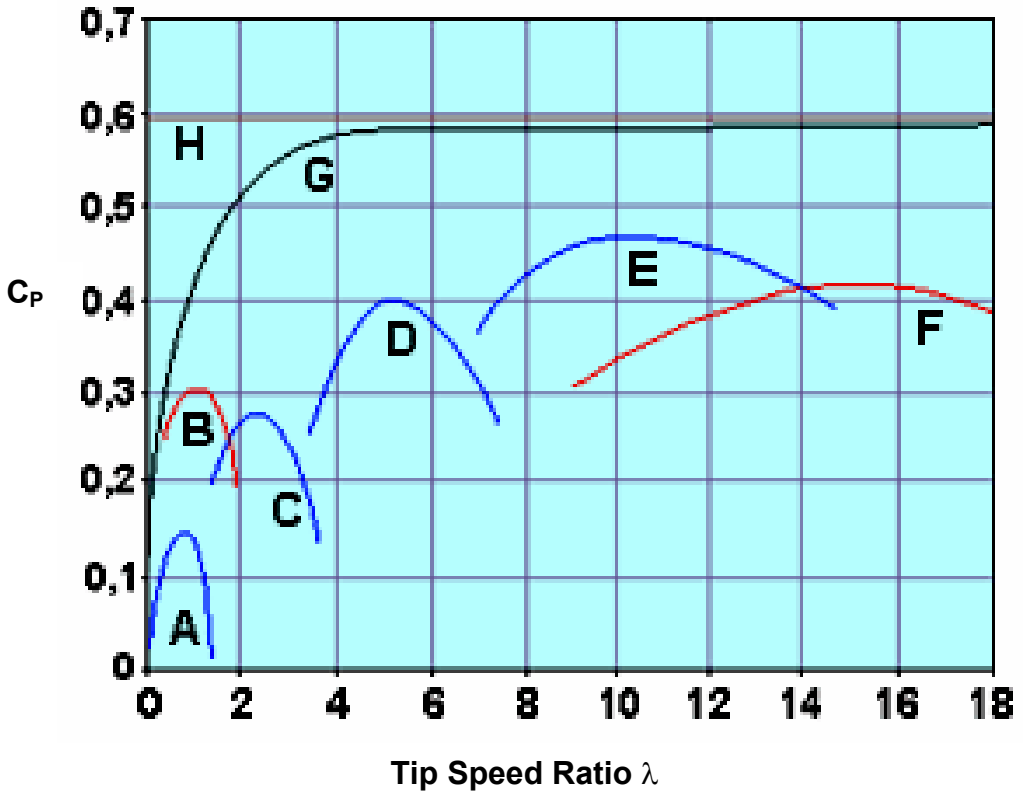

A: Savonius Rotor
B: American Multi Bladed Rotor
C: Dutch Four Arm Rotor
D: Darrieus rotor
E: Modern Two Bladed HAWT
F: Single Bladed Rotor
G: Ideal Propeller
H: Betz limit

Figure 3.3

From equation (3-3), we have

$$P_{turbine} = 0.5\, C_P\, \rho\, A\, V^3$$

The power extracted by turbine from wind can also be written as product of torque (τ) and angular speed (ω).

$$P_{turbine} = \tau\, \omega \qquad (3\text{-}10)$$

From equations (3-3) and (3-10), we have

$$\tau \omega = 0.5 C_P \rho A V^3$$

Substituting ω by $\lambda V/r$ from equation (3-9), we have

$$\tau \lambda V/r = 0.5 C_P \rho A V^3$$

$$\tau = 0.5 C_P \rho A r V^2 / \lambda \quad (3\text{-}11)$$

3.4.0 Rotor Solidity:

3.4.1 Rotor solidity, usually denoted by S, is defined as the ratio of the projected area of a rotor to its swept area.

S = Projected area of rotor / swept area of the rotor

Solidity ratio is always less than 1. A rotor with a high value of solidity ratio has usually high starting torque but low rotational speed. On the other hand, a rotor with low solidity has high operating speeds making it suitable to be coupled with an alternator for generation of electricity.

3.5.0 Ducted Systems:

Various types of ducted devices such as flow concentrators, diffusers, etc. as shown in figure 3.4 have been designed to aid the wind rotors in extraction of more power from wind. Experimental evidences suggest that these devices can increase the wind speed through the rotor up to 150% multiplying the power output by nearly 3 times[9,12]. However the cost may be prohibitively high in some cases. In addition, the operational and maintenance difficulties of huge

structure at heights particularly in case of high mounted HAWTs can be troublesome. Further the power consumed in yawing the entire assembly to face the wind can outweigh the gains. Specific designs need to be analysed in detail considering the practical aspects in the field rather than at test bed.

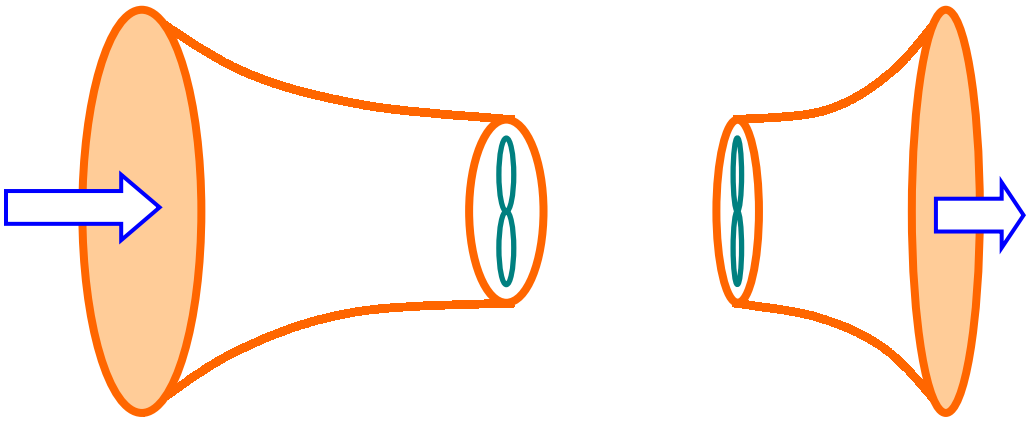

Flow Concentrator Diffuser

Figure 3.4

3.5.1 Flow Concentrators:

3.5.1.1 A Flow Concentrator is provided at the front end of a wind rotor. It improves the rotor performance in the following two ways:

a) As the wind approaches a rotor, the flow tends to diverge out. As a result, a portion of the wind bypasses the rotor. This reduces the actual volumetric flow rate of wind passing through the rotor resulting in less energy output. A flow concentrator converges the wind flow resulting in increased wind speed at inlet to rotor. The rotor is able to extract more energy from the increased kinetic energy of the wind passing through it.

b) A flow concentrator reduces the turbulence around the rotor. Turbulence causes a reduction in lift on the rotor blades. By reducing turbulence, the

aerodynamic lift on the rotor blades increases and hence the power output also increases.

3.5.1.2 There are certain losses of energy associated with the use of flow concentrators:

i) Skin friction losses at the boundary layer of the flow along the duct walls.

ii) Eddying or flow separation losses due to abrupt change in wind profile at the inlet of the ducts or inside (as shown in figure 3.5).

iii) Secondary flow losses where a portion of the streamline momentum is transferred to the secondary flow and finally dissipated as heat.

The design of the flow concentrators, therefore, needs to be optimised so that losses do not exceed the gains in energy in wind stream.

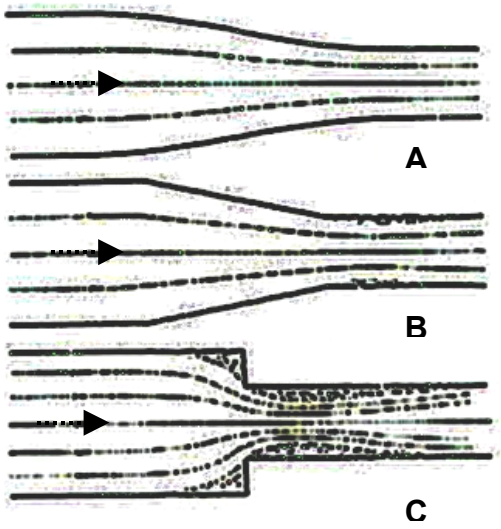

Flow losses in three different types of contractions in concentrators

A) Smooth contraction (negligible losses)
B) Flow separation due to angled contraction (losses: 5-10%)
C) Sharp contraction (losses: 30-50%)

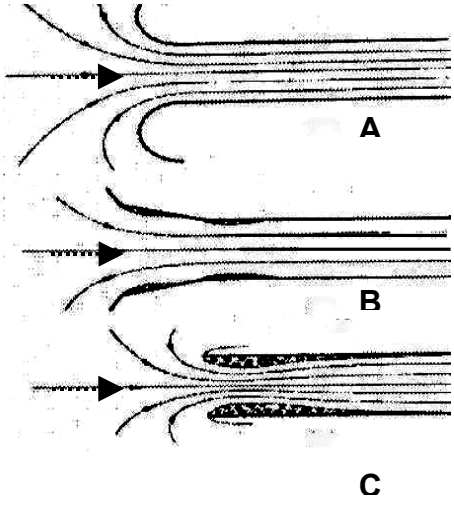

Flow losses in three different types of inlets

A) Smooth (negligible losses)
B) Flow separation in small angled inlet (5-7% losses)
C) Sharp inlet (losses: 60-70%)

Figure 3.5

3.5.2 Diffusers:

3.5.2.1 Diffusers are used to increase suction at the rear of the turbine so that the differential pressure across the rotor increases. As a consequence, the volumetric flow rate of wind through the rotor also increases resulting in higher energy output.

3.5.2.2 If the widening angle of the diffuser is small, there will be no separation of flow at the rear of the turbine and the only losses of energy will be due to skin friction. However if the rate of diffusion is increased beyond certain limit by employing larger widening angle, the boundary layer is liable to separate from the duct walls causing eddies to develop and hence more losses of energy. A typical diffuser augmented turbine is shown in figure 3.6.

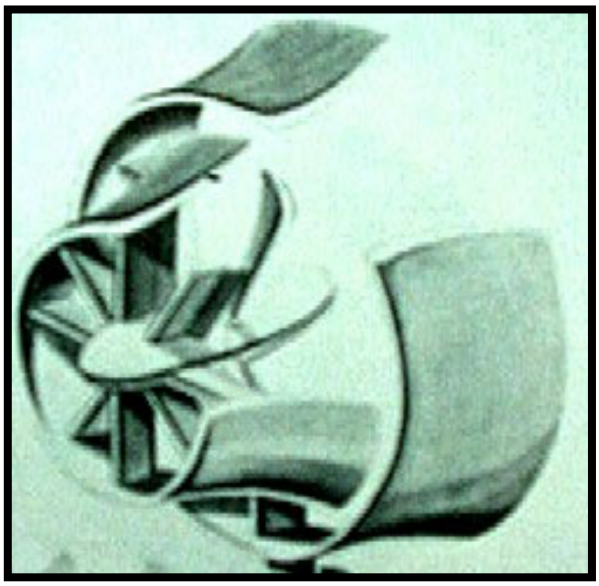

Figure 3.6

3.6.0 Alternator:

A.C. generator, more commonly known as alternator, is a rotating machine, which converts mechanical power fed into it to electrical power. The power conversion is based on the principle of production of dynamically induced e.m.f. Whenever a conductor cuts magnetic flux, dynamically induced e.m.f. is produced in it which, according to Faraday's second law of electromagnetic induction, is directly proportional to the rate of change of magnetic flux linkage. Now if the conductor forms a part of a closed circuit, the induced e.m.f. will cause a current to flow. Hence the three basic requirements of an alternator are magnetic field, conductor(s) and the relative motion between them. The figure 3.7 shows the basic construction details of a three phase alternator. The standard construction consists of an armature winding mounted on a stationary element called the stator and field excitation windings on a rotating element called the rotor. In small generators, the field windings are replaced by strong permanent magnets.

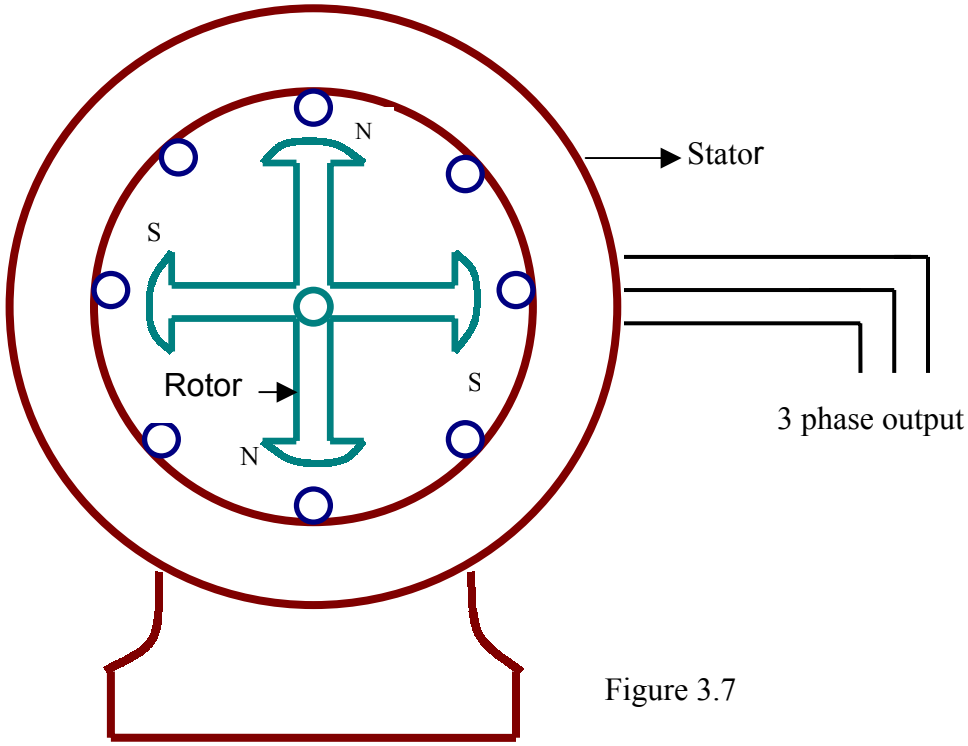

Figure 3.7

3.6.1 Frequency – Speed Relation:

3.6.1.1 The frequency of the e.m.f. induced in the alternator is given by the expression:

$$f = pN/120 \quad (3\text{-}12)$$

Where p is the number of poles and

N is the rotational speed of the rotor expressed in r.p.m.

It follows from the above expression that for a fixed number of poles, the alternator is required to be run at a constant speed known as synchronous speed for producing an e.m.f of specified frequency. For example a two pole alternator, if required to generate 50 Hz frequency voltage, should essentially run at 3000 r.p.m. All grid connected alternators are synchronous alternators.

3.6.2 Equation of Induced E.m.f.:

3.6.2.1 If n is the number of coils per phase;

p is the number of poles;

B is the magnetic flux per pole in webers;

f is the frequency of induced e.m.f. in Hz and

N is the speed of rotor in r.p.m.,

then in one revolution of the rotor (i.e. 60/N seconds), each stator coil is cut by a flux of 2p B webers.

The average e.m.f induced per coil = dB / dt = pBN/30

Total average e.m.f. induced per phase = pBNn/30

R.M.S. value of e.m.f. per phase, E = 1.11 x pBNn/30 (3-13)

= 4.44 x pBNn/120

From equation (3-12), we have f = pN/120

R.M.S. value of e.m.f. per phase, E = 4.44 x fBn Volts (3-14)

3.6.3 Alternator on Load:

3.6.3.1 As the load on an alternator is varied, its terminal voltage is also found to vary due to the following voltage drops:

a) Voltage drop due to armature resistance (R_a)
b) Voltage drop due to armature leakage reactance (X_l)
c) Voltage drop due to armature reaction

The drop due to armature reaction is theoretically accounted for by assuming a fictitious reactance X_a in armature winding. The vector sum of X_l and X_a gives synchronous reactance X_s. Hence it can be said that an alternator possesses resistance R_a and synchronous reactance X_s. The figure 3.8 shows the phasor diagram for a purely resistive load. Voltage vector V is taken as the reference vector. Current vector I is in phase with voltage V. The voltage drop IR_a due to armature resistance is in phase with V whereas drop IX_s is at right angles to it, their vector sum giving IZ_s. By combining IZ_s with V, we get induced e.m.f. E.

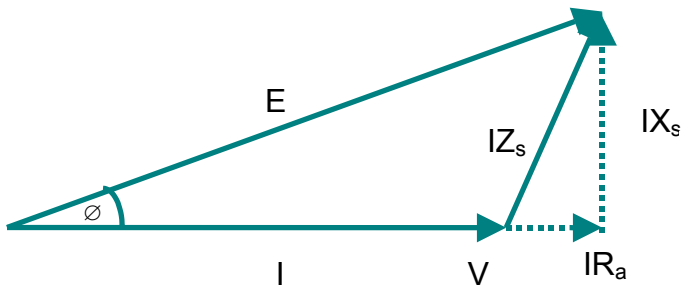

Figure 3.8

From the vector diagram, we have

$$E^2 = (V + IR_a)^2 + (IX_S)^2$$

Now if R is the resistive load on the generator, we have V = IR

$$E = I [(R + R_a)^2 + (X_S)^2]^{0.5} \quad (3\text{-}15)$$

From equations (3-13) and (3-15), we get

$$1.11 \times pBNn/30 = I [(R + R_a)^2 + (X_S)^2]^{0.5}$$

$$N = I * \{[(R + R_a)^2 + (X_S)^2]^{0.5} \times 30 / (1.11 \times pBn)\}$$

If the frequency of the induced e.m.f. is low as in case of a low speed alternator, the value of the synchronous reactance $X_S = (L_s + L_a)\omega$ will be very small and, therefore, variation in its value due to changing frequency can be neglected. Hence for all practical purposes, we can assume X_S to remain constant. Further if the alternator is of permanent magnet type, B, the magnetic flux will also be constant. With all other parameters within the bracketed term being constant, we have

$$N = I * K$$

Where K $\{= [(R + R_a)^2 + (X_S)^2]^{0.5} * 30 / (1.11*p*B*n) \}$ is a constant for a permanent magnet low speed alternator with a purely resistive load R connected across its terminals.

Therefore it follows from the above expression that the current flowing through a purely resistive load connected across a permanent magnet alternator (or

constant excitation) is directly proportional to the speed of the alternator. This conclusion was used for establishing the rotational speed of the wind rotor by measuring the current flowing through the resistive load connected across the coupled permanent magnet alternator as discussed in the succeeding chapters. It is important to point out that this conclusion holds good only in case of low speed generators as the synchronous reactance may play a significant role at higher frequencies.

3.6.4 Power Losses:

3.6.4.1 There are certain losses of power in the operation of alternator as the power flows from shaft to output terminals. The various losses are as under:

a) **Mechanical losses** comprising of

(i) **Friction losses** at bearings and commutators

(ii) Air friction or **windage losses** in rotor

The mechanical losses together account for nearly 10 to 20% of full load losses.

b) **Iron losses** (or core losses) consisting of

(i) **Hysteresis losses** due to reversal of magnetism.

For flux densities up to 1.5 Wb/m^2, the hysteresis losses are given by Steinmetz formula

$$P_h = \mu B^{1.6}_{max} f V_c$$

Where μ is hysteresis coefficient for the core material

B_{max} is the maximum magnetic flux density

f is the frequency of magnetic reversals and

V_c is the volume of the core

For keeping hysteresis losses low, the material used for the core is one having low c = 191).

(ii) **Eddy current losses** due to production of closed circuit eddy currents in the body of the core expressed by the relation

$$P_e = k B^2_{max} f^2 t^2 V_c$$

Where B_{max} is the maximum magnetic flux density

f is the frequency of magnetic reversal

t is the thickness of lamination

V_c is the volume of the iron core

From the above expression, it is clear that eddy current losses are directly proportional to the square of the thickness of lamination. In order to keep these losses low, a thin laminated core made of low electrical resistivity material is used.

The iron losses constitute 20 to 30% of total losses at full load.

c) **Copper losses** occurring in the stator and field windings expressed by the relations

$$P_{ca} = I^2_a R_a \qquad P_{cf} = I^2_f R_f$$

Where I_a and I_f are the currents flowing through the stator and field windings respectively and

R_a and R_f are the stator and field winding resistances respectively

Copper losses are nearly 40 to 60% of full load losses. In order to keep these losses low, the stator and field windings should have low resistances.

The Power Flow diagram of an alternator is shown in figure 3.9

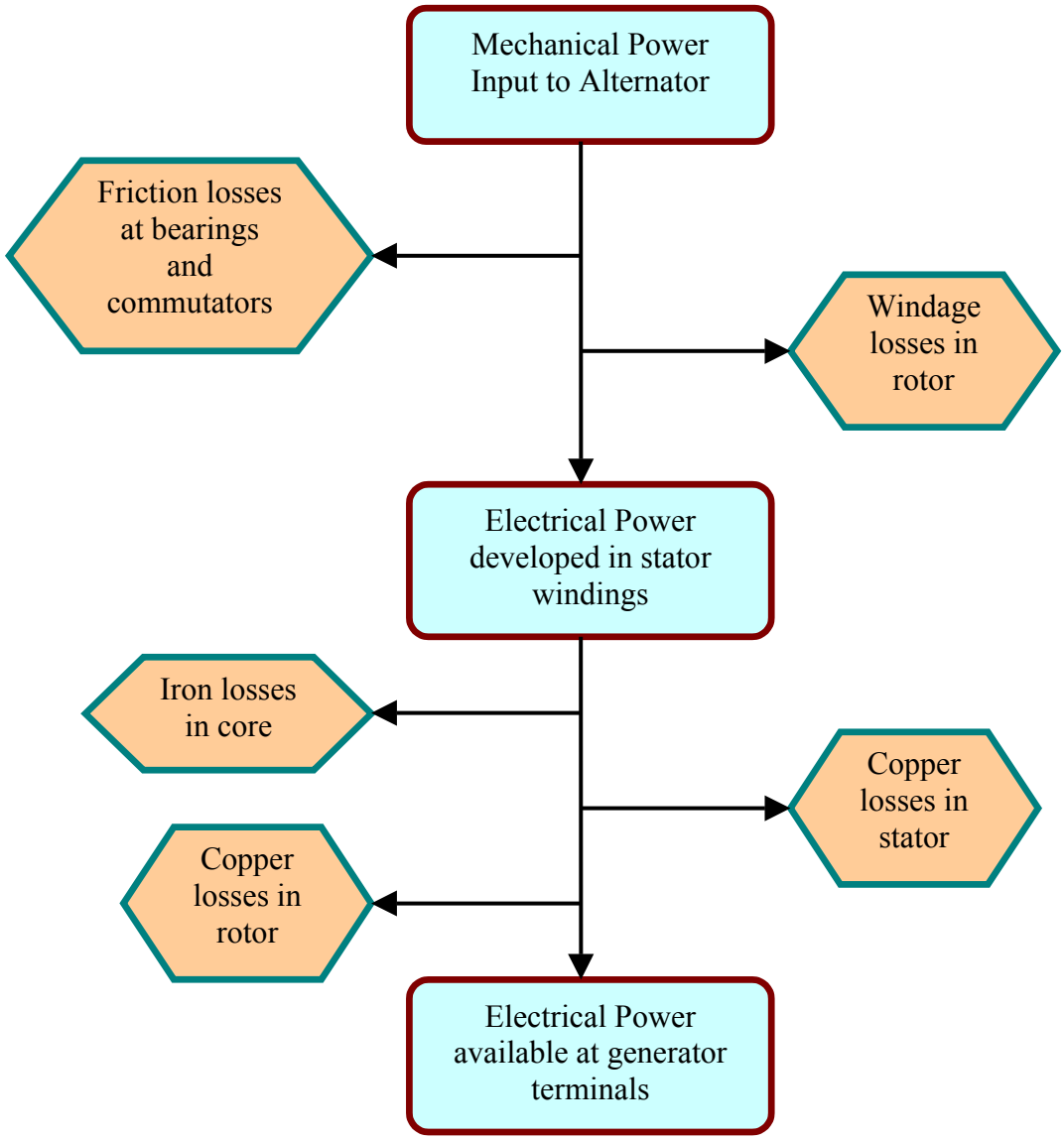

Figure 3.9

For small alternators, the efficiency is in the range of 65-80%. But large generators used in power stations have high efficiency of around 95-98%.To dissipate the heat generated in the alternators, cooling arrangements are provided in stator as well as rotor.

Chapter 4: Delta Wind Turbine

General

This chapter describes the basic construction and operational features of Delta Wind Turbine prototype, which has been developed by Mr. Chris L. Baigent for Delta Wind Turbines Ltd. The novel wind turbine has been patented in Great Britain in August 1998. The turbine prototype has been erected at Fionnphort, Isle of Mull in Scotland.

4.1.0 Delta Wind Turbine:

4.1.1 Delta Wind Turbine comprises of two contra rotating vertical axis rotors, which are housed in a ducted system. Each rotor is directly coupled to its own generator providing two independent power sources. The entire structure is required to be turned into the wind as it changes direction. But the yaw mechanism used for this purpose is automatic without requiring any external aid such as yawing motor and gear train. The figures 4.1, 4.2 and 4.3 show the rear, front and the side views of the novel VAWT.

Figure 4.1

Figure 4.2

Figure 4.3

The basic components of Delta wind turbine are:

4.2.0 Wind Collection Housing:

4.2.1 The Wind collection housing is essentially a rectangular duct, which serves the purpose of flow concentrators at the inlet of the rotors and diffusers at the rear end. An aerodynamically designed central section (see figure 4.2) bifurcates the rectangular duct providing two independent guided paths for the wind stream towards the respective rotors. The inlet duct for one rotor is shown in figure 4.4.The guided paths reduce the turbulence around the rotors resulting in extraction of higher energy from the wind. Since the wind turbine is mounted close to the ground level where the level of turbulence in the wind is higher, the reduction in turbulence by wind collection housing is likely to have a marked effect on the power extraction capabilities of the rotors. Further the reducing cross sectional area of the duct with the depth increases the wind speed, and hence the kinetic energy available in the wind for extraction at entry to the rotors is higher than that in free flowing wind stream. The ratio of cross sectional area of throat (i.e. inlet of rotor) to the inlet of the duct is around three. The ceiling

Figure 4.4

and the side flaps of the housing are extended in front (see figures 4.2 and 4.3) to capture higher wind energy.

4.2.2 At the rear end, the diffuser provides a wind suction effect which aids in increasing the volumetric flow rate of wind through the rotors (see the increasing duct flow size at the rear end in figure 4.1).

4.3.0 Rotors:

4.3.1 The rotors are primarily drag based vertical axis type using certain amount of lift by virtue of aerodynamic airfoil blades. Each rotor comprises of three sub-rotors which are mounted over one another with a common vertical axis of rotation and fastened together to form a single assembly as shown in figure 4.5. Each sub-rotor houses twelve blades making a total of thirty-six blades per rotor, uniformly distributed over the entire periphery. Further the rotors are supported on top and bottom by tapered roller bearings. The blades are carved out of aluminum so as to keep the entire assembly light as well as durable. The rotor has high solidity ratio providing it with high starting torque. The machine is self-starting. The overall aspect ratio of rotor (= height / diameter) is around 1.95.

Figure 4.5

4.3.2 The two rotors are working in independent flow streams, presumably without any interference (This could not be verified in the field testing as one of the generators was not operating satisfactorily). Further the clearances along the rotor sides, top and bottom have been kept minimal to prevent bypassing of rotors by wind stream. At the same time these clearances are sufficient to avoid the revolving rotor touching the housing.

4.4.0 Generators:

4.4.1 Each rotor is directly coupled with a generator mounted on the top of the housing (visible in top portion of the figure 4.1). The generators are of variable frequency permanent magnet type, asynchronous in operation. Further each generator has twelve poles. The turbine prototype incorporates workshop made generators, whose rated power output and characteristic curves are not known. However since the aim of the thesis was to investigate the performance characteristics of wind turbine, it had no bearing on the results. The generator was calibrated at University workshop for determination of power available at the rotor shaft as explained in the next chapter.

4.5.0 Yawing Mechanism:

4.5.1 As stated earlier, the machine is required to be aligned to the wind direction so that the wind collection housing always faces upwind. The turbine uses a simple automatic yawing mechanism for this purpose. The required alignment is achieved by using unbalanced forces due to wind thrust on the side walls of the housing. The entire assembly is allowed to rotate freely around a vertical steel shaft (see figure 4.6) using two tapered roller bearings – one

Figure 4.6

on the top and the other at the bottom The vertical shaft is positioned in such a way that nearly two thirds of the housing projects on one side and the remaining one third hangs on the other side. In order to balance the weight, the counterweights have been used as visible at the bottom in the front view of the turbine in figure 4.2. The entire weight of the structure rests on the bottom tapered roller bearing which is very strong and robust in operation.

4.5.2 For understanding the principle of operation of yawing mechanism, consider a horizontal rectangular cross section bar AB which is allowed to rotate freely about a vertical axis passing through its hinge point O as shown in figure 4.7. The arm length OA is nearly double OB. Initially let us assume that the bar is aligned to the wind direction, shown by dotted lines in the figure 4.7. After some time, the wind changes the direction by about 90^0 as shown by solid lines in figure 4.7.

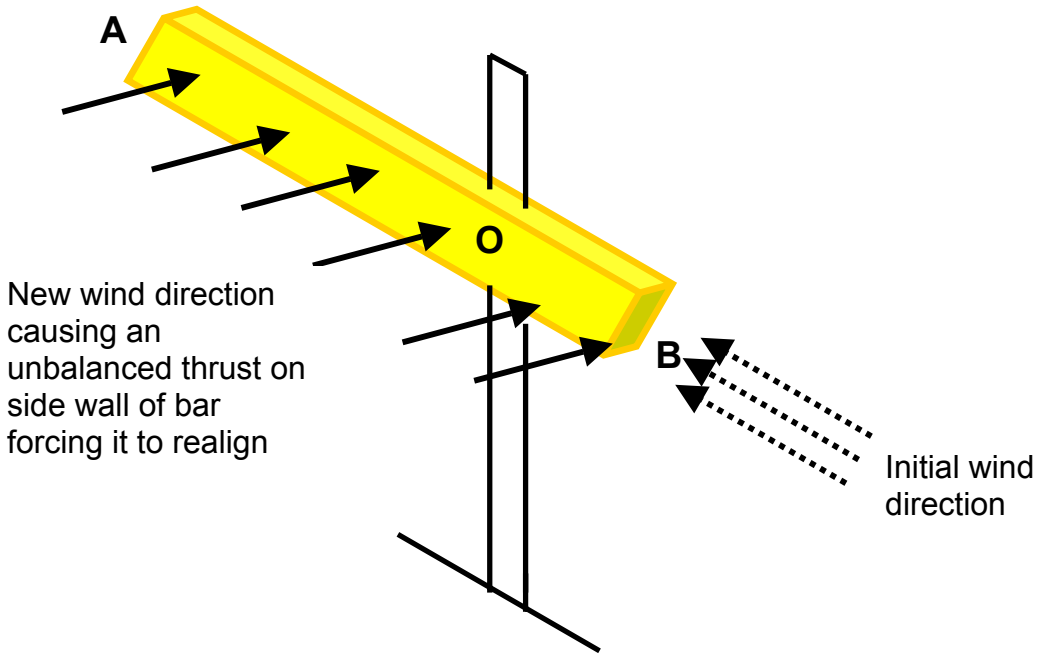

Figure 4.7

4.5.3 If P is the wind pressure and A is the surface area of the side wall, the portion OA experiences force 2PA/3 whereas the portion OB receives a thrust PA/3 due to wind pressure acting against the side wall. The unbalanced forces cause the bar to rotate until the net force on the side wall due to wind pressure becomes nil. This will happen only when the bar realigns itself parallel to the new wind direction as shown in figure 4.8. Therefore, the bar will always be turned into the wind with B facing the upwind.

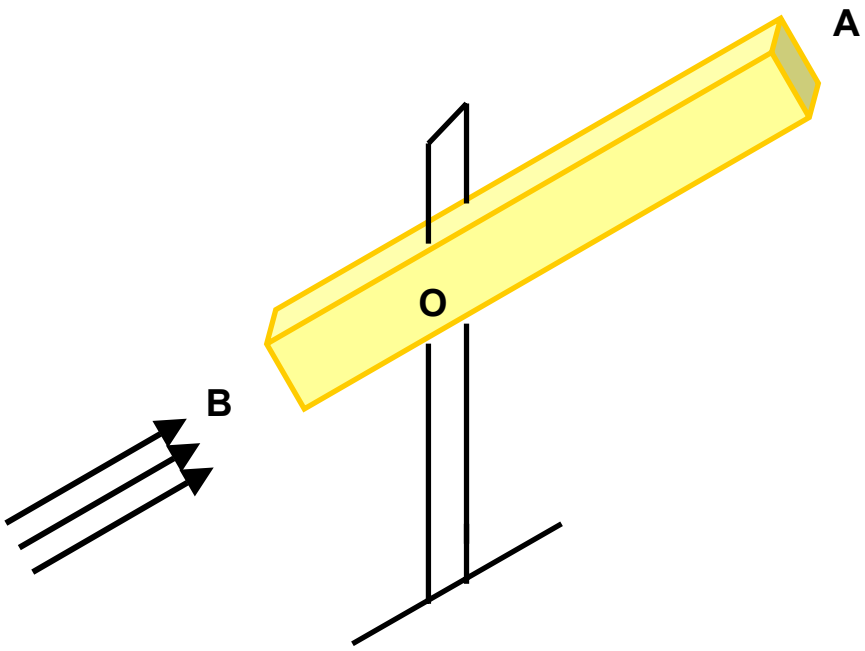

Figure 4.8

4.6.0 Other Features:

4.6.1 Since the rotors are entirely housed inside the duct, the revolving parts are not likely to come in physical contact. Hence the machine may be considered safe into operation. However, the wind collection housing requires a defined circular footprint of around 10 meters diameter for swinging around following the wind direction.

4.6.2 The machine is almost noiseless in operation because of absence of gear trains. Even two persons standing within a distance of 5 meters from the turbine can easily talk and hear each other.

4.6.3 The overall height of the machine from the ground is around 2.5 meters and is therefore likely to cause less visual impact on the surroundings when compared with its HAWT counterparts which are required to be mounted at considerable hub heights.

4.6.4 The engineering drawing for the turbine (incorporating top, front and the sectional views from the side) is shown in figure 4.9.

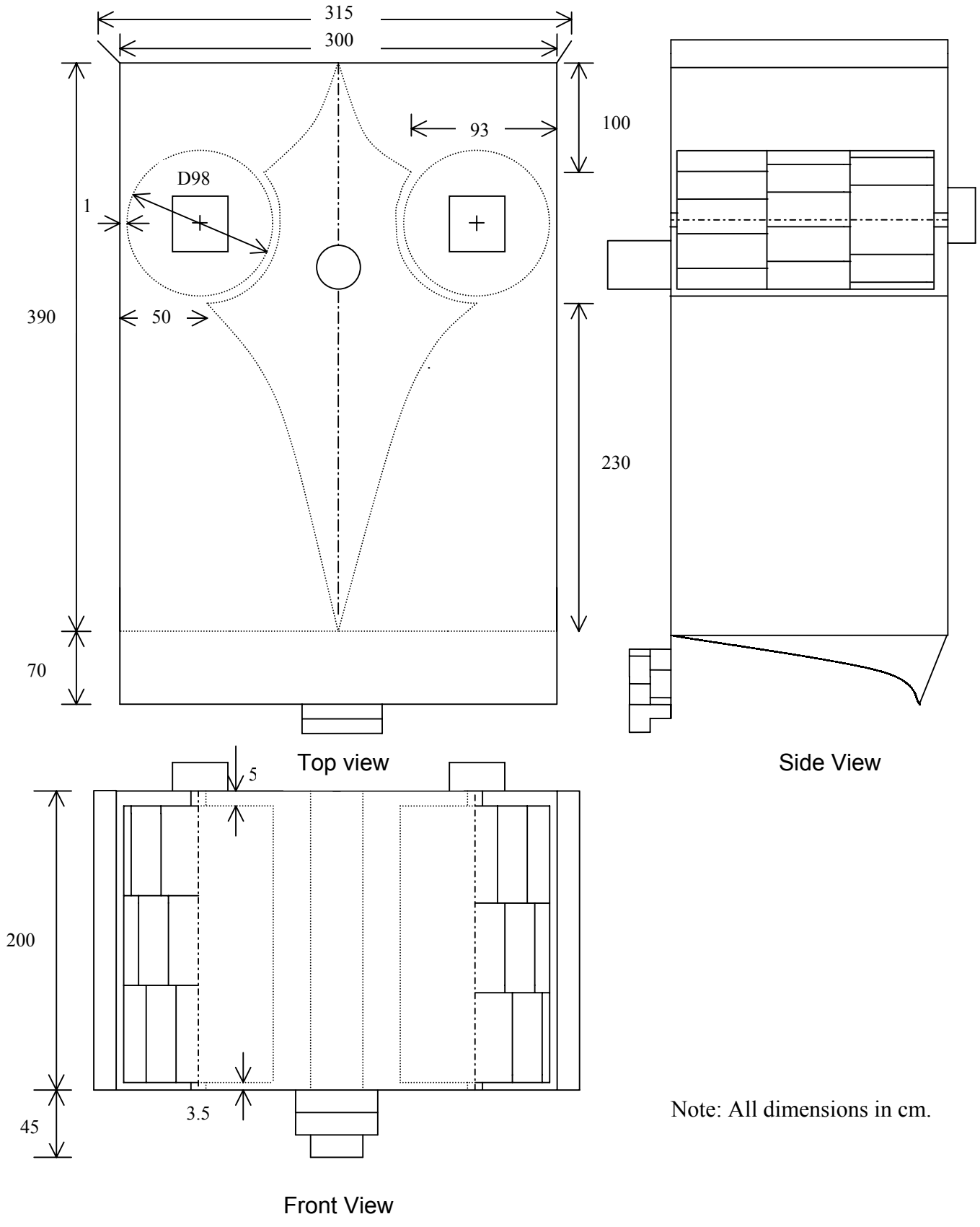
315
300
93
100
D98
1
390
50
230
70
Top view
Side View
5
200
3.5
45
Front View
Note: All dimensions in cm.

Figure 4.9

Chapter 5: Instrumentation:

General

This chapter is focussed on the various instruments used for field testing of the novel VAWT. At present, there is no common Standard or Procedure for power performance measurements of wind turbines. A number of Standards such as International Standard IEC 61400-12 released by technical committee (TC 88) of International Electro-chemical Commission in March 1998, draft Standard for power performance measurements from MEASNET (an European agency with around 36 member institutions), National Standards of Dutch, Denmark and Germany, etc. are in vogue. However a common feature among all these Standards is that these require all instruments, which are deployed for power measurements of wind turbines, to be calibrated/verified in the lab before hand. Accordingly all instruments used for field testing were calibrated and verified for accuracy of measurements. The test procedures and the test reports are included in this chapter along with brief discussions on test results.

5.1.0 Wind Anemometer:

A wind anemometer is a device used for measuring wind speed. In the expression for power extraction by rotor from the wind (3-3), the free flowing wind speed appears as the cube and is, therefore, one of the most important parameters. A small error in its measurement can introduce a relatively big error in the results. The selection of a proper anemometer was, therefore, crucial.

5.1.1 Selection of Anemometer:

5.1.1.1 Anemometers come in different designs and make use of various techniques including hot-wire, laser doppler, ultrasonic, etc., the most popular being the

cup-anemometer. The following table describes, in brief, the various kinds of anemometers currently available on the market.

Type	Description
Cup Anemo-meter	The instrument consists of a cup assembly (usually three or four cups) connected to a vertical shaft for rotation. It is in fact the most direct application of a Savonius drag based wind rotor. As the wind blows, the thrust due to wind pressure is converted into rotational torque. Rotations per minute are electronically registered by a transducer, integrated with the instrument, which converts the rotational movement into electronic signals. These electronic signals are then interpreted in terms of wind speed. A cup anemometer is shown in figure 5.1 on next page.
Fixed – Axis Propeller	It uses a propeller having a fixed axis in one direction to measure wind speed in that direction. Speed of rotation of propeller is directly proportional to wind speed in the direction of the fixed axis. The magnitude of this component is proportional to the cosine of the angle between the wind velocity and the fixed axis. If wind turbulence data is required for a site, propeller anemometers are used for obtaining three dimensional wind speed data.
Propeller Vane	This instrument makes use of a propeller, which is directed into the wind direction by a tail or vane. Speed of rotation is proportional to wind speed. The vane often has a transducer attached to it for measuring direction. It, therefore, measures wind speed as well as direction.
Acoustic Doppler	The device uses the Doppler shift of sound scattered by atmospheric inconsistencies from an acoustic beam projected into the atmosphere. It measures mean wind velocity in strata approx. 50 m thick from 60 m to 600 m. It is generally used for air-pollution studies for which long period wind data above tower levels are required.
Deflection	The device uses a simple hinged flapper to indicate wind speed against a set scale. It is suitable only for airflow applications or in low-speed winds.

Laser Doppler	This instrument uses the Doppler shift of laser light scattered from particles in air to measure the velocity of the particles. The size, concentration and refractive index of the particles have a direct bearing on the quality of the measurement. The instrument finds wide application in dusty weather conditions where the abrasive dust particles contained in high-speed winds can reduce the life of ordinary cup anemometers.
Hot wire	The anemometer measures the wind speed by interpreting the rate of cooling (i.e. temperature drop) of a hot wire of known resistance, kept in a wind stream, through which a measured current is passed. Alternately, the current required for maintaining the wire at the same temperature is calibrated for wind speed.
Ultra-sonic	This instrument measures wind velocity components by transmitting and receiving acoustic signals along fixed paths in one, two or three directions. Since there are no moving parts to come into dynamic equilibrium with the flow, the sonic anemometer reacts rapidly to wind velocity fluctuations but these are expensive. The figure 5.2 shows an ultra-sonic wind anemometer

Figure 5.1

Figure 5.2

5.1.1.2 Out of the various anemometers described above, the cup anemometer was considered most suitable as the conditions prevailing at the testing site did not require use of any specific type of anemometer such as laser doppler based anemometer, which is generally used for dusty conditions or icy weather. The ultra-sonic and hot-wire anemometers were cost prohibitive. The relative marginal gain in accuracy in wind speed measurements over the cup anemometer, which tends to slightly over-estimate the decelerating wind speed usually known as "over-run error", did not justify the difference in cost (nearly 4 to 8 times). Further the propeller anemometer, which is primarily used for three-dimensional wind speed measurement for obtaining the wind turbulence data, was not considered feasible. Finally, the low power cup anemometer (Model A100L2, VICTOR INSTUMENTS, UK Make), which is considered to be one of the most rugged for outdoor applications was decided upon. It measures the wind speed from all directions in the horizontal plane and to ±20° vertically with an approximate cosine law.

5.1.1.3 The anemometer (see figure 5.1) comprises of a 3-cup rotor fastened to a steel spindle by a unique gravity sensing arrangement in which the rotor gets locked up with the spindle on pressing from the top. To unlock, the anemometer is required to be inverted and rotor hub is pressed upwards. The 3-cup rotor consists of three conical cups of weather-resisting plastics attached to an anodised aluminium alloy hub/arms assembly. The stainless steel spindle turns a slotted disc, which interrupts a light beam to measure rotation speed. This arrangement results in a low threshold and allows highly accurate wind speed measurements. The internal electronic modules convert the light beam signal into the required analogue or pulse output. The anemometer is mounted on a mast by fixing a screw at the base.

5.1.1.4 The anemometer has a speed measurement range of 0 to 150 knots. It provides both analogue (0 to 2.5 V) and pulse outputs. The threshold starting and

stopping speeds are 0.4 knots and 0.2 knots respectively. The distance constant for the anemometer is 2.3 m ±10%. (Distance constant is the length of the column of air that must pass the head for the anemometer to respond to 63.2% of the step change. The distance constant depends only upon air density and is independent of the wind speed. It is a measure of the anemometer sensitivity).

5.1.2 Anemometer Calibration:

5.1.2.1 It was decided to use analogue output of the anemometer for measuring wind speed for two reasons. Firstly, the data logger (described later in this chapter at paragraph 5.4.0) could interpret DC voltage signals up to ± 2.097 V and secondly the manufacturer of the anemometer provided a combined output curve for ratemeter and rotor non-linearity.

Nominal output voltage range : 0 to 2500 mV
Nominal wind speed range : 0 to 150 knots

Nominal analogue output calibration = Z = 2500/150 = 16.67 mV per knot

Nominal frequency calibration = 10 Hz per knot
= 10 x 1.9426 Hz per m/s = 19.426 Hz per m/s
(*1 m/s = 1.9426 knots. Units of knots used are UK knots based on nautical mile of 6080 ft/hr. The international knot is based on 1.852 Km, approx. 0.06% less*)

Number of pulses per rotor revolution = 25
Theoretical corresponding rotor calibration constant, R_{th} = 19.426 x 60/ 25
= 46.62 rpm per m/s

Further each rotor is individually calibrated by manufacturer in a wind tunnel at one air speed (9 m/s) by comparing with a 'reference' rotor which is traceable to UK national standards.

Actual Rotor calibration constant, R_{act} = 46.4 rpm per m/s

The correction curve for analogue output for combined effects of ratemeter and R30 rotor non-linearity is shown in figure 5.3.

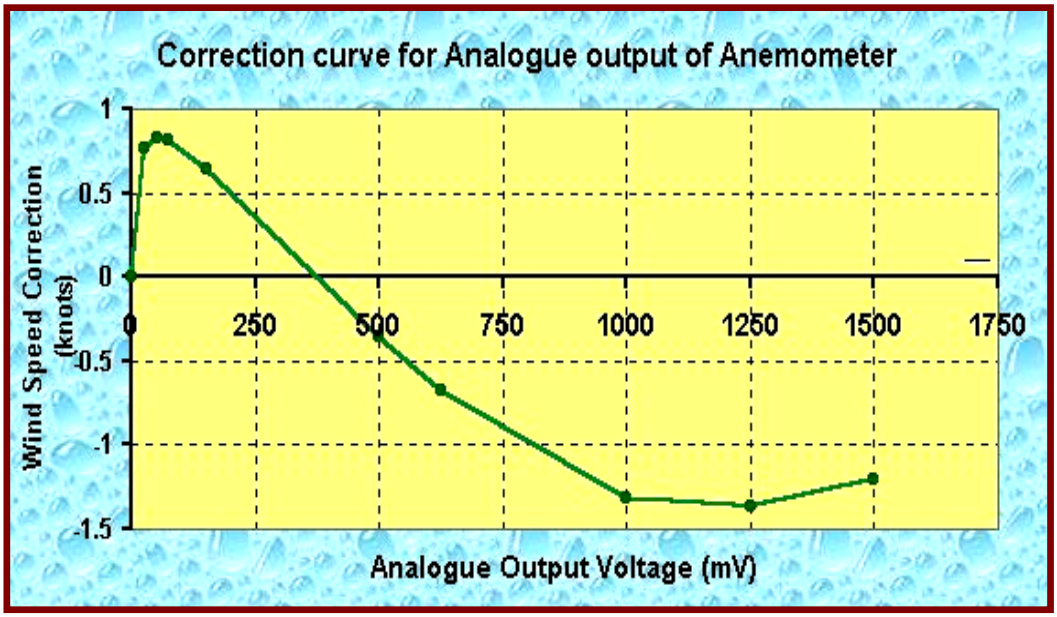

Figure 5.3

Let E mV be the analogue output corresponding to a wind speed V knots

V_{corr} be the correction in wind speed obtained from the correction curve corresponding to the analogue output voltage E.

Z be nominal analogue output calibration

The actual wind speed V is given by the following expression:

$$V = (E / Z + V_{corr}) \times R_{act} / R_{th}$$

$$V = (E / 16.67 + V_{corr}) \times 46.4 / 46.62$$

$$V = (0.06 \times E + V_{corr}) \times 0.99528 \quad (5\text{-}1)$$

The relation between V_{corr} and E was determined for different linear parts of the correction curve shown in figure 5.3 by using linear regression technique in MSEXCEL.

For example up to 25 mV of analogue output, E and V_{corr} are related by the following expression:

$$V_{corr} = .0304 \times E$$

Substituting V_{corr} from the above expression in (5-1), we get

$$V = (0.06 \times E + .0304 \times E) \times 0.99528$$
$$E = 11.1144\ V$$

For V= 2 knots, the analogue output voltage, E, works out to be 22.229 mV. Likewise, the analogue output voltages were determined for various wind speeds ranging from 0 to 64 knots. A linearisation table (see Table 5.1) was generated for interpreting wind speed from the measured analogue voltage output of the anemometer. The linearisation table was registered in the data logger and a new sensor (Sensor Code: WS) was added in the sensor list of the data logger for recording and storage of wind speed.

Wind Speed (knots)	**Analogue Voltage Output Signal (mV)**	**Wind Speed (knots)**	**Analogue Voltage Output Signal (mV)**
0	0	34	578.589
2	22.229	36	613.535
4	53.009	38	648.174
6	87.408	40	682.661
8	122.235	42	717.149
10	157.137	44	751.637
12	192.305	46	786.125
14	227.473	48	820.612
16	262.640	50	855.100
18	297.808	52	889.588
20	332.976	54	924.075
22	368.143	56	958.563
24	403.311	58	993.051
26	438.479	60	1026.831
28	473.646	62	1060.434
30	508.699	64	1094.038
32	543.644		

Table 5.1

5.1.3 Verification:

5.1.3.1 The wind anemometer was verified for accuracy of measurement of wind speed over a range of 0 to 56 knots by an experimental set up in low wind speed tunnel.

5.1.3.2 Test Set up:

S.No.	Equipment Description	Quantity
1.	Low speed (0-45 m/s) wind tunnel	1 set
2.	Wind anemometer A100L2 with R30 rotor	1 No.
3.	Mast	1 No.
4.	Data logger with power supply unit (12V)	1 No.
5.	Pilot static tube connected to an inclined manometer	1 set
6.	Mercury Barometer	1 No.
7.	Thermometer	1 No.
8.	Spirit level	1 No.
9.	Connecting wires	1 set
10.	Computer with data logger software	1 set

1. Erect the mast at the centre of the wind tunnel and check that the plate, welded on its top on which the anemometer is to be fixed, is perfectly horizontal by a spirit level.
2. Press the rotor hub gently on top of the anemometer spindle and check for engagement by trying to pull it out gently. The rotor, if positively locked with anemometer, would not come out.
3. Mount the anemometer on the top of the mast by fixing the fastening screw at the bottom of the anemometer.

4. Prepare a configuration file for the delta logger (For configuration files, refer delta logger at paragraph 5.4.3 in this chapter) with the new sensor (WS) for recording wind speed at channel 2 with a sampling interval of 1 second.
5. Connect the anemometer wires to channel 2 as per the recommendations of manufacturer for analogue output. The channel 2 is connected to LAC1 input card in the logger.
6. Tie up the anemometer cable with tape to mast to prevent it from vibrating in the airflow during testing.
7. Level the inclined manometer by using levelling screws.
8. Adjust the level of the inclined manometer liquid so that it reads zero with wind tunnel fan off.
9. Remove any loose material, tools, etc. from the wind tunnel.

The final test set up is shown in figure 5.4.

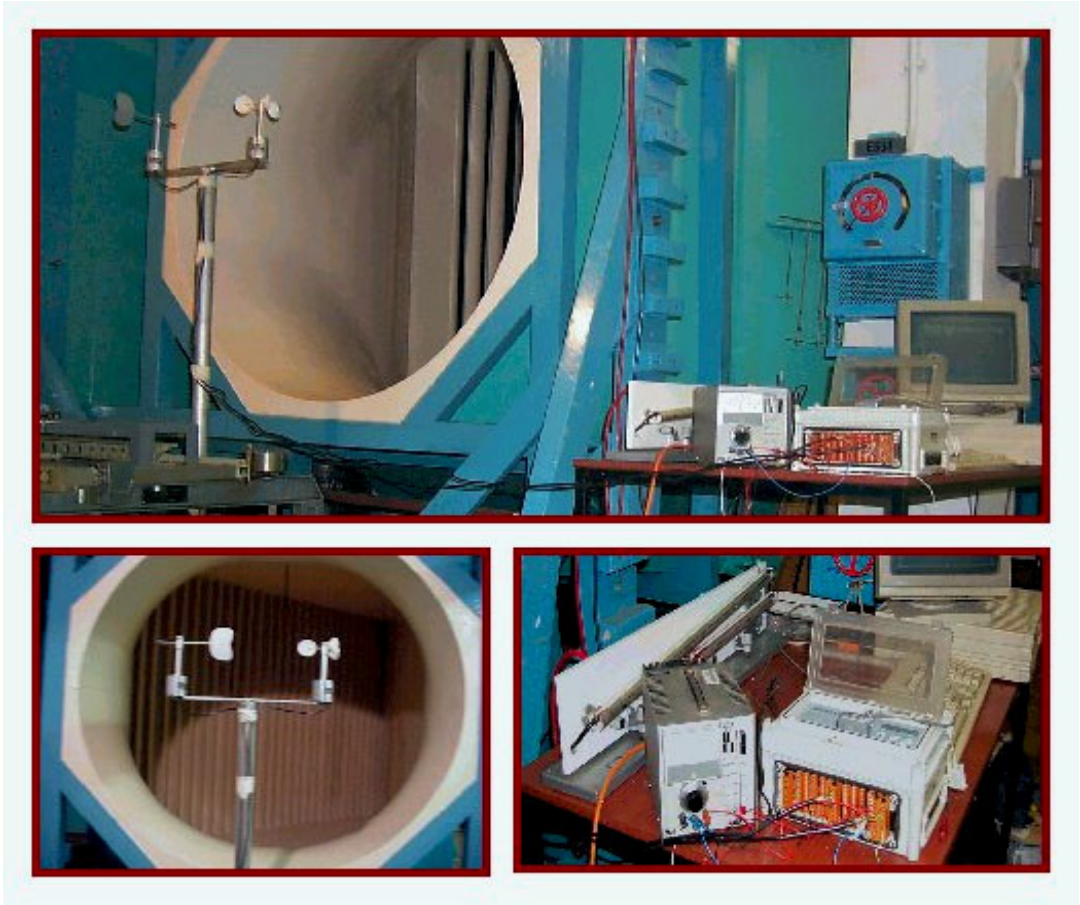

Figure 5.4

5.1.3.3 Test Procedure:

1. Start-up the wind tunnel motor.
2. Set certain wind speed and allow it to stabilise for some time (say 3 minutes).
3. Record the level of liquid in inclined manometer.
4. Record the wind speed as interpreted by data logger.
5. Repeat steps 2 to 4 over the entire scale of manometer with the rising wind speed.
6. Repeat step 5 for the declining wind speed and then random wind speeds.
7. Record the temperature from thermometer with its bulb exposed to airflow in wind tunnel.
8. Record the atmospheric pressure from mercury barometer.

5.1.3.4 Theory:

The wind speed is measured by the pilot-static tube located in the airflow tunnel. It measures the airflow static pressure, which is interpreted from liquid level in the inclined manometer (Scale: 1mm = 1 N/m^2). The wind speed and the airflow static pressure (P_{st}) are related by the expression:

$$0.5\ \rho\ V_{act}^{\ 2} = P_{st}$$

$$V_{act} = (2 \times P_{st} / \rho)^{0.5}$$

Where ρ is the air density given by expression (3-2) reproduced hereunder for ready reference.

$$\rho = P / R\ T$$

If V is the wind speed interpreted by the data logger, then percentage error is given by:

$$\% \text{ error} = (V_{act} - V) \times 100 / V_{act}$$

5.1.3.5 Test Results and Discussions:

The test results for verification of wind anemometer calibration are enclosed at Appendix-1. The figure 5.5 shows a graph between the percentage error and the actual wind speed recorded by pilot tube (V_{act}).

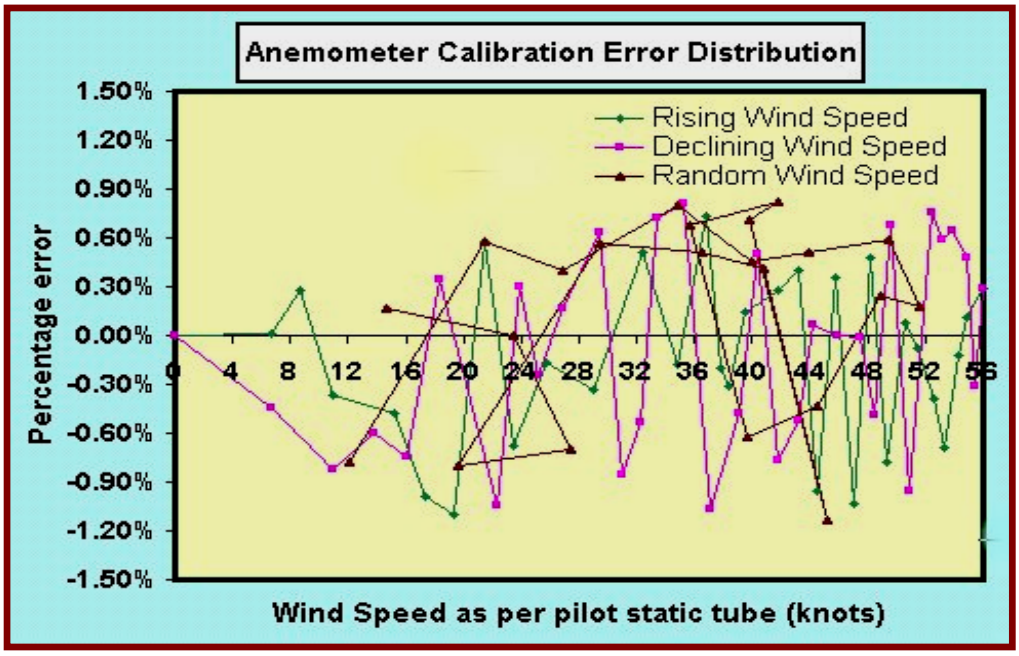

Figure 5.5

From the graph it can be seen that there was no apparent trend in error i.e. either increasing/decreasing with rising/declining wind speed or steady over a range of speeds. The errors were varying at random between –1.13 % and +0.82 %. Sometimes for the same wind speed as measured from static pilot tube (e.g. 23.41 knots highlighted in Appendix-1), there was no error in one reading while the other reading indicated an error of -0.68%. The randomly distributed nature of small errors suggested that these might be due to the fact that while the wind anemometer responded to small variations in the airflow in the wind tunnel, these could not be recorded from pilot tube at the same time. There was no scope for any improvement in calibration of the anemometer. It was, therefore,

concluded that the anemometer calibration for wind speed measurement and the corresponding linearisation table registered in the logger were reasonably accurate.

5.2.0 Wind Vane:

A wind vane is used for measuring wind direction. It consists of a fin attached to a horizontal rod with a counterweight on the other side of the rod. The rod is mounted on a vertical spindle at the point of balance. The wind vane is able to rotate freely around in a horizontal plane. As the wind blows from one direction, the wind vane adjusts itself to point in the wind direction (Wind direction is defined as the direction, which the wind is blowing from.). The position of the pointer is interpreted by a transducer, which produces an electrical signal relative to a reference position. Normally a potentiometer is used as the transducer.

5.2.1 Selection of Wind Vane:

5.2.1.1 The wind vanes can be broadly divided into two categories:

a) Fixed-referencing wind vane in which wind direction is measured relative to the body of the instrument which is required to be aligned with one particular direction (usually north) as the reference direction on installation.
b) Self-referencing wind vane, which uses a powerful compass magnet to align the transducer so that the output is referenced to magnetic north. A vane turns the body of the instrument. Power and signal wires are connected by means of slip-rings.

5.2.1.2 The fixed-reference wire-wound potentiometer wind vane (Model W200P, VICTOR INSTUMENTS, U.K. Make shown in figure 5.6) was selected for measuring wind direction. Like the wind anemometer, the wind vane has a

fixing screw at the base for mounting it on a mast and a gravity sensing fastening arrangement for securing the vane arm assembly on the potentiometer spindle. A notch on the spindle ensures that the vane arm assembly is always mounted in one particular angular position on the spindle. The stainless steel spindle runs in a hard plastic upper bearing and a lower thrust ball bearing and is connected to a potentiometer wiper.

Figure 5.6

The potentiometer output is proportional to the resistance element covered by the wiper of the potentiometer, with a small section of dead band of 3.5 degrees near the ends due to the small gap required between terminals (see figure 5.7).

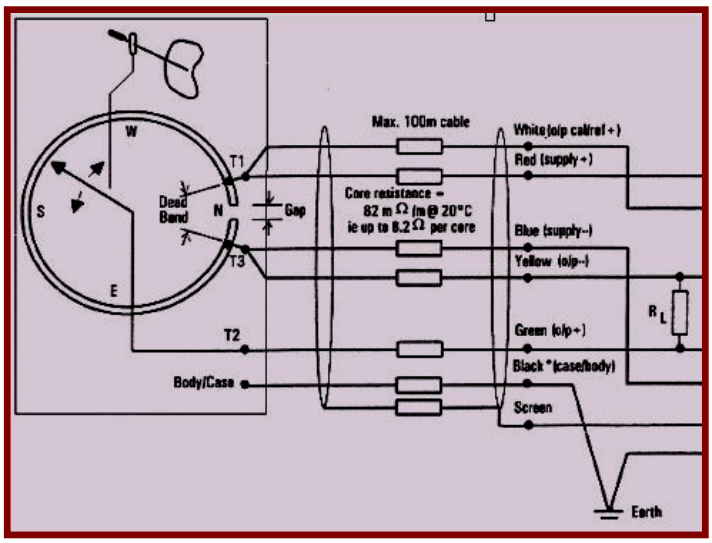

Figure 5.7

The gap is filled with an insulator to provide smooth transition from one terminal to the other. As the wind blows from North through East, South, West around to North, the wiper moves along the track from terminal T3 to T1. The threshold starting speed for the wind vane to respond is 1.2 knots with the vane aligned at 45 degrees to the flow. The distance constant is 2.3 m ±10%.

5.2.2 Wind Vane Calibration:

A fixed measured voltage (V_{ref}) is applied across the terminals T1 and T3 of the potentiometer integrated with the wind vane and the output voltage is measured. The output voltage expressed as percentage over the supply/reference voltage (V_{ref}) is interpreted as the wind direction. The graph of wind direction versus the output as percentage of reference voltage is shown in figure 5.8.

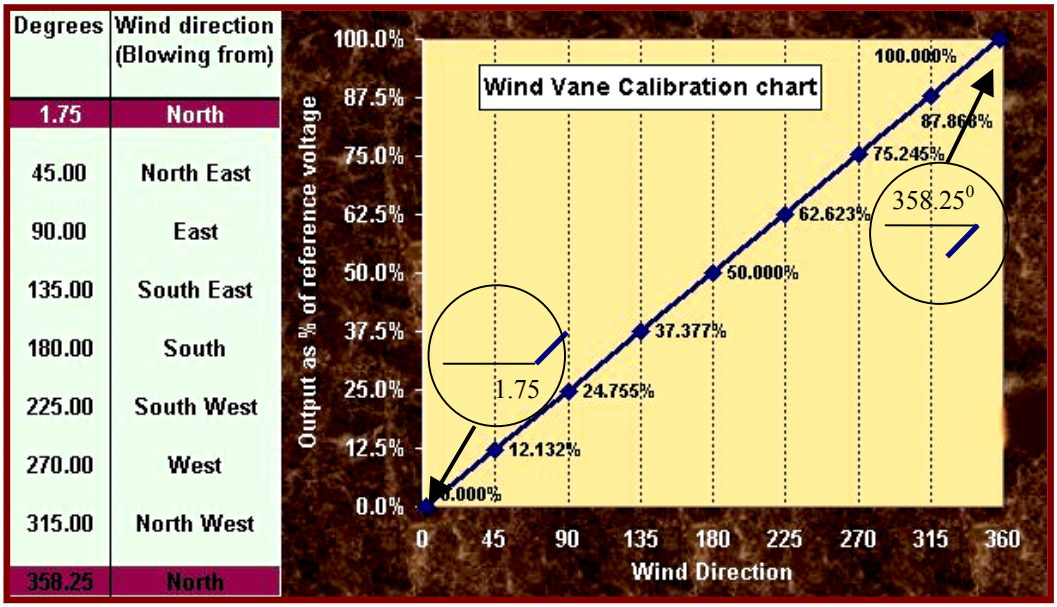

Figure 5.8

From the graph it is clear that the 1.75 degrees and 358.25 degrees are interpreted as north. Ideally these should have been 0 degree and 360 degrees respectively. But a gap is required to be kept between the terminals T1 and T3 to

make them as positive and negative terminals as explained previously. In this potentiometer, an electrical gap of 3.5 degrees is maintained.

If V_{out} is the voltage output of the potentiometer, the wind direction in degrees from north (reference direction) is given by

$$\theta = V_{out} \times (360 - 3.5) / V_{ref} + (3.5/2)$$
$$= V_{out} \times 356.5 / V_{ref} + 1.75 \quad (5\text{-}2)$$

In the delta logger, the LFW1 card is used for recording the potentiometer output. The logger was programmed to supply a measured voltage (V_{ref} = 521 mV) across the potentiometer terminals at the time of taking reading and the output voltage (V_{out}) was interpreted by logger as the wind direction.

For this purpose, the voltage signal is referred to as the Base unit and the interpreted unit in which the channel reading is to be stored is called as the Engineering Unit. The relation between the Engineering unit and the Base unit is graphically shown in figure 5.9. Mathematically it is expressed as follows:

Value in Engineering unit = Value in Base unit/Conversion factor + Offset

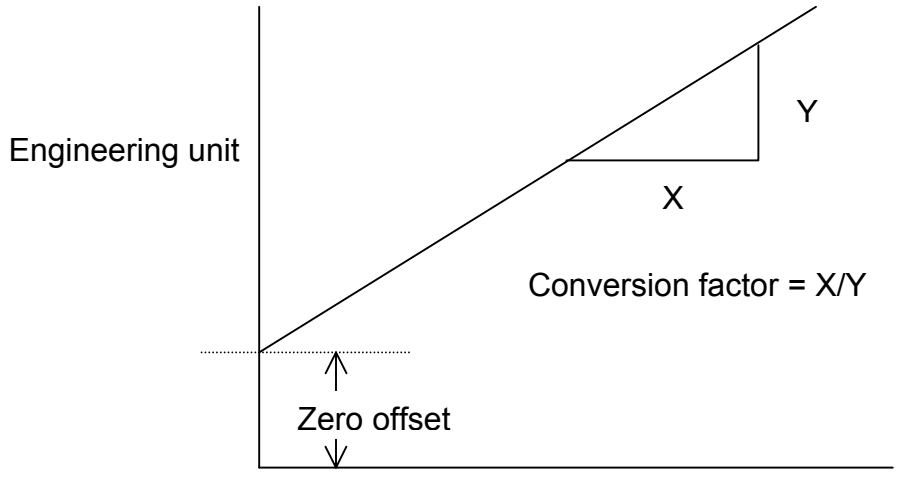

Figure 5.9

Comparing the above equation with equation (5-2), the conversion factor and offsets for the wind direction are

Conversion factor = V_{ref} / 356.5 = 521/356.5 = 1.4614 mV/degree
Offset =1.75 degrees

A new sensor (Sensor code: WD2) for wind direction was added in the sensor list of the data logger with a conversion factor of 1.461 mV/degree and offset of 1.75 degrees.

5.2.3 Verification:

5.2.3.1 The wind vane was verified for accuracy of measurement of wind direction over a range of 1.75 degree to 358.25 degrees as described in the succeeding paragraphs.

5.2.3.2 Test Set up:

S.No.	Equipment Description	Quantity
1.	Wind vane W200P	1 No.
2.	Card-board piece (25cm x 25 cm)	1 No.
3.	Mast	1 No.
4.	Magnetic compass	1 No.
5.	Data logger with power supply unit (12V)	1 No.
6.	Spirit level	1 No.
7.	Connecting wires	1 set
8.	Computer with data logger software	1 set

1. Draw a circle on a piece of paper with its radius equal to the distance of the outer edge of tail fin from the centre of the hub so that the circle matches with the footprint of vane arm assembly.
2. Divide the circle into various sectors (say 20) subtending different angles at the centre.
3. Mark one chord as zero and North (N) and draw two more chords at angles of 1.75 degrees on either side of this zero sector chord. Mark all other chords in terms of angular rotation from the zero marked chord.
4. Paste the paper on the card-board and make a hole through the centre of the circle.
5. Mount the potentiometer on a mast with the cardboard sand-witched in between and north mark of potentiometer aligned with the chord marked north on the cardboard. Also align the north direction marked on the potentiometer of the vane with the north direction pointed by magnetic compass. (While looking at the North marked on the potentiometer, the user back should face the north pointed by compass) and tighten the fixing screw at the base of the wind vane.
6. Modify the configuration file prepared for anemometer by using another terminal (number 31 connected to LFW1 card in logger) for wind direction (Sensor Code: WD2) and register it in logger.
7. Connect the potentiometer wires as per manufacturer supplied wiring diagram to logger terminal no. 31.

5.2.3.3 Test Procedure:

1. Align the tail fin with a chord and record the reading from the cardboard.
2. Record the reading as per logger.
3. Repeat steps 1 and 2 for various sectors on the card-board.

5.2.3.4 Test Results and Discussions:

The test results are enclosed at Appendix- 2. From the results, it can be seen that the error is varying from –1.71% to 2.29%. The figure 5.10 shows a graph between the percentage error and the angular rotation (in degrees) from reference direction.

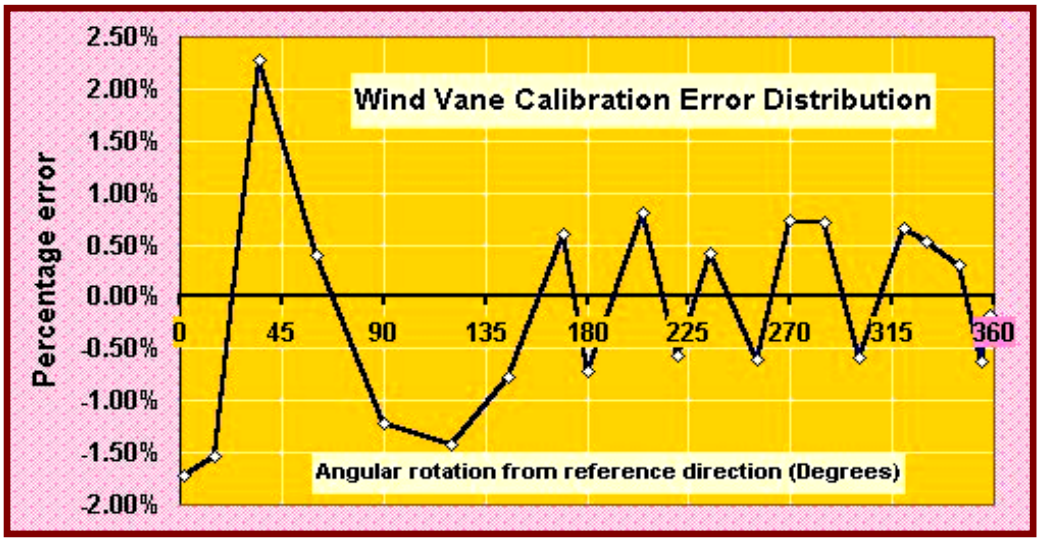

Figure 5.10

From the graph it emerges that the errors were randomly distributed without showing any visible trend based on which the instrument could have been re-calibrated. These small errors might be due to parallax in aligning the tail fin with the chords on the cardboard. The results were, however, within reasonable limits of acceptability. Further, it was verified that the logger was recording readings over the entire range of 0^0 to 360^0 for one complete rotation of vane.

5.3.0 Thermocouple:

Thermocouples are used for measuring temperature. They basically comprise of junctions of two dissimilar metals such as copper and constantan. If the two junctions are kept at different temperatures, a potential difference is developed between them. This potential difference is proportional to the temperature

difference between the two junctions for a pair of metals used. This forms the principle of operation of all thermocouples. A K type thermocouple was used for measuring the free wind stream temperature in degrees C.

5.3.1 Thermocouple Calibration:

5.3.1.1 The hot junction of the thermocouple is exposed to the body/surface whose temperature is to be measured while the cold junction is maintained at a reference temperature. In order to measure the absolute temperature, the potential difference developed between the hot and cold junction is interpreted for the temperature difference between the two junctions and then the cold junction temperature is added to it. In the Delta-T logger used in the test set up, the logger's terminal panel is designed to be isothermal and it has a thermistor mounted on it to measure its temperature. The thermistor can be optionally switched to channel 1 to provide a cold junction temperature for use in conjunction with a thermocouple. Further the logger has resident linearisation tables for K type thermocouple for temperature measurements between -120^0 C and 200^0 C.

5.3.2 Verification:

5.3.2.1 The K type thermocouple was verified for measurement of temperature between 3^0 C and 100^0 C in lab as described in the following paragraphs:

5.3.2.2 Test Set up:

S.No.	Equipment Description	Quantity
1.	K-type thermocouple pair of wires	1m.
2.	Boiling cattle	1 No.
3.	Thermometer	1 No.

4.	Ice cubes	5-10 Nos.
5.	Thermos flask	1 No.
6.	Data logger with power supply unit (12V)	1 No.
7.	Connecting wires	1 set
8.	Computer with data logger software	1 set

1. Make a thermocouple hot junction from the pair of K type thermocouple wires.
2. Connect the other ends of thermocouple wires to terminal no.4, which is connected to input card LAC1 of the Delta-T logger.
3. Modify the configuration file prepared for verifying calibration of anemometer and wind vane to the extent that the terminal 1 records the cold junction temperature (Sensor Code TM1 readily available in sensor list) and terminal 4 measures the voltage signal from K type thermocouple (Sensor code TCK) with cold junction referred as terminal 1.
4. Register the modified configuration file in the logger.

5.3.2.3 Test Procedure:

1. Boil some water in the cattle and put it in the thermos flask.
2. Dip the thermometer bulb in the water.
3. Immerse the hot junction of the thermocouple wire in the water almost near the bulb of the thermocouple.
4. Record the temperature readings – one measured by the thermometer and the other interpreted by the logger on terminal 4 from the connected computer.
5. Repeat step 4 for different temperatures of hot water as it gradually cools down to room temperature.
6. Put some cold water in the thermos flask along with ice cubes.
7. Repeat steps 4 for different temperatures of cold water as it gradually comes to room temperature.

5.3.2.4 Test Results and Discussions:

The test results are enclosed in Apendix-3. A graph indicating the variation in thermocouple calibration error with temperature is shown in figure 5.11. From the results, it can be seen that the error in calibration was varying from –0.38 ^{0}C to +0.47 ^{0}C over the temperatures range of 3 ^{0}C to 100 ^{0}C. This was due to non-linearity in the variation of potential difference between thermocouple junctions with the temperature difference between them. Another source of error was the limitation of least count of the thermometer. While the thermometer could measure temperature up to first decimal place in degrees C, the thermocouple recorded temperature up to the second decimal place. This explanation holds good for accounting variations of only ±0.05 ^{0}C. However the results were found to be within acceptable limits of accuracy.

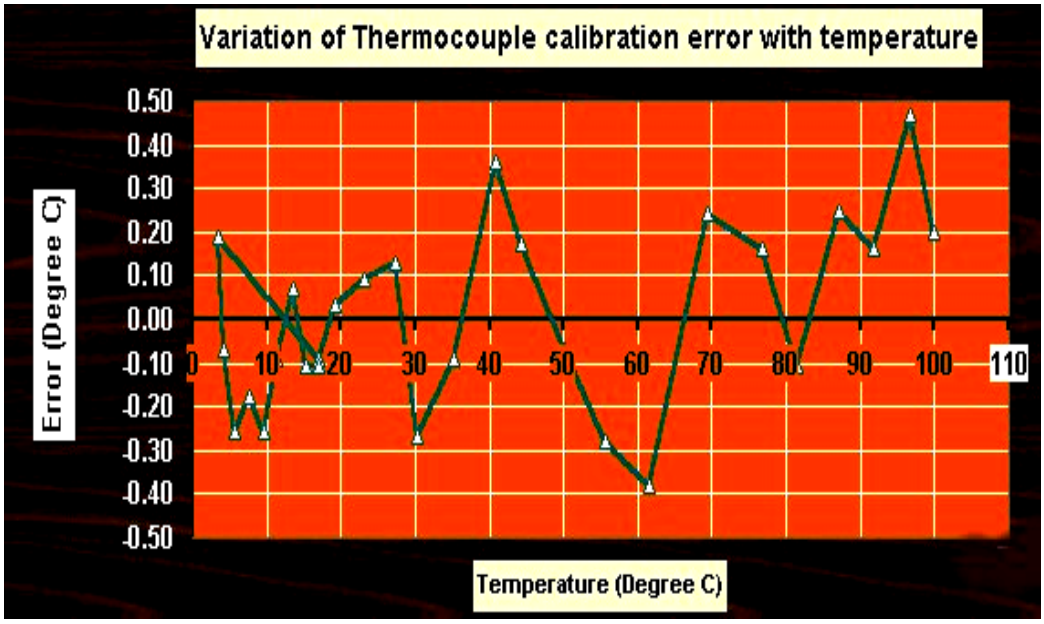

Figure 5.11

5.4.0 Data Logger:

A data logger is an electronic device, which can be programmed to read and record measurements such as temperature, voltage, current, on/off, open/closed events, etc. over a long time without requiring the physical presence of any personnel. Typically, data loggers are small battery-powered devices equipped with a microprocessor and data storage facility. Data loggers are used where manual data collection and recording are impractical due to the quantity of data, the location of instrumentation (remote areas) or where a real time alarm system is required. They enable more data to be recorded than manual data collection methods, giving engineers/scientists the ability to pick up trends that would otherwise be missed with infrequent manual reading. Systems range from simple standalone units to complex networks with remote access via phone line, cell phone, radio or the Internet.

Each data logger is provided with computer software which is first used to program the logger for what parameters are to be recorded (sensors), frequency of recording each parameter (sampling intervals), start time, finish time, etc. Once configured, the logger is then disconnected from the computer and deployed in the desired location. The logger records each measurement and stores it in memory along with the time and date. Periodically, the data are taken out from the logger's memory in the form of a predefined file format and is transferred to a computer. The software is used again to read out the data. The tabular data can be exported to a spreadsheet or databases for further processing and analysis.

5.4.1 Delta – T Logger:

5.4.1.1 A Delta-T Logger (see figure 5.12) was deployed for recording and storage of data for field testing of the novel VAWT. The Delta-T logger is modular in design and is powered by an external DC supply (12 V) or its own internal batteries. In case of power failure, it is backed up by 6 internal AA alkaline cells, which provide sufficient power for recording up to 500K readings, followed by a lithium cell to retain the readings stored in the memory for 2 months. Depending upon the internal input cards, the logger can record data from up to 62 sensors.

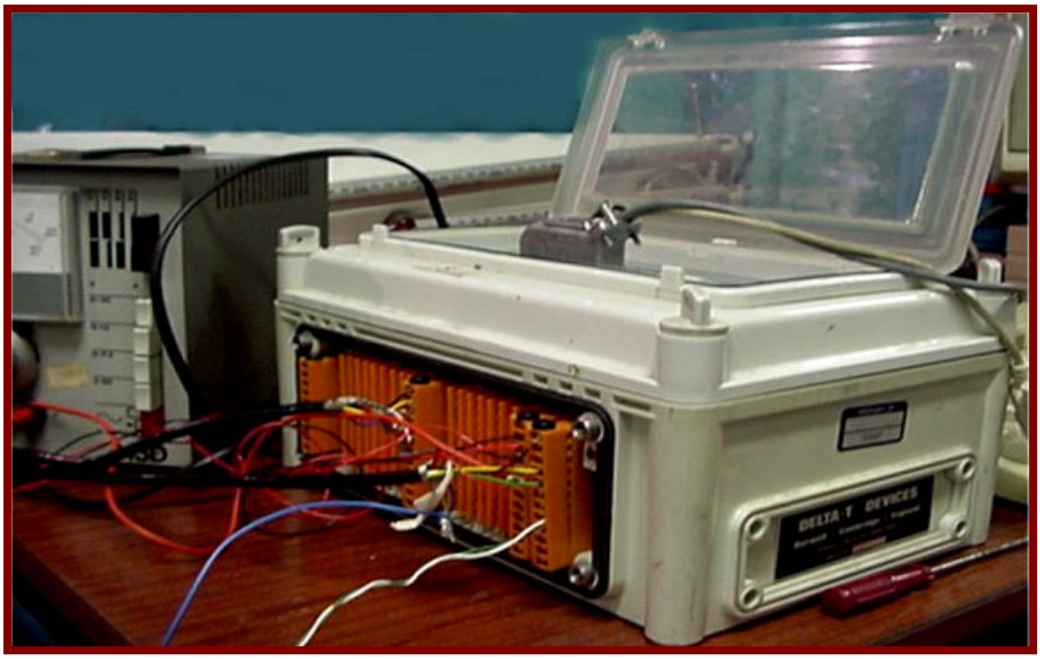

Figure 5.12

5.4.1.2 Input cards are available for analogue and pulse output sensors. The logger has the capability of recording both Timed data (recording of data at regular time intervals) as well as Event Triggered data. Besides, it has two relays for powering up sensors or simple control applications. The logger is fitted with a

cold junction thermistor for measuring its temperature as described earlier. The logger can be programmed to measure resistances, voltages (up to ± 2.097 V DC), current, counting, frequency or digital status (for event triggered data) or sensors providing these output signals. The software has a readily available list of 30 sensors. However more sensors can be added depending upon individual requirements as was done for wind speed and wind direction. The logger is provided with computer software called DELTA for its configuration and retrieval of stored data from its memory. The data file transferred from the logger can be used in MSEXCEL for further processing.

5.4.2 Data Compression:

5.4.2.1 The logger has the ability to record timed data at a sampling interval of 1s, 5s, 10s, 30s, 1m, 5m, 10m, 30m, 1h, 2h, 4h, 12h and 24h. It can also compress the recorded data into average, minimum or maximum value storing only the compressed data in its memory. However, only one operation can be specified out of the three in any given sensor. The permitted intervals for data compression are 5s, 10s, 30s, 1m, 5m, 10m, 30m, 1h, 2h, 4h, 12h and 24h.

5.4.3 Logging Configuration:

5.4.3.1 The logging configuration is a program file, which is set up by using the computer software and is then stored in the logger. It provides the following information for the logger to record and store the data:

a) The number of input channels in use;
b) Type of signal fed to each channel;
c) Interpretation of the signal in terms of 'real world' (engineering units) i.e. either by way of conversion factor and offset (e.g. wind direction) or through the use of linearisation table (e.g. wind speed, thermocouple);

d) Time duration of the excitation signal to be supplied to each sensor such as in case of wind vane, supply voltage to be applied across potentiometer terminals;
e) Sampling interval and data compression intervals, if in use;
f) Maximum, minimum or average function to be applied in case of data compression;
g) Action to be taken in case of malfunctioning of any input signal such as being noisy, outside limits or over-run and
h) Password for the stopping, retrieval and removal of data from loggers memory

In nutshell, the configuration file is the mindset of the logger for all its operations.

5.5.0 Full Wave Bridge Rectifier, Current Transducer and Filter Circuit:

The generators coupled with the novel VAWT rotors are of variable frequency permanent magnet type as described in paragraph 4.4.0 of chapter 4. Further the peak open circuit voltage across their terminals was stated to be around 90 V by DWT. However, the logger is capable of measuring ± 2.097 V DC voltage signals. A Full Wave Bridge Rectifier was used to convert AC output of the alternator into DC output. The device essentially comprises of 4 diodes (semiconductor PN junction diodes) connected in a forward biased bridge fashion (see figure 5.13). The AC current is fed from two diametrically opposite corners of the bridge (A and B in figure 5.13) and the unidirectional current is drawn from the other two diametrically opposite ends (C and D in figure 5.13).

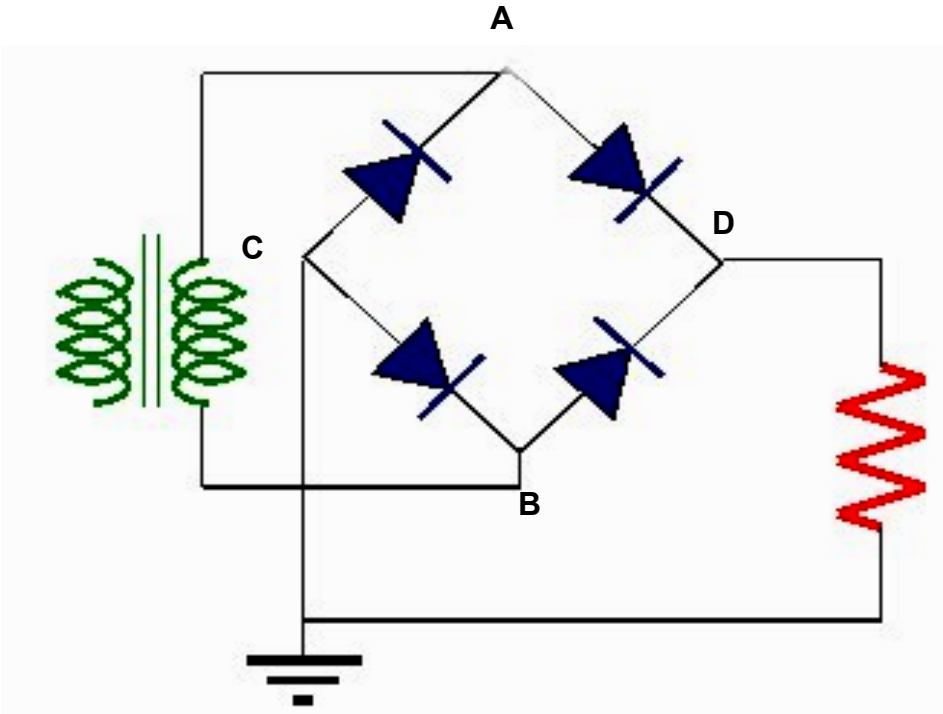

Figure 5.13

5.5.1 Principle of Operation of Full Wave Bridge Rectifier:

In order to understand the operation of full bridge wave rectifier, consider one cycle of AC input MNOPQ shown by the red line in figure 5.14.

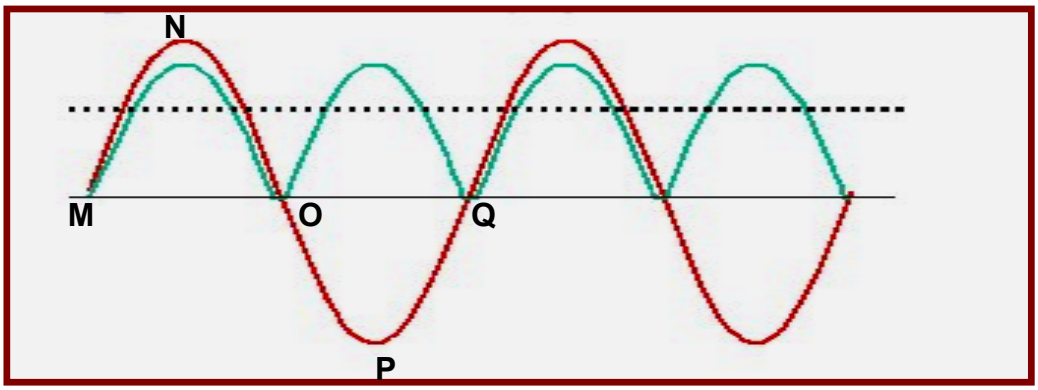

Figure 5.14

In the positive half cycle MNO, the top end of the secondary (see figure 5.15 (i)) becomes positive and hence red diodes get forward biased, resulting in current flowing through the external load in a downward direction. During the negative half cycle OPQ, the lower end of the secondary becomes positive and now it is the turn of green diodes (figure 5.15(ii)) to conduct the current. During the entire cycle, the current flows through the external load in the same downward direction. The output current cycle is shown by green line in figure 5.14.

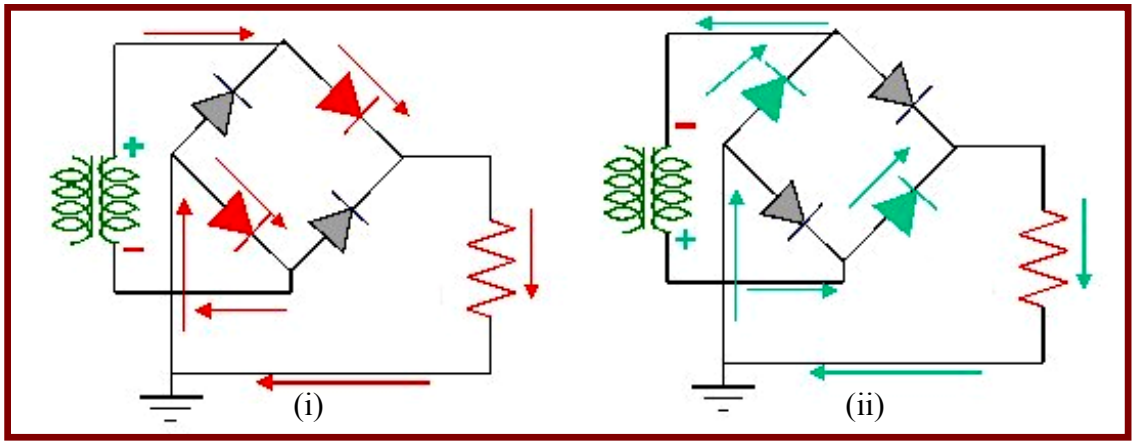

Figure 5.15

It is important to note that there is some voltage drop in the diodes due to which the instantaneous value of output current is less than that of input. Further the output of the full wave rectifier is unidirectional but varying with time (as distinguished from a pure DC shown by a dotted line in figure 5.14).

5.5.2 Current Transducer and Filter:

5.5.2.1 In order to measure the current flowing through the external resistance load, a Current Transducer (CT) with a turn ratio of 1:1000 was used. The CT makes use of 'Hall effect' for its operation and provides instantaneous voltage output, which can be interpreted for the current flowing through the current transducer. Further to increase the sensitivity of the current transducer, four turns of winding were passed through CT resulting in an overall turn ratio of 1:250.

5.5.2.2 In order to have a smooth output from the CT, which was necessary for the operation of the logger, a filter circuit was used. A capacitor was connected across the output terminals of the CT. When the voltage is increasing along MR (see figure 5.16), the capacitor gets charged. When the voltage tends to decline, the capacitor gets discharged as shown by portion RS in figure 5.16 and, therefore, tends to maintain a constant voltage in the output circuit. The resultant voltage in fact still carries some ripples but the output is sufficiently smooth for the logger to interpret the current.

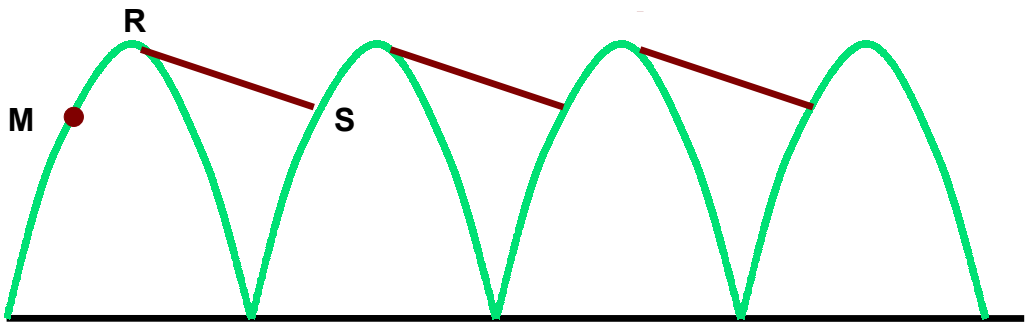

Figure 5.16

The composite circuit of CTs with capacitors is shown in figure 5.17.

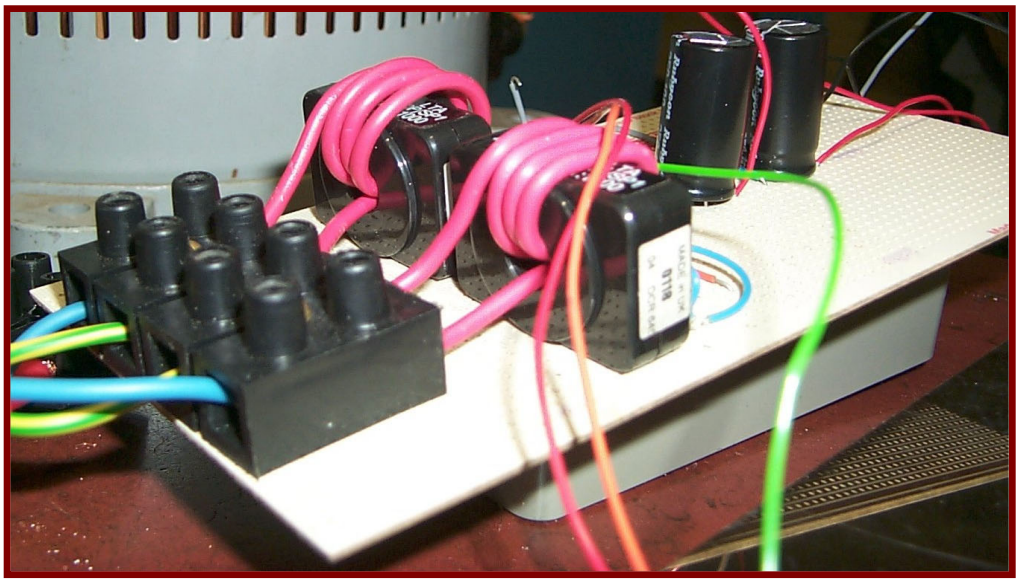

Figure 5.17

5.5.3 Calibration:

5.5.3.1 The CT provides almost linear voltage output for the current passed through it but some amount of non-linearity is expected at lower currents due to lack of sensitivity. In order to reduce errors in the measurement of current, which appears squared in the expression of power, it was decided to calibrate the CT with a test set up as explained in succeeding paragraphs.

5.5.3.2 Calibration Set up:

S.No.	Equipment Description	Quantity
1.	Composite CT filter circuit with power supply unit (30 V)	1 No.
2.	AC Voltage Variac 0-240 Volts, 8 A	1 No.
3.	Full wave bridge rectifier	1 No.
4.	Digital multimeter	1 No.

5.	Resistive Loads (100 ohms, 100 w)	4 Nos.
6.	Data logger with power supply unit (12V)	1 No.
7.	Connecting wires	1 set
8.	Computer with data logger software	1 set

1. Connect the four resistors, each of 100 ohms, in parallel and mount them on a flat aluminium plate so as to increase their heat dissipation capacity.
2. Measure the total resistance across the resistors so as to adjudge the maximum current, which can be passed through them without exceeding their heat dissipation capacity. The total resistance in the above arrangement would be around 26 ohms permitting a current up to 3.92 A (= $(400/26)^{0.5}$).
3. Modify the configuration file by using terminal 6 for reading input voltage signal. Terminal 6 is internally connected to LAC1 card in logger. Use a sampling interval of 1s.
4. Register the modified configuration file in the logger.
5. Connect the wires as per circuit diagram shown in figure 5.18.

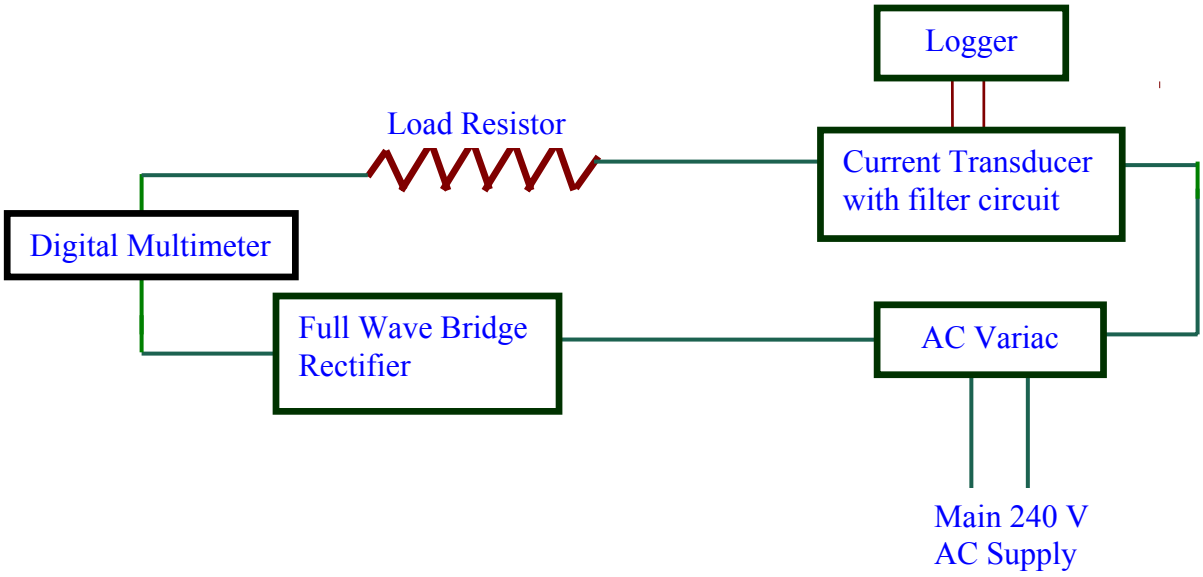

Figure 5.18

The test set up is shown in figure 5.19.

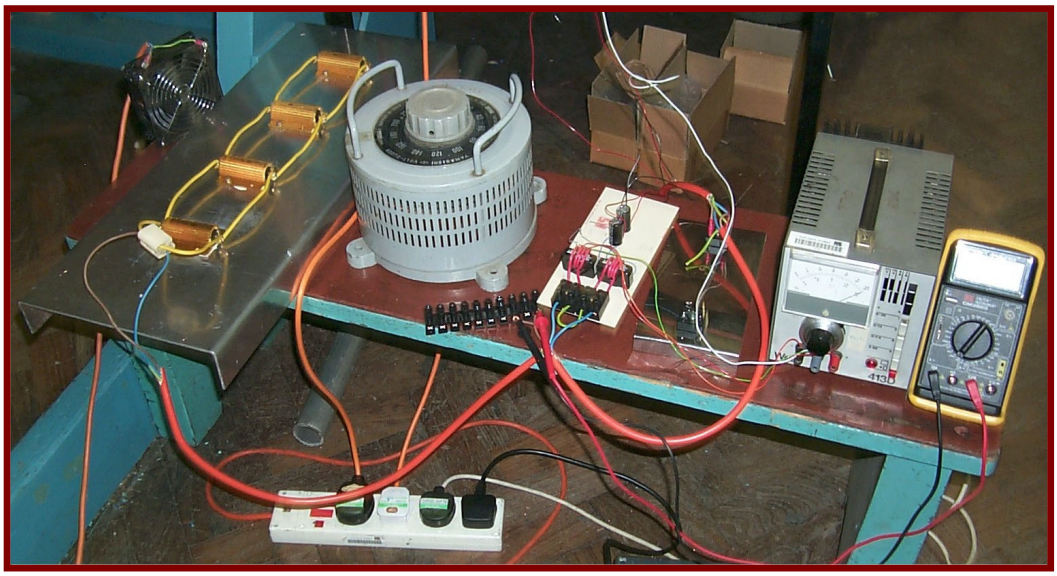

Figure 5.19

5.5.3.3 Procedure:

1. Bring the AC variac to zero position and switch on the power supplies to variac, composite CT filter circuit, data logger and computer.
2. Set the voltage of power supply units to CT filter circuit and data logger as per manufacturer recommendations (30V and 12 V respectively).
3. Increase the voltage applied across the load through variac and set it to a position at which the current through the load as recorded by mulimeter is 0.12 A.
4. Record the value of voltage output signal from CT through logger.
5. Increase the current through the load in steps of 0.12 A (up to 3.84 A) by increasing the voltage through the variac and record the voltage output signal through logger each time.
6. Repeat step 5 for decreasing current again in steps of 0.12 A.

5.5.3.4 Calibration Table:

The results for the calibration are shown in table 5.2. The graphs between the current through the CT and the voltage output signals for rising and falling currents are shown in figure 5.20. The graphs are nearly linear. Further the differences between the voltage signals for rising and falling currents are very small. A linearisation table (Table 5.3) between the current and the average value of voltage signals was registered in the delta logger with a new sensor (Sensor Code: I-1).

Current Through CT (A)	Voltage Output Signal		Current Through CT (A)	Voltage Output Signal	
	Rising Current (mV)	Falling Current (mV)		Rising Current (mV)	Falling Current (mV)
0	0	0	2.04	947.73	947.67
0.12	62	62.04	2.16	1006.13	1006.07
0.24	115.79	115.77	2.28	1063.57	1063.43
0.36	169.56	169.64	2.4	1116.17	1116.23
0.48	226.81	226.83	2.52	1172.48	1172.52
0.6	280.08	280.12	2.64	1230.85	1230.75
0.72	336.38	336.42	2.76	1284.63	1284.57
0.84	392.18	392.22	2.88	1339.93	1339.87
0.96	448.48	448.52	3	1389.12	1389.08
1.08	502.26	502.34	3.12	1447.86	1447.94
1.2	559.07	559.13	3.24	1503.23	1503.17
1.32	614.08	614.12	3.36	1554.86	1554.94
1.44	671.18	671.22	3.48	1615.42	1615.38
1.56	726.49	726.51	3.6	1670.73	1670.67
1.68	781.28	781.32	3.72	1730.58	1730.62
1.8	836.27	836.33	3.84	1770.51	1770.49
1.92	894.48	894.52			

Table 5.2

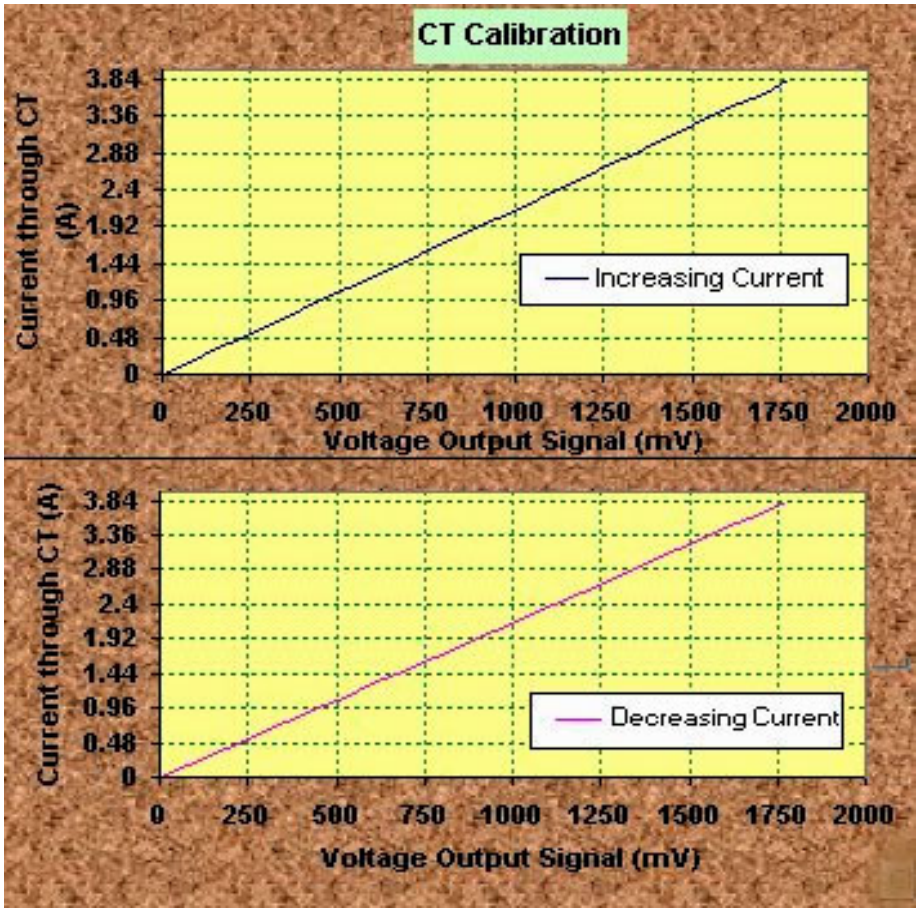

Figure 5.20

Current Through CT (A)	Avg. Voltage Output Signal (mV)	Current Through CT (A)	Avg. Voltage Output Signal (mV)	Current Through CT (A)	Avg. Voltage Output Signal (mV)
0	0	1.32	614.1	2.64	1230.8
0.12	62.02	1.44	671.2	2.76	1284.6
0.24	115.78	1.56	726.5	2.88	1339.9
0.36	169.6	1.68	781.3	3	1389.1
0.48	226.82	1.8	836.3	3.12	1447.9
0.6	280.1	1.92	894.5	3.24	1503.2
0.72	336.4	2.04	947.7	3.36	1554.9
0.84	392.2	2.16	1006.1	3.48	1615.4
0.96	448.5	2.28	1063.5	3.6	1670.7
1.08	502.3	2.4	1116.2	3.72	1730.6
1.20	559.1	2.52	1172.5	3.84	1770.5

Table 5.3

5.5.4 Verification:

5.5.4.1 The test set up and the procedure used for calibration was repeated to verify the accuracy of measurement of current. But this time the current was changed at random rather than in the fixed steps used for calibration.

5.5.4.2 Test Results and Discussions:

The test results are enclosed in Appendix-4. From the results, it can be seen that the values of the current recorded by the multimeter and the logger were in exact conformity except in a few readings (3 out of 36 readings), which showed a difference of 0.01 amperes between the multimeter reading and the current reading interpreted by the logger. It was, therefore, concluded that the composite CT filter circuit was accurately measuring the current flowing through the load resistance.

5.6.0 Calibration of Alternator:

The alternator along with the rectifier were calibrated to determine the composite efficiency versus the output current characteristics so that input shaft power to alternator, which was the same as the power output of the wind rotor, could be computed by measuring the current flowing through the load resistor connected to the rectifier. Further it was established in chapter 3 that the output current flowing through the resistive load connected across a permanent magnet alternator (or constant excitation) is directly proportional to the speed of the alternator (see paragraph 3.6.3 for details). This conclusion was used for establishing the rotational speed of the wind rotor by measuring the output current. Hence the output current versus rotational speed characteristics were also drawn for the two resistive loads of 56.7 ohms and 104 ohms.

The calibration of the alternator along with the rectifier was carried out by using a DC shunt motor in following three stages:

a) Stage I: Calibration of DC generator tachometer directly coupled with the shaft of DC shunt motor
b) Stage II: Calibration of DC shunt motor
c) Stage III: Calibration of alternator with calibrated DC shunt motor

5.6.1 Calibration of Tachometer Coupled with DC Shunt Motor:

A small permanent magnet DC generator was directly coupled with the shaft of the DC shunt motor. The voltage output of the generator tachometer was calibrated for speed of the motor by using the following test set up:

5.6.1.1 Test Set up:

S.No.	Equipment Description	Quantity
1.	DC shunt motor (1.5 h.p., 1500 r.p.m.)	1 No.
2.	DC power supply unit for field winding	1 No.
3.	DC power supply unit for armature winding with a rheostat	1 No.
4.	Permanent magnet DC generator directly coupled with the shaft of the motor	1 No.
5.	Optical Tachometer	1 No.
6.	Multimeter	1 No.
7.	Connecting wires	1 set

Connect the wires as per the circuit diagram shown in figure 5.21. Paste a thin rectangular silver metal strip on the motor shaft.

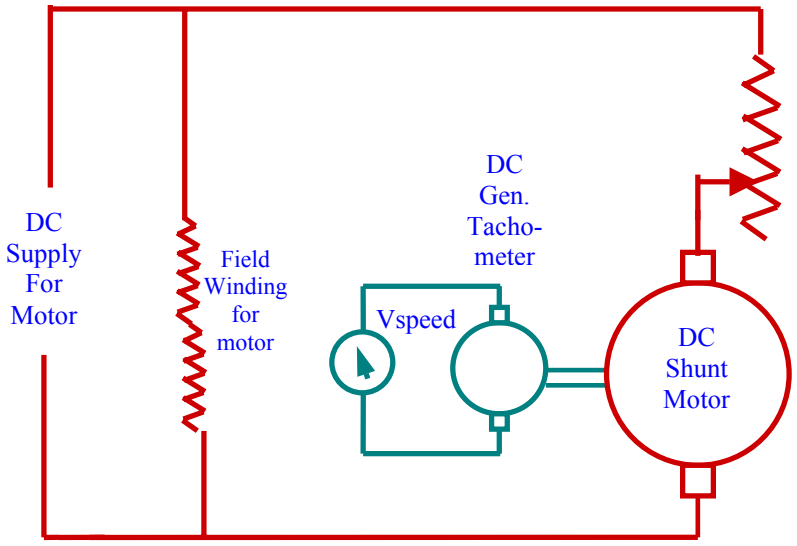

Figure 5.21

5.6.1.2 Calibration Procedure:

1. Bring the rheostat connected with the armature winding to minimum position and switch on the DC power supply unit for field and armature windings.
2. By reducing resistance in the rheostat, start the motor and check for any unusual noise or vibrations in the motor.
3. Allow the motor to stabilise at this speed.
4. Bring the optical tachometer near the motor shaft and target its light against the silver strip on the shaft.
5. Hold the tachometer firmly keeping its button pressed till the neon lamp glows continuously indicating a stable speed.
6. Note the voltage output of the DC generator tachometer from the multimeter.
7. Recall the last reading recorded in the tachometer and note it down.
8. Repeat steps 3 to 7 by increasing the motor speed gradually through the rheostat control.
9. Repeat steps 3 to 7 for decreasing speed of the motor.

5.6.1.3 Calibration Results and Discussions:

The results of the calibration are enclosed in Appendix-5. Further the figure 5.22 shows the graph between the voltage output of DC generator tachometer and the speed recorded by tachometer.

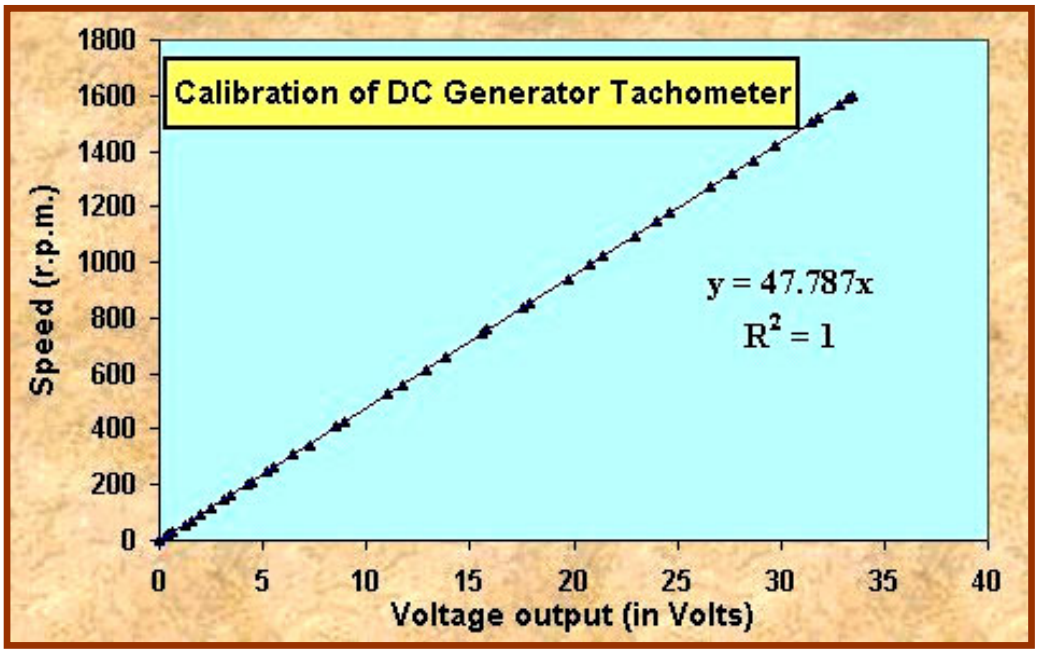

Figure 5.22

From the graph it can be seen that the voltage output of DC generator tachometer was varying linearly with the speed. By using linear regression technique in MSEXCEL, the relation between the voltage output of DC generator, in volts (V_{speed}) and speed (N), in r.p.m., was determined as following:

$$N = 47.787\ V_{speed} \qquad (5\text{-}3)$$

The correlation coefficient was found to be 1 (precisely 0.9999), suggesting a very high degree of linear correlation. It was also found that the voltage output

of the DC generator was rated 20.8 volts per 1000 rpm, which works out to be 48.077 r.p.m per Volt. It was quite close to the value of 47.787 r.p.m per Volt determined experimentally (see the relation (5-3) between V_{speed} and N).

5.6.2 Calibration of DC Shunt Motor:

The DC shunt motor was calibrated for efficiency versus the armature current characteristics as described in the following paragraphs:

5.6.2.1 Test Set up:

S.No.	Equipment Description	Quantity
1.	DC shunt motor (1.5 h.p., 1500 r.p.m.)	1 No.
2.	DC power supply unit for field winding	1 No.
3.	DC power supply unit for armature winding with a rheostat	1 No.
4.	Permanent magnet DC generator tachometer coupled with the motor	1 No.
5.	Eddy current dynamometer	1 No.
6.	DC Power supply for dynamometer with a variac	1 No.
7.	Multimeter	5 Nos.
8.	Connecting wires	1 set

Set up the test bed by coupling the motor with dynamometer and connect the wires as per the circuit diagram shown in figure 5.23.

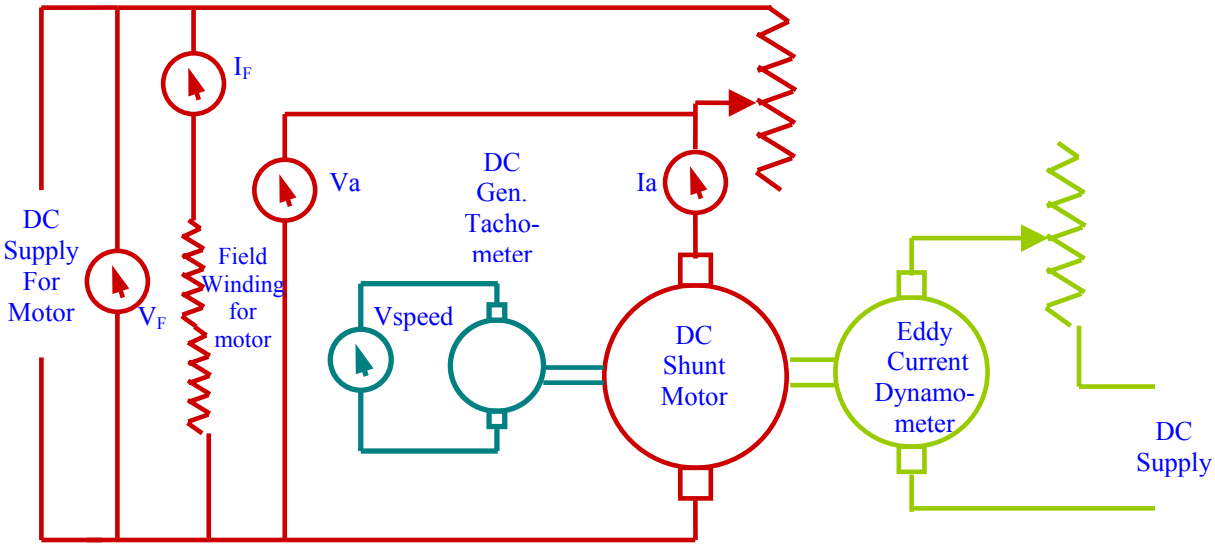

Figure 5.23

The test set up is shown in figure 5.24.

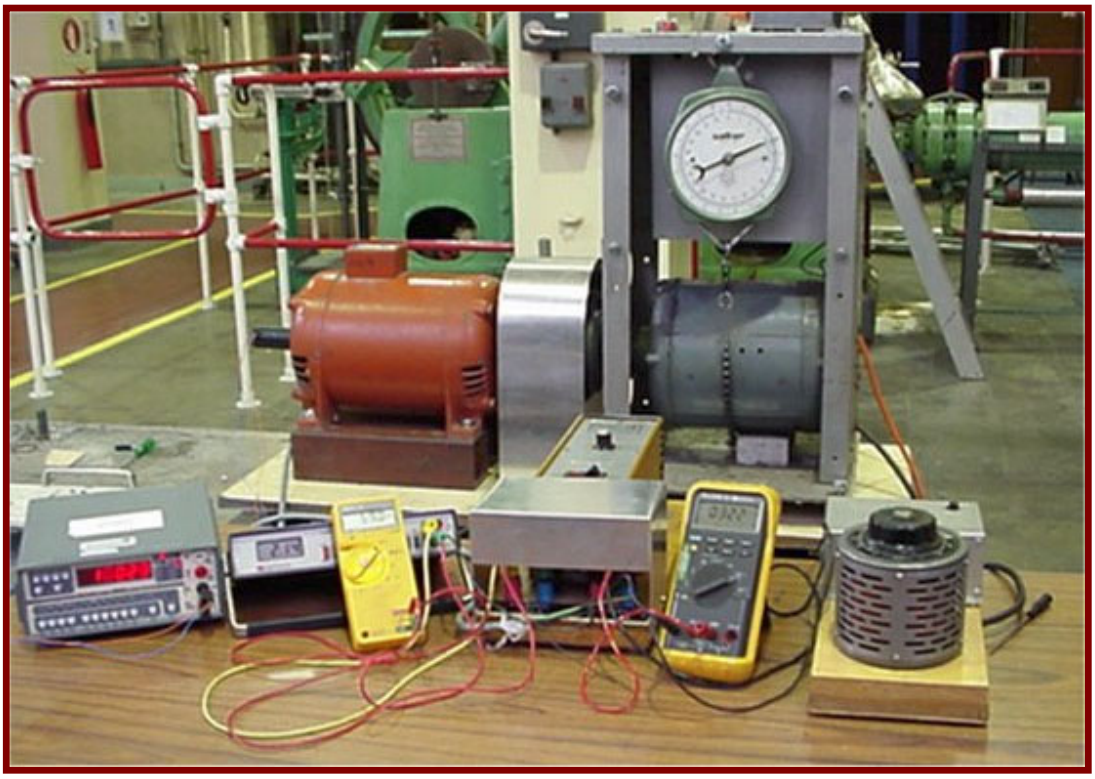

Figure 5.24

5.6.2.2 Calibration Procedure:

1. Bring the rheostat, connected with the armature winding of motor, and DC variac, connected with the eddy current dynamometer, to minimum positions and switch on the DC power supply units for the motor and dynamometer.
2. By reducing resistance in the rheostat, start the motor and check for any unusual noise or vibrations in the motor.
3. Gradually raise the speed of the motor and bring it to a speed of nearly 600 r.p.m. This speed would correspond to the generator tachometer voltage output of around 12.5 volts.
4. Allow the motor speed to stabilise for around 3 minutes.
5. Increase the DC voltage across the dynamometer gradually and note the increasing current in the armature and the load on the spring balance.
6. Allow the system to stabilise for about 3 minutes for a certain load (start with a light load of around 0.4-0.6 kg).
7. Take down the readings of field current (I_f), armature current (I_a), voltage across field winding (V_f), voltage across armature winding (V_a) and voltage output of generator tachometer (V_{speed}) from respective multimeters.
8. Note down the load from spring balance of dynamometer.
9. Increase DC power supply to dynamometer by using DC variac.
10. Repeat steps 6 to 9 till the motor starts stalling.
11. Bring the DC supply through dynamometer to minimum.
12. Reduce the motor speed and repeat steps 4 to 11.
13. Obtain several sets of readings by varying motor speed and load on dynamometer.
14. Measure arm length of the dynamometer.

5.6.2.3 Theory

The electrical power input to motor is determined from the following expression:

$$P_{input} = V_f I_f + V_a I_a$$

Where V_f is the voltage applied across field winding;

I_f is the current in field winding;

V_a is the voltage applied across armature winding and

I_a is the current in armature winding

The shaft power output is computed by using the equation:

$$P_{output} = 2 \pi N \tau / 60$$

Where τ = Shaft torque = Load x 9.81x arm length of dynamometer

N = Shaft speed in r.p.m

The rotational speed of the motor is determined by inputting the value of voltage output of DC generator tachometer (V_{speed}) in the expression (5-3).

The efficiency of the motor is computed using the following relation:

$$\eta_{motor} = P_{output} / P_{input}$$

5.6.2.4 Calibration Results and Discussions:

The results of the calibration are enclosed in Appendix-6. Further the figure 5.25 shows the graph between the armature current and the motor efficiency.

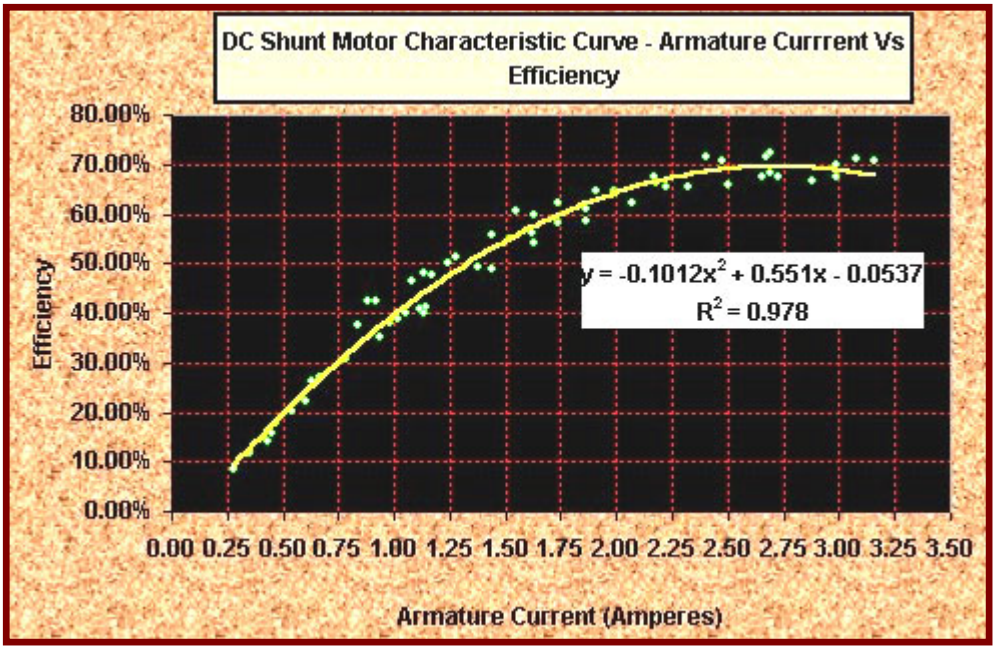

Figure 5.25

As can be seen from the graph, the efficiency of the motor was very low at low values of armature current. This is due to the fact that constant losses absorb a significant proportion of the input power at low armature current (iron losses, mechanical losses and shunt copper losses in DC shunt motor are collectively called constant losses. Please refer to paragraph 3.6.4 in chapter 3 for further details). The efficiency of the motor increased steadily with armature current and became maximum (around 70%) at 2.72 amperes beyond which it started falling.

By using best curve fitting technique in MSEXCEL, the relation between the armature current, in amperes (I_a), and motor efficiency (η_{motor}) was determined as following:

$$\eta_{motor} = -0.1012\ I_a^{\,2} + 0.551\ I_a - .0537 \qquad (5\text{-}4)$$

The correlation coefficient was found to be 0.978, which is quite close to unity, establishing the validity of the relation. Further it is clear from the aforesaid equation that the efficiency curve leaves a positive intercept on X-axis, representing no load armature current at starting speed.

5.6.3 Calibration of Alternator with Rectifier:

The alternator with rectifier was calibrated by using the calibrated DC shunt motor. The test set up, procedure and results are described in the following paragraphs.

5.6.3.1 Test Set up:

S.No.	Equipment Description	Quantity
1.	DC shunt motor (1.5 h.p., 1500 r.p.m.)	1 No.
2.	DC power supply unit for field winding	1 No.
3.	DC power supply unit for armature winding with a rheostat	1 No.
4.	Permanent magnet DC generator tachometer coupled with the motor	1 No.
5.	Alternator	1 No.
6.	Composite CT filter circuit with power supply unit (30 V)	1 No.
7.	Full wave bridge rectifier	1 No.
8.	Multimeter	5 Nos.
9.	Resistive loads mounted on heat dissipating aluminium plates (56.7 ohms,400 W and 104 ohms,400 W)	2 sets
10.	Data logger with power supply unit (12V)	1 No.
11.	Connecting wires	1 set
12.	Computer with data logger software	1 set

Set up the test bed by coupling the motor with alternator and connect the wires as per the circuit diagram shown in figure 5.26.

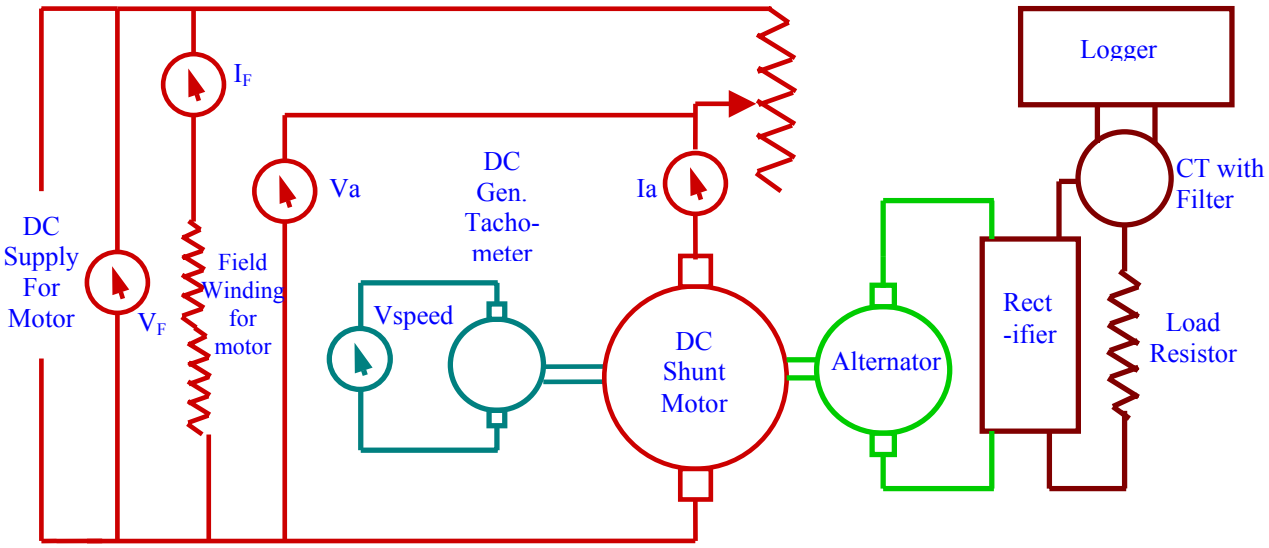

Figure 5.26

The test set up is shown in figure 5.27

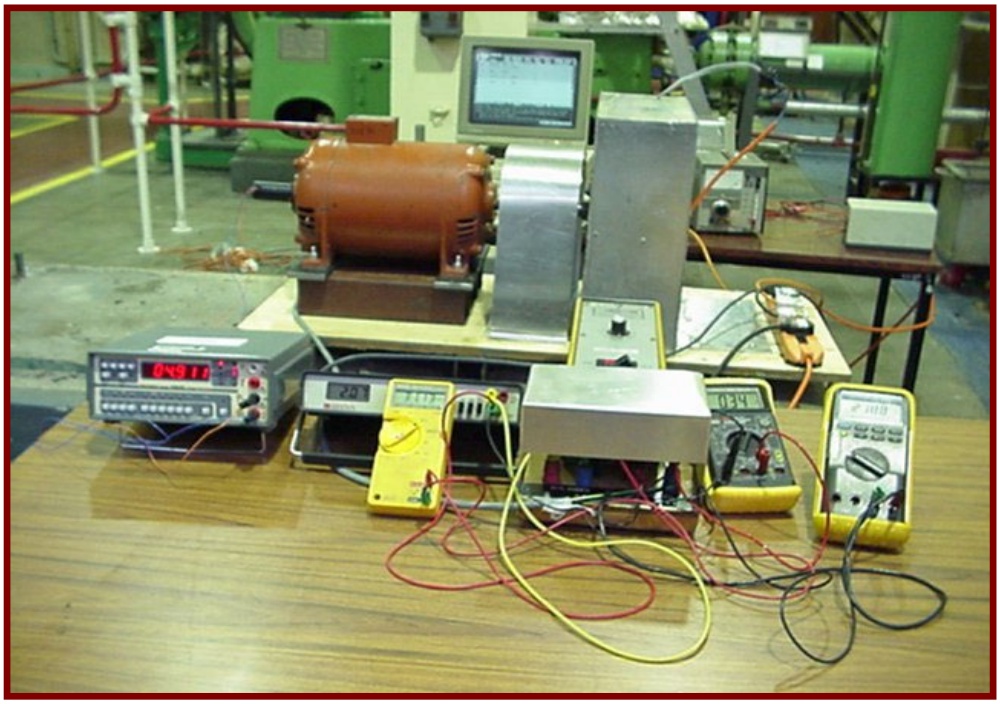

Figure 5.27

5.6.3.2 Calibration Procedure:

1. Measure the resistance of armature winding.
2. Connect the load resistance plate of 104 ohms with the rectifier.
3. Bring the rheostat, connected with the armature winding of motor, to minimum position and switch on the DC power supply units for the motor and data logger.
4. By reducing resistance in the rheostat, start the motor and check for any unusual noise or vibrations in the motor and alternator.
5. Gradually raise the speed of the motor and bring it to a speed of nearly 50 r.p.m. This speed would correspond to the generator tachometer voltage output of around 1.05 volts.
6. Allow the motor speed to stabilise for around 3 minutes.
7. Take down the readings of field current (I_f), armature current (I_a), voltage across field winding (V_f), voltage across armature winding (V_a) and voltage output of generator tachometer (V_{speed}) from respective multimeters.
8. Note down the reading of the output current of the rectifier from data logger.
9. Gradually raise the motor speed.
10. Repeat steps 6 to 9 till the output current of the rectifier reaches a value of 1 ampere.
11. Change the load resistance plate from 104 ohms to 56.7 ohms and repeat steps 3 to 10.

5.6.3.3 Theory

The electrical power input to motor is determined from the following expression:

$$P_{input} = V_f I_f + V_a I_a$$

Where V_f is the voltage applied across field winding;

I_f is the current in field winding;

V_a is the voltage applied across armature winding and
I_a is the current in armature winding

The motor shaft power output is computed by using the equation:

$$P_{output} = P_{input} \times \eta_{motor}$$

The motor efficiency is determined from the expression (5-4) established experimentally as described in paragraph 5.6.2 above. The relation is reproduced here for ready reference.

$$\eta_{motor} = -0.1012 I_a^2 + 0.551 I_a - .0537 \quad (5\text{-}4)$$

The shaft power input to alternator (P_{in}) is same as the shaft power output of the motor. Further the power output (P_{out}) of the alternator with rectifier is determined from the following relation:

$$P_{out} = I^2 R$$

Where I is the output current as recorded by data logger based on voltage signal from composite CT filter circuit and
R is the load resistance connected with the rectifier.

Hence the following relation gives the composite efficiency of the alternator with rectifier unit:

$$\eta_{com} = P_{out} \times 100 / P_{in}$$

The rotational speed of the motor is determined by inputting the value of voltage output of DC generator tachometer (V_{speed}) in the expression (5-3).

5.6.3.4 Calibration Results and Discussions:

The results of the calibration are enclosed in Appendix-7. Further the following figures show the various characteristic curves of the alternator.

Figure 5.28: Output current versus composite efficiency

Figure 5.29: Power output versus shaft power input to alternator

(It is important to note here that power output of the wind rotor would be same as the shaft power input to alternator)

Figure 5.30: Output current versus speed

By using the best curve fitting technique, the relations between the various characteristic parameters were established as shown in the respective figures. The values of the correlation coefficients were also determined. As can be seen, the values of the correlation coefficients were near unity.

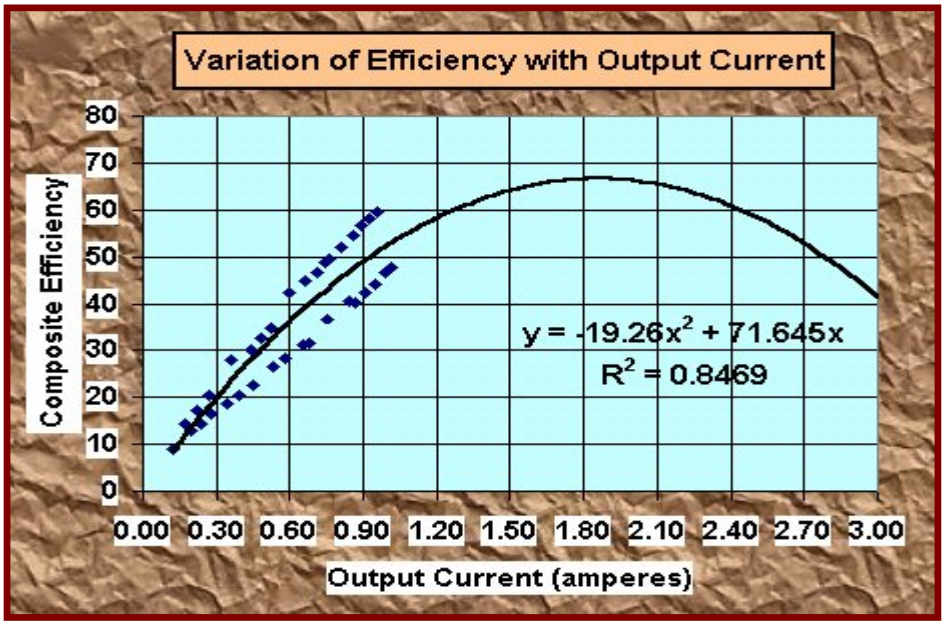

Figure 5.28

In case of output current versus efficiency, the correlation coefficient was found to be 0.8469. It is important to mention here that the efficiency curve was

plotted based on test results with maximum output current being restricted to 1 amperes. The resistance of the stator winding of the alternator was found to be nearly 19.3 ohms and the alternator had no provision for cooling of the stator winding. It was, therefore, decided not to take the output current above 1 amperes as the stator winding might have been damaged.

The efficiency curve obtained experimentally was extrapolated for higher values of stator current based on the relation established between the output current and the efficiency. It can be seen in the figure 5.28 that the efficiency curve increased steadily and reached a peak value of 67% at output current of 1.87 amperes. The curve drooped down for further increase in current. This is the normal characteristic curve of an alternator, which supported the validity of the relation established experimentally.

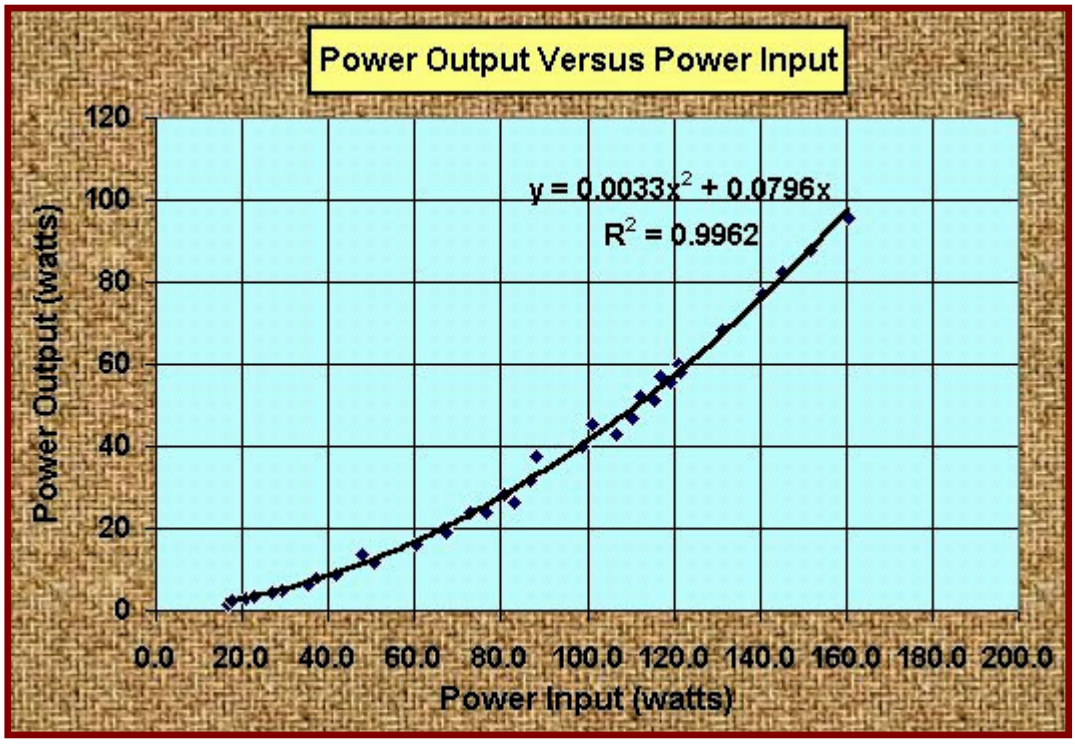

Figure 5-29

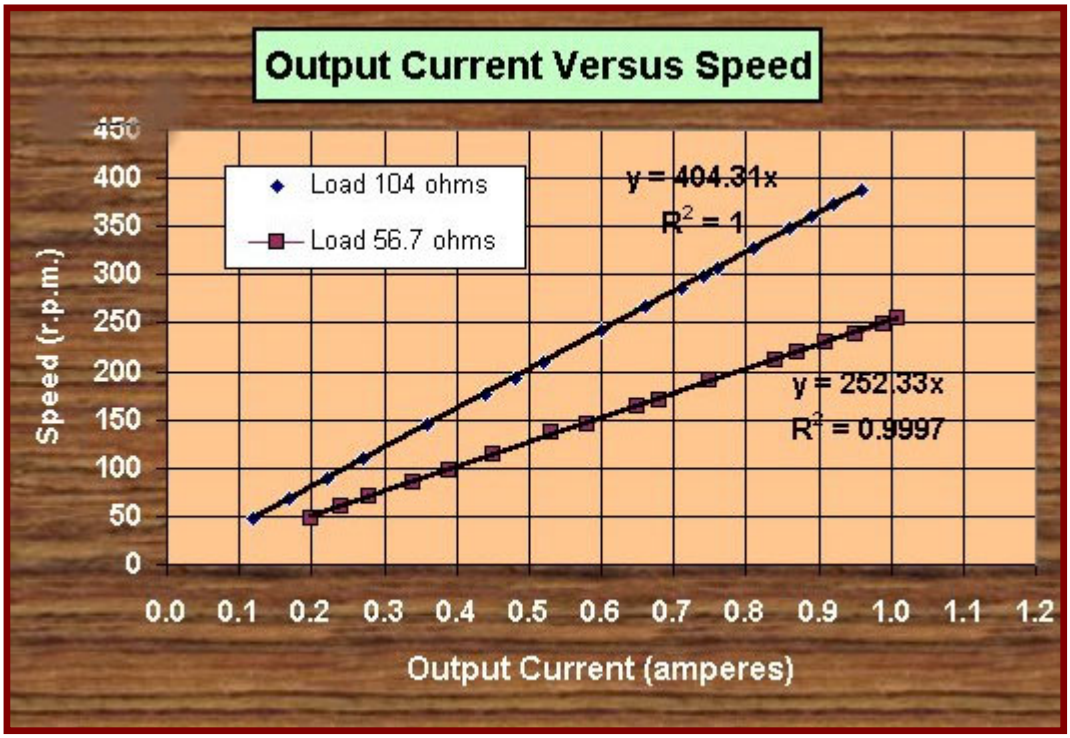

Figure 5.30

The following relations were established experimentally for the alternator coupled with the novel VAWT.

$$\eta_{com} = -19.26\ I^2 + 71.645\ I \quad (5\text{-}5)$$

$$P_{out} = .0033\ P_{in}^{\ 2} + 0.0796\ P_{in} \quad (5\text{-}6)$$

$$N = 404.31\ I \quad \text{(for load of 104 ohms)} \quad (5\text{-}7)$$

$$N = 252.33\ I \quad \text{(for load of 56.7 ohms)} \quad (5\text{-}8)$$

Where I is the output current of the rectifier, in amperes

P_{in} is the shaft power input to alternator, in watts

P_{out} is the electrical power output of the alternator with rectifier, in watts

N is the alternator rotational speed, in r.p.m.

Chapter 6: Field Test Set up and Data Acquisition

General

This chapter deals with the installation of the test set up at the project site, Fionnphort, which is on the Island of Mull off the West Coast of Scotland. The chapter also describes certain problems, which were observed in the test set up after the trial run. These were analysed in detail and the test set up was fine-tuned based on early experiences.

6.1.0 Test Site:

6.1.1 The figure 6.1 shows some photographs of the test site. As can be seen from these photographs, the site terrain was nearly flat but the field surrounding the turbine was covered with long grass, which was expected to provide considerable shear and turbulence effects on the wind near the ground. However since DWT had claimed that the turbine would generate sufficient power output when mounted at ground level, despite the shear effects near the ground, the field conditions existing at the test site were considered ideal for testing of the novel VAWT.

6.1.2 Further there were no trees, hills or any tall structures in the vicinity of the turbine, which could obstruct the free flow of wind to the turbine. However on the West Side, a house of about 12 meters height was noted at a distance of around 90 meters from the turbine. This house could cast a wake over the wind turbine for the winds coming from western side. The directions of wind, in degrees, from the referencing north direction, which could have been obstructed by the house, were determined using a magnetic compass as discussed in the

paragraph 6.6.0 of this chapter. The data collected for the wind coming from these directions was filtered out and not taken into consideration for analysis.

Figure 6.1 (a)

Figure 6.1 (b)

Figure 6.1 (c)

Figure 6.1 (d)

6.2.0 Positioning of Mast for Anemometer and Wind Vane:

6.2.1 Currently there is no common Standard for power performance measurements of wind turbines. Various standards such as International standard IEC 61400-12, draft standard for power performance measurements from MEASNET, National standards of Dutch, Denmark and Germany, etc. are in vogue. These standards differ in their recommendations for positioning of the wind anemometer mast relative to the wind turbine. However the most common accepted practice is to position the mast at a distance of 2 to 6 times the rotor diameter. Since the novel VAWT is housed inside a ducting, the width of the housing rather than the rotor diameter was used as the referencing dimension for calculation of separation distance between the mast and the turbine. The mast was erected at a distance of around 4 times the width of the housing from the turbine. Further the anemometer and the wind vane were mounted at a height coinciding almost with the centre of the turbine. The horizontal position of the mounting bar on which the anemometer and the wind vane rested, was checked with a spirit level.

6.3.0 Alignment of Wind Vane with Referencing Direction:

6.3.1 As stated in chapter 5, the referencing direction for the wind vane was north. Using a magnetic compass, the north marking on the potentiometer of the wind vane was aligned with the north direction and the fixing screw at the bottom of wind vane was tightened.

6.4.0 Thermocouple:

6.4.1 To measure the outside temperature, the hot junction of the thermocouple (i.e. the welded end of the thermocouple pair of wires) was exposed to the free flowing wind. It was kept under a shelter to prevent it from getting wet by

rainwater otherwise the evaporative cooling would have reduced the temperature and caused an error in temperature measurement.

6.5.0 Configuration File:

6.5.1 The configuration file was prepared for recording the field data as per the following details:

a) Cold junction temperature, in degrees C, on terminal 1 with a sampling interval of 10 minutes;
b) Wind speed, in knots, on terminal 2 with a sampling interval of 1 second and data compression (averaging) over 10 minutes;
c) Outside temperature, in degrees C, on terminal 4 with a sampling interval of 10 minutes;
d) Current flowing through the load resistor, in amperes, on terminal 6 with a sampling interval of 1 second and data compression (averaging) over 10 minutes;
e) Wind direction, in degrees from north, on terminal 31 with a sampling interval of 1 second and data compression (averaging) over 10 minutes.

The terminals 1 through 15 were inputting to the LAC1 card and terminal 31 to the LFW1 card in logger. The configuration file was registered in the logger.

6.6.0 Determination of Waking Wind Directions for Turbine and Anemometer:

6.6.1 The figure 6.2 shows the relative positions of the wind turbine, anemometer and the house casting a wake over them for the winds coming from west side.

In the figure 6.2, PQ represents the side-wall of the house; W represents the wind turbine position and A indicates the position of the mast for anemometer and wind vane.

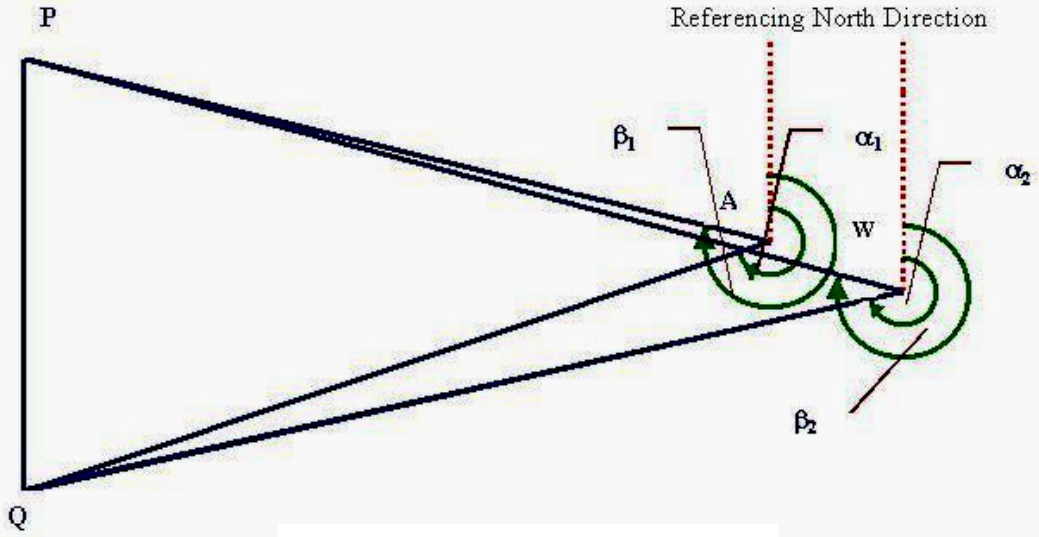

Figure 6.2

By pointing the magnetic compass along AP, AQ, WP and WQ, the various angles were recorded as under:

$\alpha_1 = 230^0$ $\beta_1 = 268^0$ $\alpha_2 = 220^0$ $\beta_2 = 242^0$

Based on the above, it was decided that the winds coming from the directions in between 220^0 and 268^0 from north were obstructed by the house for the anemometer (resulting in wrong wind speed measurement) or the turbine (resulting in generation of less power and hence measurement of less current) or both. Hence the data recorded for wind directions falling in between 220^0 and 268^0 from north were not considered for analysis.

6.7.0 Early Experiences and Fine Tuning of Field Test Set up:

After commissioning of the field test set up, it was put up on trial run for about ten days. A detailed review of the data file (see file TRIAL enclosed as Appendix-8 here) pointed out certain deficiencies and the field test set up was fine tuned as detailed in the succeeding paragraphs:

6.7.1 Review of Sampling Interval:

6.7.1.1 A preliminary examination of the data file pointed out that the logger stopped working after two days due to power failure. This could not be detected early, as it was not possible to interrogate the logger on line. Since the wind speed, wind direction and current were recorded at a sampling interval of 1second, the logger remained busy in logging the data all the time and did not respond to communication calls. Any attempt to interrogate the logger on line resulted in a communication error.

6.7.1.2 The use of the smallest sampling interval also resulted in 'over-run error' in certain sets of readings. Due to the limiting logging speed, the logger was busy in recording the previous set of readings while the next set of readings became due. The logger, therefore, used the data from the previous set of readings and attached over-run error flag (#) to the next set of readings. It was, therefore, decided to change the sampling interval from 1 second to 5 seconds. This change also enabled on line interrogation of the logger to find out whether it was logging. Further it was decided to extract the data from the logger on a weekly basis.

6.7.2 Review of Auto Range for Temperature Measurement:

Certain sets of readings in the data file showed noise errors (see noise error flag ($) on temperature channels 1 and 4 in data file TRIAL in Appendix-8), although the temperature recording values were consistent with their neighbouring values. It was due to the fact that the logger was unable to auto-range both up and down during the same reading. It was, therefore, decided to use fixed range for measuring temperature rather than auto-range. The sacrifice in resolution due to use of fixed range was negligible. This change reduced the noise errors in temperature measurements.

6.7.3 Review of Data Compression:

On the review of data file, it was found that the logger sensed the highest instantaneous wind speed of 18.8 knots with the corresponding current of 0.25 amperes in the circuit (see maximum value of wind speed and current in data file TRIAL in Appendix-8). But the highest average wind speed recorded was 11.46 knots with the corresponding average current of 0.13 amperes. It was, perhaps, due to the fact the wind gusts in that part of year were of short duration making the average wind speed over 10 minutes period low as compared to the maximum wind speed in the averaging interval. Thus the following changes were made in data compression for wind speed, current and the wind direction:

(i) The logger was configured to compress data for wind speed and current for recording the maximum value rather than the average value. The purpose of using the average value earlier was that the response time of the wind rotor with respect to changing wind speeds was not known. It was, therefore, thought that averaging over a large interval of 10 minutes would cover this aspect. But the use of maximum values rather than average had no bearing on this purpose as the maximum power produced

would correspond to the maximum wind speed and both were being recorded for a fixed time interval. However in the case of peak of wind speeds falling near the end of a compression interval, there were chances of the corresponding peak of power falling in the next interval. This situation might introduce some element of error in readings. But it was not expected to have these situations very frequently.

(ii) It was felt that the data compression interval of 10 minutes was too long to cover up the response time aspect of the wind turbine. In fact the readings were taken over a sampling interval of 5 seconds without any data compression for nearly 24 hours. A review of the data file was carried out by focussing over small windows of 5 minutes. The review pointed out that the wind turbine was normally responding to changing speed within 5 minutes. Accordingly, it was decided to use a data compression interval of 5 minutes.

(iii) The averaging of wind direction over a period of 10 minutes was not serving any purpose. In case of wind blowing from north, it could have generated errors, as it would have been interpreted as wind blowing from some other direction. For example averaging of four values of wind direction for wind blowing from north ((358 +358 + 5 + 5) /4 = 181.5) would be interpreted as wind blowing from south. It was, therefore, decided to use an instantaneous value for wind direction at interval of 5 minutes rather than averaging out.

6.7.4 The configuration file was revised as per the changes above and registered in the logger again. Before it could be achieved, the data continued to be obtained using the old configuration. It is important to point out that the data files with pre-revised configuration were not providing any erroneous data as changes were made only to obtain the wider range of data (i.e. use of data compression

for 5 minutes instead of 10 minutes and for maximum values rather than average values) and avoid unnoticed stopping of the logger. Even in the case of wind direction, averaging of wind blowing from north might lead to wrong interpretation of wind direction in the range of 220^0 and 268^0 from north (e.g. (356 + 355 + 15) /3 = 242). It would only mean that this data point would be excluded from the analysis but the wrong interpretation would not lead to inclusion of spurious data points in the analysis. Thus all data files with pre-revised configuration were used for analysis as discussed in chapter 7.

Chapter 7: Data Compilation and Analysis

General

This chapter describes the various procedures and tools used for compilation and analysis of the data obtained from the field testing of the novel VAWT. The chapter is broadly divided into three sections. The first section describes the methodology adopted for storage of the raw and processed data files. The next section deals with the filtration of erroneous data. The last section focuses on the data analysis tools and also includes some sample calculations for ease of understanding.

7.1.0 Data Compilation:

7.1.1 Like any other experimental work, the project involved handling of huge amounts of data. A pre-determined methodology for data compilation resulted in ease of data storage and quick retrieval. Broadly the data files were divided in the following two categories:

a) Raw data files and
b) Processed data files.

7.1.2 All data files containing the raw data were stored in a folder named 'RAW-DATA'. The individual file names and description of the data contained in them are described in Table 7.1.

Folder: RAW-DATA*		
S.No.	**File Name**	**Description**
1.	TRIAL	Raw data obtained from the trial run of field test set up for around 50 hours.
2.	RD-LOAD1	Raw data obtained for load resistance of 104 ohms.
3.	RD-LOAD2	Raw data obtained for load resistance of 56.7 ohms.

Table 7.1

7.1.3 The processed data files were maintained in another folder called 'PROCESSED-DATA'. The individual file names and description of the data contained in them are described in Table 7.2.

Folder: PROCESSED-DATA*		
S.No.	**File Name**	**Description**
1.	PD-LOAD1	Processed data for load resistance of 104 ohms.
2.	PD-LOAD2	Processed data for load resistance of 56.7 ohms.

Table 7.2

7.2.0 Data Filtration:

7.2.1 As stated in the previous chapter, the wind turbine and the anemometer fell in the wake of a house on the West Side of the test site. Therefore the data corresponding to the wind, which could have been obstructed by the house on its way to turbine or anemometer, was not considered in evaluating the performance of the wind turbine. Such data corresponded to the wind directions in between 220^0 and 268^0 from north and was identified by using asterisk (*) in the error flag column in the processed data files.

** Data files are not included in the PDF version of the thesis but are available separately as MSEXCEL flies.*

In certain sets of readings, the current flowing through the load resistance was found to be exceptionally low or high as compared to the other readings for the same wind speed bin (see paragraph 7.3.4 in this chapter for explanation of 'wind speed bin'). Such readings were determined by drawing graphs between wind speed and the current for various wind speed bins for each load separately. A sample graph for wind speed bin of 0-1 m/s for load of 104 ohms is shown in figure 7.1. From the graph it is clear that certain data points were lying apart from the rest, indicating exceptional and hence erroneous values. Such points are appearing with a background colour of red in the graph. All such erroneous readings were identified by using identifier '@' in the error flag column in processed data files and were excluded from further processing.

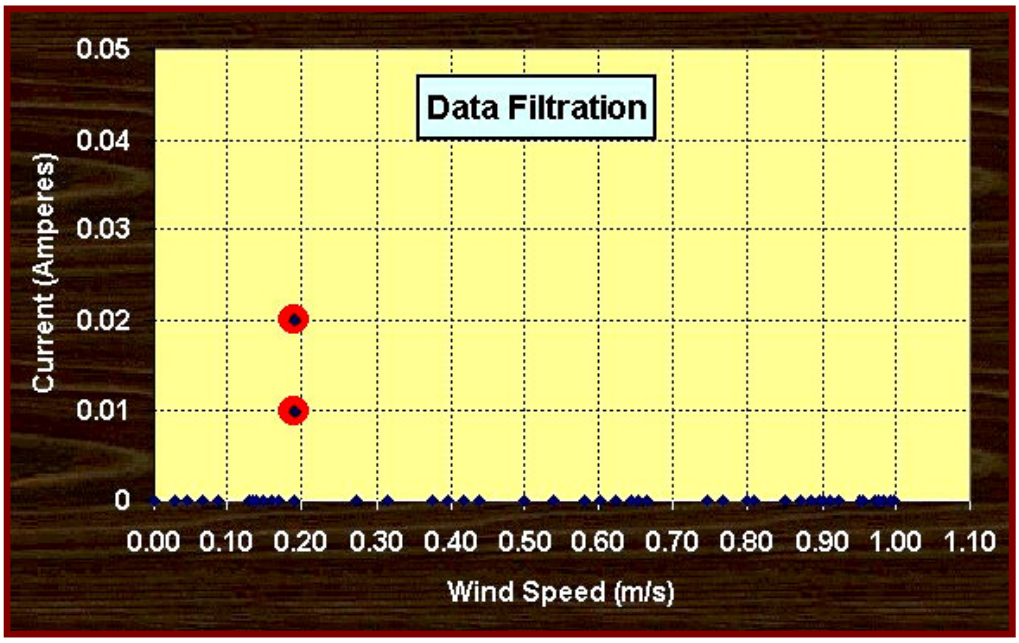

Figure 7.1

7.2.2 The data which carried the over-run error flag (#) in raw data files was not considered for data analysis and hence filtered out. The over-run error indicated that the data logger ran short of time for taking the readings and hence carried out data compression based on the previous readings available to it. However, certain temperature readings carried the noise error flag ($) as described in the

chapter 6. These readings were found to be in close agreement with their neighbouring values and, therefore, not discarded for performance measurements of the turbine.

7.3.0 Data Analysis:

The power extracted by the wind turbine from freely flowing wind is given by the expression (3-3), which is reproduced here for ready reference:

$$P_{turbine} = 0.5\ C_P\ \rho\ A\ V^3 \qquad (3\text{-}3)$$

Where C_P is the coefficient of performance

ρ is the air density

A is the swept area of the rotor and

V is the speed of freely flowing wind stream.

7.3.1 Computation of Rotor Swept Area:

7.3.1.1 The swept area of the rotor is given by the expression

$$A = DH$$

Where D is the rotor diameter and

H is the rotor height

For the novel VAWT, D = 0.98 m and H = 1.915 m

Swept Area, A = 0.98 x 1.915 = 1.8767 m^2

7.3.2 Determination of Air Density:

7.3.2.1 The air density is derived from the following expression based on Perfect Gas equation, as described in paragraph 3.1.0 of chapter 3:

$$\rho = P/ RT$$

Where P is the absolute pressure in N/m^2

T is the absolute temperature in K and

R is the gas constant for dry air = 287.1 J/kg K

$$\rho = (P_{Hg} \times 10^5) / (750 \times 287.1 \times (T + 273.15)) \quad (7\text{-}1)$$

Where P_{Hg} is the atmospheric pressure measured in mm of mercury column and

T is the temperature of freely flowing wind stream in degrees C

The test site, Fionnphort, is nearly at same elevation from sea level as Glasgow. Further the atmospheric conditions existing at Fionnphort, as far as their effect on atmospheric pressure is concerned, can be considered same as existing in Glasgow. The atmospheric pressure at test site was, therefore, assumed to be nearly the same as at Glasgow and was measured on a daily basis from a mercury barometer in the university workshop. The temperature of the freely flowing wind was recorded by the logger on channel 4. By inputting P and T in the equation (7-1), the air density was determined for each set of readings.

7.3.3 Measurement of Turbine Power and its Standardisation for Air Density:

7.3.3.1 As stated in chapter 4, the wind rotor was connected to a variable frequency permanent magnet alternator. By measuring the electrical power output from the alternator, the power extracted by the wind rotor from the freely flowing wind

was determined. For this purpose, the AC output of the alternator was converted into DC output by using a full wave bridge rectifier and a purely resistive load was connected across the rectifier. The alternator along with the rectifier circuit was calibrated for efficiency versus the output current. The output current flowing through the resistive load was recorded in the logger using a current transducer filter circuit as described in paragraph 5.5.2 of chapter 5 and the electrical power through the resistive load was computed using the expression

$$P_{el} = I^2 R \qquad (7\text{-}2)$$

The input shaft power to alternator, which is same as the power extracted by the rotor from wind, was determined from the following expression

$$P_{turbine} = 100\ P_{el} / \eta_{com} \qquad (7\text{-}3)$$

Where η_{com} is the combined efficiency of the alternator and rectifier and is related to output current by the following expression as determined experimentally (For details, please refer to paragraph 5.6.3 of chapter 5):

$$\eta_{com} = -19.26\ I^2 + 71.645\ I \qquad (7\text{-}4)$$

As evident from expression (3-3) (see paragraph 3.2.0 in chapter 3 for expression (3-3)), the power output of the wind turbine varies with the air density. It is a common practice to determine the power output of a turbine for the standard air density at sea level (P_{Hg} = 750 mm) at 15 degrees C temperature. The power output of the novel VAWT at standard air density was computed using the following expression:

$$P_{Std\text{-}turbine} = P_{turbine} \times \rho_0 / \rho \qquad (7\text{-}5)$$

Where ρ_0 = Dry air density at sea level at 15 degrees C = 1.225 kg/m^3

ρ = Air density at observed pressure and temperature

7.3.3.2 The data was processed using MSEXCEL software. The layout of processed file is as follows:

Column A: Error Flag

Column B: Date and time of recording the observation (t).

Column C: Atmospheric pressure, in mm of mercury (P_{Hg}).

Column D: Temperature of freely flowing wind, in degrees C (T).

Column E: Air density, in kg/m^3, calculated by inputting values of pressure and temperature from columns C and D respectively in expression (7-1) (ρ).

Column F: Speed of freely flowing wind, in knots (British knots based on nautical mile of 6080 ft/hour) (WS).

Column G: Speed of freely flowing wind, in m/s (1 m/s = 1.9426 knots) (V).

Column H: Current, in amperes, flowing through the resistive load (I).

Column I: Electrical power, in watts, dissipated in load calculated by inputting the value of the current from column H and the load resistance in the expression (7-2) (P_{el}).

Column J: Combined efficiency of generator and rectifier computed by inputting the value of the current from column H in the expression (7-4) (Eff.)

Column K: Power, in watts, extracted by wind turbine from freely flowing wind ($P_{turbine}$) computed by inputting the values of electrical power and combined efficiency from columns I and J in expression (7-3)

Column L: Power, in watts, extracted by wind turbine from freely flowing wind at standard air density ($P_{std\text{-}turbine}$) calculated by inputting values of air density and turbine power from columns E and K in expression (7-5).

Column M: Wind direction, in degrees, from North

Any row showing ' * ', ' # ' or ' @ ' in the error flag column does not contain any values in columns E, G, I, J, K and L as the corresponding data was not considered for evaluating performance of novel VAWT as described in paragraph 7.2.0 in this chapter.

A portion of the spreadsheet depicting the use of various columns is enclosed in Appendix-9.Further it is supplemented with a sample calculation in Appendix-10.

7.3.4 Power Performance Characteristics: BINS Method

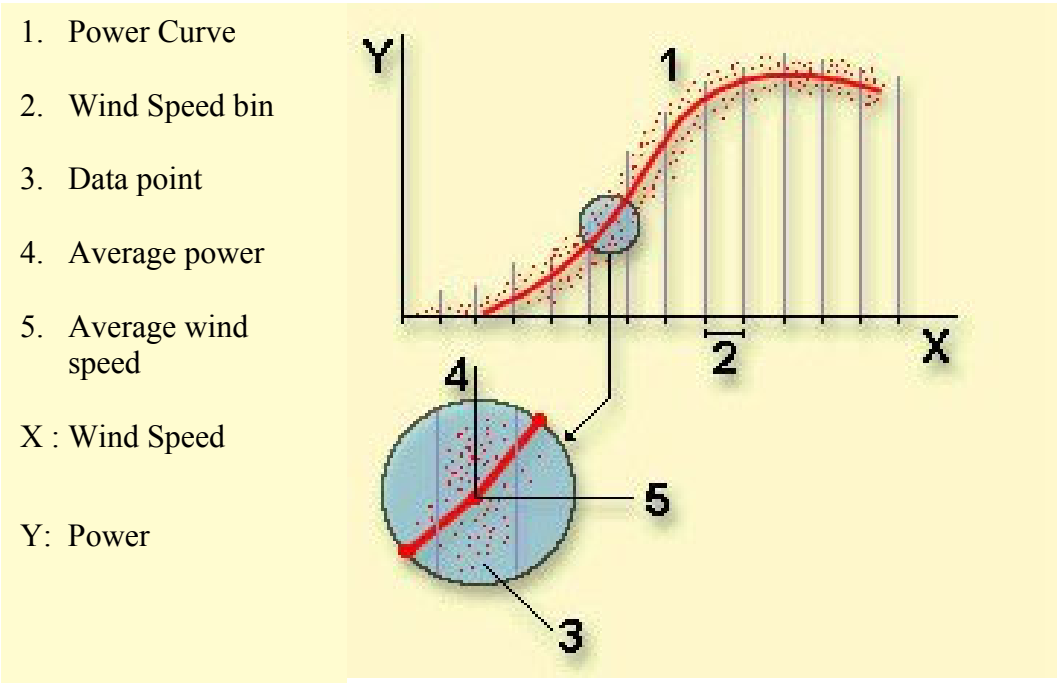

Figure 7.2

7.3.4.1 The unsteady nature of the wind required development of a statistical method of determining turbine performance. The method used is known as BINS method, which is graphically shown in figure 7.2. The method involved dividing the wind speed range into equally spaced bins. The bin size was selected as 1 m/s. The power developed in the wind turbine corresponding to each wind speed was

inputted in the respective bin. Average power for each wind speed bin was computed by dividing the sum of the values of power by the number of inputted values in that bin i.e. bin frequency. The average power so computed corresponded to the average wind speed of that bin. The BINS method was implemented using MSEXCEL software for computation of power performance characteristics of the novel VAWT for two load resistances of 104 ohms and 56.7 ohms.

7.3.5 Computation of Coefficient of Performance:

7.3.5.1 The Coefficient of Performance, C_p, corresponding to average wind speed of each bin was computed by dividing the average power output of rotor by the power contained in freely flowing wind given by the expression:

$$P_{wind} = 0.5\ \rho_0 A V^3$$

Where ρ_0 = Dry air density at sea level at 15 degrees C = 1.225 kg/m^3
A = Swept area of rotor = 1.8767 m^2 and
V = average wind speed for the bin

The characteristic curves showing variation of C_p with wind speed were drawn for the two external loads of 56.7 ohms and 104 ohms.

7.3.6 Determination of Tip Speed Ratio:

7.3.6.1 The alternator along with the rectifier was calibrated in the university laboratory as described in paragraph 5.6.0 of chapter 5 and the following characteristic curves were drawn:

a) Output current (I) versus combined efficiency (η_{com});

b) Output current (I) versus rotational speed (N) for loads of 104 ohms and 56.7 ohms and

c) Power output (P_{out}) versus power input (P_{in})

Further a relation (see equation (5-6) in paragraph 5.6.3.4 of chapter 5) was established between the power output (P_{out}) and shaft power input (P_{in}) for alternator by using the best curve fitting method in MSEXCEL The relation is as follows:

$$P_{out} = .0033\ P_{in}^{\ 2} + 0.0796\ P_{in} \qquad (5\text{-}6)$$

It is important to mention here that power output of the alternator with rectifier was same as the electrical power dissipated in the load resistor i.e. $P_{out} = P_{el}$ and the power input was same as the rotor power output i.e. $P_{in} = P_{std\text{-}turbine}$.

The equation (5-6) was used to determine the electrical power output dissipated in the load corresponding to average wind speed of each bin by inputting the average power output of rotor as computed by using BINS method described at paragraph 7.3.4 above. Further the average current flowing through the load corresponding to average wind speed of each bin was determined from the following expression:

$$I = (P_{out}/ R)^{0.5}$$

7.3.6.2 The following relations were also established experimentally between the output current and alternator speed for load resistances of 104 ohms and 56.7 ohms (see equations (5-7) and (5-8) in paragraph 5.6.3.4 of chapter 5 for details).

For load of 104 ohms, N = 404.31 I

For load of 56.7 ohms, N = 252.33 I

By inputting the average current as determined in paragraph 7.3.6.1 above, the rotational speed of the wind rotor was established for average wind speed of each bin. Hence the tip speed ratio was computed from the following equation:

$$\lambda = \pi DN /60V$$

Where D = Rotor diameter = 0.98 m

V = Average wind speed for the bin

The variation of coefficient of performance with tip speed ratio was worked out for each load.

7.3.7 Computation of Shaft Torque:

7.3.7.1 The shaft torque corresponding to average wind speed of each bin was determined from the following expression:

τ = Average power output of rotor / angular speed

Where angular speed (ω) was computed from rotational speed (N) by using the relation

$$\omega = 2\pi N/60$$

The variation of shaft torque (τ) with rotor speed (N) was plotted for the two load resistances.

Chapter 8: Test Results and Discussions:

General

The field tests were carried out on the novel VAWT prototype with two different loads. The data obtained from these test results was compiled and analysed by using various tools as described in the previous chapter. This chapter presents the field test results in tabular as well as graphical form and includes a detailed analysis of the test results to reason out the trends obtained.

8.1.0 Field Test Results:

8.1.1 The Table 8.1 shows the performance characteristics of the novel VAWT computed on the basis of the BINS method described at paragraph 7.3.4 of chapter 7. The power performance results are based on a purely resistive load of 104 ohms connected across the alternator, which was directly coupled with the rotor. However the performance results are only of the turbine rotor and do not include the performance of the coupled alternator. Further since the power extracted by the rotor from the wind varies with air density, the power output of the wind rotor obtained at different air densities was computed for a standard air density of 1.225 kg/m^3 (density of dry air at sea level at 15^0 C). The details for measurement of turbine power and its standardisation for air density are given in paragraph 7.3.3 of the previous chapter.

8.1.2 During the testing of the novel VAWT with external load resistance of 104 ohms, the wind anemometer, which was mounted at a height of 1.45 m from ground, recorded a maximum wind speed of 17.06 m/s. However, there were very few samples of the wind speed above 16 m/s. Hence it was not considered

statistically appropriate to include the data for wind speeds above 16 m/s for evaluating the power performance.

Wind speed bin	**Avg. wind speed**	**Power extracted by rotor at standard air density**	**Power contained in free wind stream**	**Coeffici-ent of Perform-ance**	**Avg. electrical power output**	**Avg. output current**	**Rotati-onal speed**	**Tip speed ratio**	**Shaft Torque**
	V	$P_{Std\text{-}turbine}$	P_{wind}	C_p	P_{el}	I	N	λ	τ
(m/s)	(m/s)	(W)	(W)		(W)	(A)	(r.p.m.)		(Nm)
0 – 1	0.5	0.000	0.14	0.0000	0.000	0.000	0	0.00	0.00
1 – 2	1.5	0.300	3.88	0.0773	0.024	0.015	6	0.21	0.47
2 – 3	2.5	3.385	17.96	0.1885	0.307	0.054	22	0.45	1.47
3 – 4	3.5	9.344	49.28	0.1896	1.032	0.100	40	0.59	2.22
4 – 5	4.5	16.056	104.75	0.1533	2.129	0.143	58	0.66	2.65
5 – 6	5.5	21.641	191.24	0.1132	3.268	0.177	72	0.67	2.88
6 – 7	6.5	23.705	315.68	0.0751	3.741	0.190	77	0.61	2.95
7 – 8	7.5	24.645	484.94	0.0508	3.966	0.195	79	0.54	2.98
8 – 9	8.5	31.913	705.92	0.0452	5.901	0.238	96	0.58	3.17
9 – 10	9.5	33.465	985.53	0.0340	6.360	0.247	100	0.54	3.20
10 – 11	10.5	39.393	1330.67	0.0296	8.257	0.282	114	0.56	3.30
11 – 12	11.5	43.613	1748.21	0.0249	9.749	0.306	124	0.55	3.37
12 – 13	12.5	62.016	2245.08	0.0276	17.628	0.412	166	0.68	3.56
13 – 14	13.5	67.110	2828.15	0.0237	20.204	0.441	178	0.68	3.60
14 – 15	14.5	76.274	3504.33	0.0218	25.270	0.493	199	0.70	3.66
15 – 16	15.5	71.241	4280.52	0.0166	22.419	0.464	188	0.62	3.63

Table 8.1

8.1.3 The power performance results of the turbine for external load of 56.7 ohms are given in Table 8.2. The performance characteristics were restricted to average wind speed of 10.5 m/s as the number of samples beyond this average speed were not enough to give true representation of the data.

Wind speed bin	**Avg. wind speed**	**Power extracted by rotor at standard air density**	**Power contained in free wind stream**	**Coefficient of Performance**	**Avg. electrical power output**	**Avg. output current**	**Rotational speed**	**Tip speed ratio**	**Shaft Torque**
	V	$P_{Std\text{-}turbine}$	P_{wind}	C_p	P_{el}	I	N	λ	τ
(m/s)	(m/s)	(W)	(W)		(W)	(A)	(r.p.m.)		(Nm)
0 – 1	0.5	0.000	0.14	0.0000	0.000	0.000	0	0.00	0.00
1 – 2	1.5	0.342	3.88	0.0880	0.028	0.022	6	0.19	0.59
2 – 3	2.5	1.876	17.96	0.1044	0.161	0.053	13	0.28	1.33
3 – 4	3.5	6.751	49.28	0.1370	0.688	0.110	28	0.41	2.32
4 – 5	4.5	11.824	104.75	0.1129	1.403	0.157	40	0.45	2.85
5 – 6	5.5	17.188	191.24	0.0899	2.343	0.203	51	0.48	3.20
6 – 7	6.5	22.202	315.68	0.0703	3.394	0.245	62	0.49	3.44
7 – 8	7.5	26.803	484.94	0.0553	4.504	0.282	71	0.49	3.60
8 – 9	8.5	31.635	705.92	0.0448	5.821	0.320	81	0.49	3.74
9 – 10	9.5	33.460	985.53	0.0340	6.358	0.335	84	0.46	3.78
10 – 11	10.5	40.872	1330.67	0.0307	8.766	0.393	99	0.48	3.94

Table 8.2

8.1.4 The figures 8.1 through 8.4 show the graphical representation of the tabulated data for performance characteristics of the novel VAWT. The various characteristic curves are as follows:

a) Figure 8.1: Power curves illustrating the variation of the power output of the rotor ($P_{std\text{-}turbine}$) with the wind speed (V).

b) Figure 8.2: Variation of coefficient of performance (C_p) with wind speed (V).

c) Figure 8.3: Variation of coefficient of performance (C_p) with tip speed ratio (λ).

d) Figure 8.4: Variation of shaft torque (τ) with rotor speed (N).

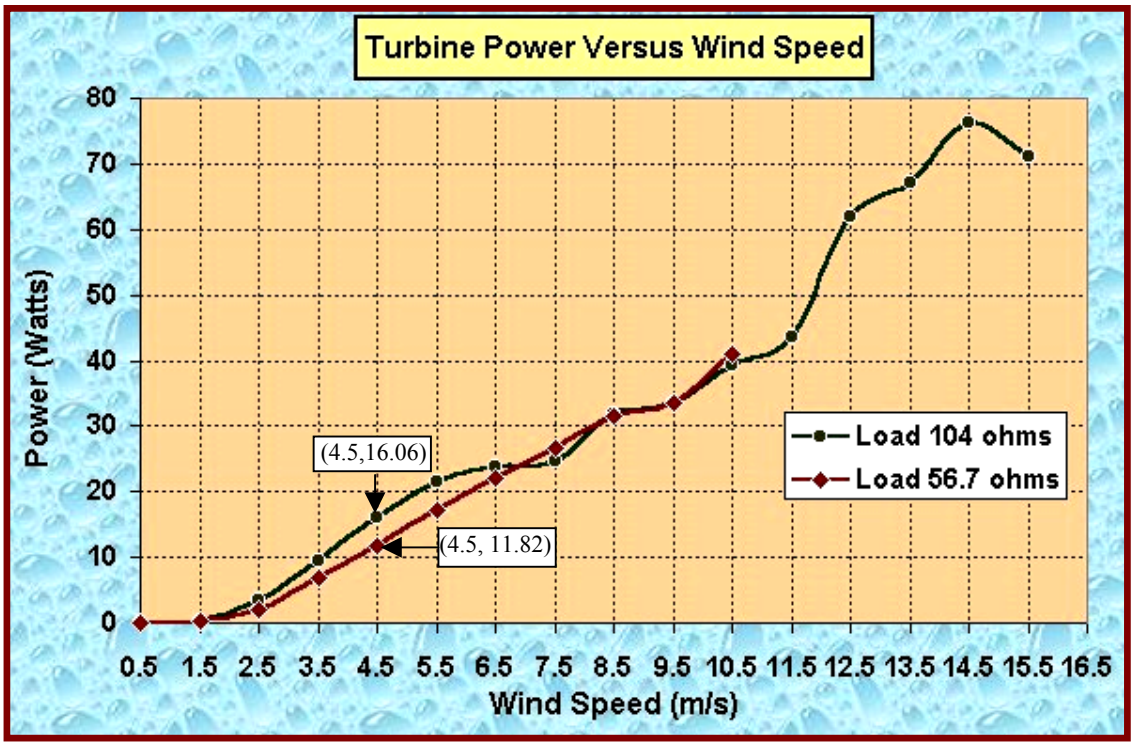

Figure 8.1

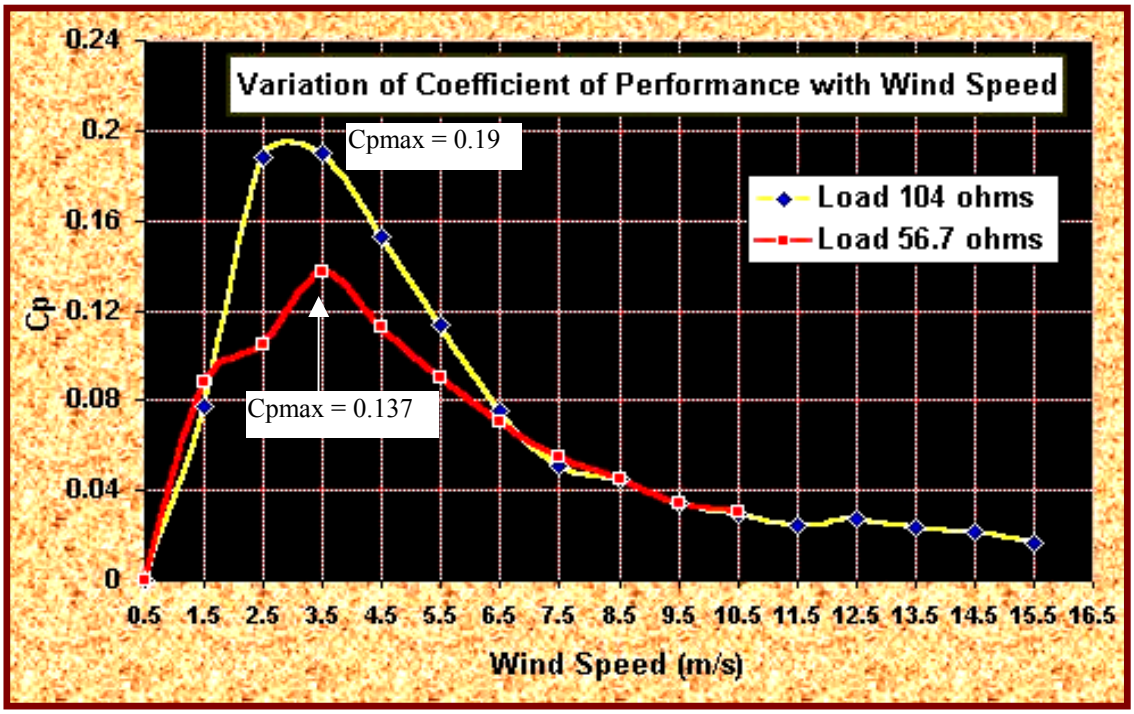

Figure 8.2

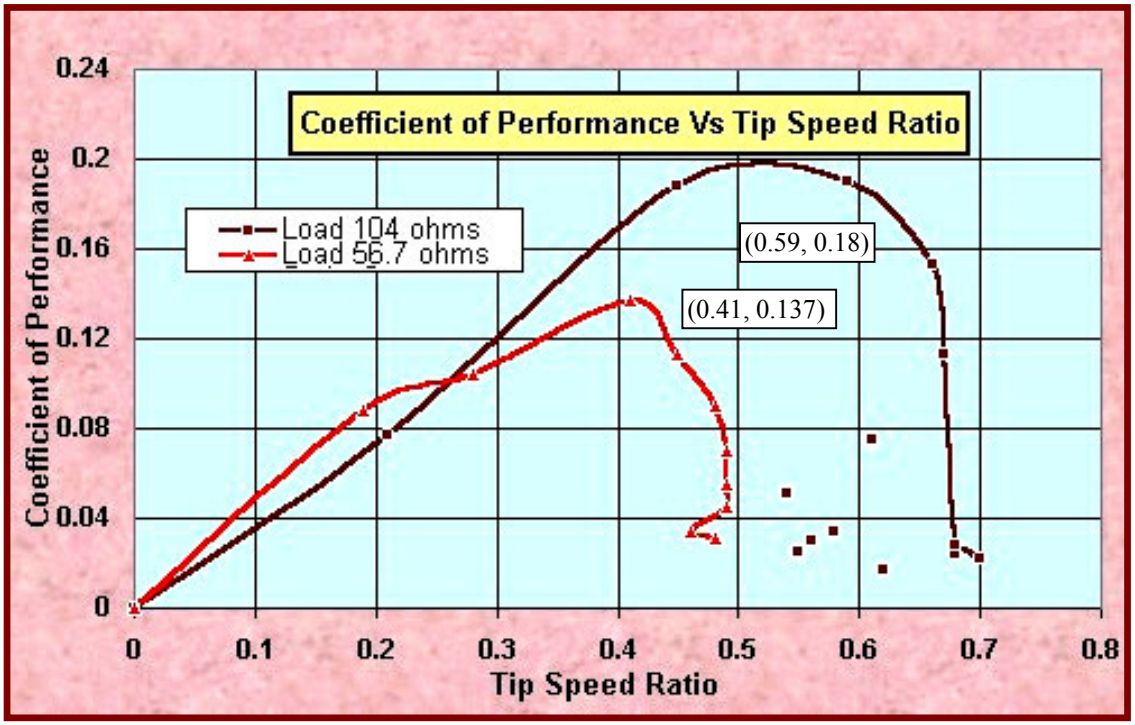

Figure 8.3

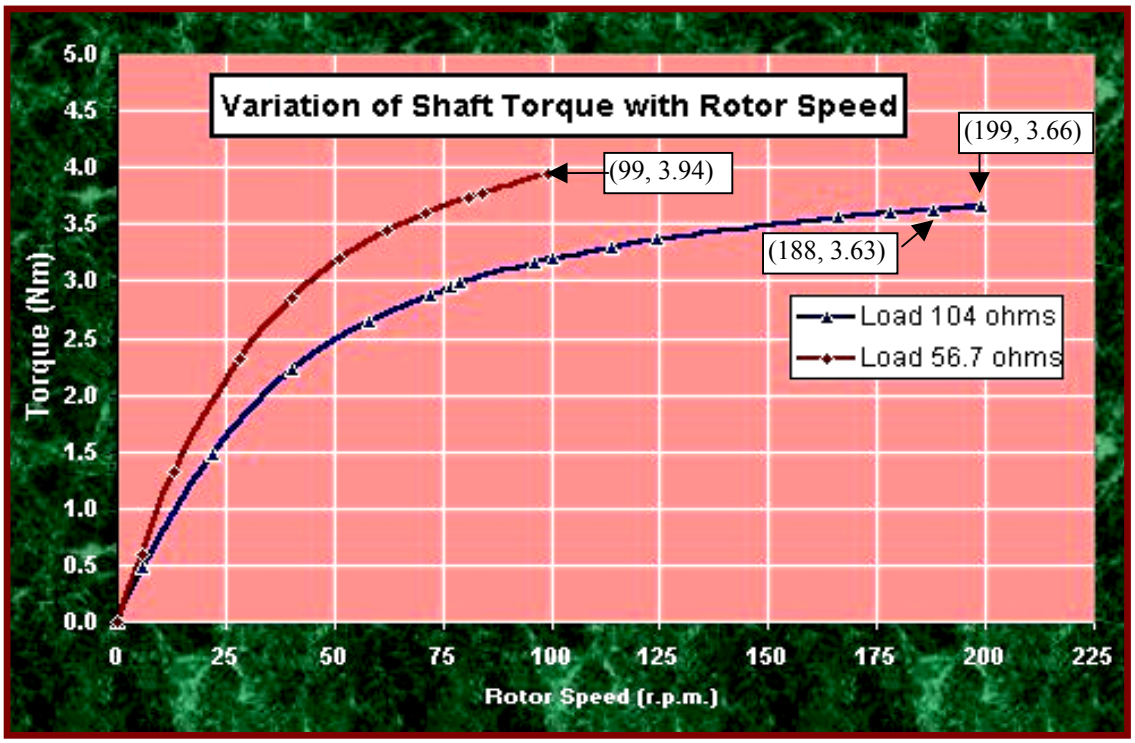

Figure 8.4

8.2.0 Discussions on Test Results:

8.2.1 Family of Power Curves:

8.2.1.1 The figure 8.1 illustrates two power curves for the novel VAWT, one for each of the two external loads of 104 and 56.7 ohms. As can be seen from these power curves, the power extracted by the rotor at any wind speed varied depending upon the load on the rotor. For example the power output of the rotor with external load of 104 ohms was 16.06 watts at average wind speed of 4.5 m/s, which was 36% higher than the power output of 11.82 watts with external load of 56.7 ohms at same wind speed (see values of $P_{std\text{-}turbine}$ in tables 8.1 and 8.2). This dependency of power extraction ability of the rotor on the load emerges more clearly in the figure 8.2, which shows variation of coefficient of performance (C_p) with wind speed for the two loads. As can be seen from the graph, the coefficient of performance reached a value of 0.19 at average wind speed of 3.5 m/s in case of external load resistance of 104 ohms whereas it was only 0.137 in case of 56.7 ohms load at same average wind speed. In fact a family of power curves could be obtained by varying the external load resistance.

8.2.1.2 It is customary to expect a single power curve for a wind turbine irrespective of its loading, which can be used for estimating the average annual energy production for any of its installation. It is an unusual experience of having a family of power curves for a wind turbine. This unusual experience is due to the fact that most of the wind turbines, which are currently available on the market, are of fixed rotational speed type. However, the novel VAWT is a variable speed machine for which it is not possible to obtain a single power curve unless its rotational speed is optimised to vary with the wind speed on a fixed pattern irrespective of the load on the machine. This fact has been explained mathematically in the succeeding paragraph.

8.2.1.3 The power extracted by a wind turbine from freely flowing wind stream is given by the expression:

$$P_{turbine} = 0.5\ C_P\ \rho\ A\ V^3$$

For a rotor of fixed swept area (A) and standard air density, the power extracted by a wind turbine is a function of coefficient of performance (C_P) and wind speed (V)

$$P_{turbine} = f\ (C_P,\ V) \qquad (8\text{-}1)$$

Further the coefficient of performance, C_P, is a function of tip speed ratio (λ), which is dependent upon two independent variables – rotational speed and the wind speed. Hence it can be stated that coefficient of performance is a function of rotational speed and the wind speed. Mathematically, we have

$$C_P = f\ (\omega,\ V) \qquad (8\text{-}2)$$

Substituting C_P from (8-2) in (8-1), we have

$$P_{turbine} = f\ (f\ \ (\omega,\ V),\ V)$$

It follows from the above expression that that power output of a wind turbine is a function of its rotational speed and the wind speed.

In case of fixed rotational speed, the only independent variable is wind speed. Therefore, the power extracted by a fixed speed rotor varies with wind speed only. However, in the case of a variable speed rotor, the power is not only a function of the wind speed but also of the rotational speed of the turbine.

For each wind speed, the power extracted by the rotor varies with the rotational speed of the rotor. In fact by carrying out a series of experiments spread over a long time period, in which wind speed is available over a wide spectrum, it is possible to obtain a family of power curves, each curve showing the variation of power with wind speed for a fixed rotational speed. For each wind speed, the rotational speed which corresponds to the maximum power can be determined. By joining such points, the power maximisation curve can be obtained. Therefore it follows from the above discussions that a variable speed rotor can be advantageously used to capture maximum energy from winds by allowing the rotor speed to vary optimally with the wind speed. For obtaining a constant frequency output from the coupled alternator irrespective of the rotor speed, both differential (e.g. mechanical or electrical frequency changing devices) and non-differential (e.g. static frequency changers or rotary devices) are available.

8.2.1.4 The power curves for the novel VAWT as shown in figure 8.1 indicate that the power output of the turbine varied between 0 and 76.27 watts for wind speed ranging from 0 to 15.5 m/s for the external load of 104 ohms on the alternator. With the external load of 56.7 ohms, the variation in power output was 0 to 40.87 watts for wind speed ranging from 0 to 10.5 m/s. The power/weight ratio of the novel VAWT is not very promising. However the turbine started generating power at average wind speed of 1.5 m/s, which is lower than cut in speeds of most of the wind turbines currently available on the market. The cut-in wind speed usually ranges from 3 to 4 m/s.

8.2.1.5 Further the power output of the turbine steadily increased with wind speed, which is a usual trend. However the peaks or the plateaux of the power curves, if existing, were not visible in the curves obtained here. The power curve for external load of 104 ohms did show a decline in the value of power beyond a wind speed of 14.5 m/s. But the declining part of the curve was too small to establish 76.27 watts as the peak value. The figure 8.4 shows the variation of

shaft torque with rotor speed. As can be seen from the graph the shaft torque reached near saturation at rotor speed of 165 r.p.m. in the case of an external load of 104 ohms. The torque reached a maximum value of 3.66 Nm at average rotor speed of 199 r.p.m. The saturating torque points out that the power curve might be reaching its peak or plateau at the corresponding wind speed of 14.5 m/s because the rotor speed as well as torque showed decline beyond this wind speed (see last two rows of data in table 8.1).

8.2.2 Variation of Coefficient of Performance with Wind Speed:

8.2.2.1 The figure 8.2 depicts the variation of coefficient of performance with wind speed. As already stated, the power extracted by the variable speed novel VAWT at any wind speed is dependent upon the load. Hence separate curves were drawn for loads of 104 ohms and 56.7 ohms. In both cases the coefficient of performance rose sharply with the wind speed and reached its peak ($C_{P\ max}$ = 0.19 for 104 ohms and 0.137 for 56.7 ohms) at average wind speed of 3.5 m/s beyond which it started declining. However the declining portions of the curves are relatively much flatter than their rising counterparts.

8.2.2.2 An important feature worth noting in the curves is that the coefficient of performance of the novel VAWT remained relatively higher in the most probable wind speed range (1.5 m/s to 7.5 m/s) than the rest of the wind spectrum. The figure 8.5 plots the probability distribution of wind speed recorded during the testing period with the external load of 56.7 ohms. As can be seen from the graph, the wind speed varied between 1.5 and 7.5 m/s for over 80% of the testing period. In this most probable wind speed range, the coefficient of performance increased from 0.088 at 1.5 m/s to 0.137 at 3.5 m/s of wind speed and then gradually rolled down to 0.055 at 7.5 m/s. The annual energy yield from this pattern of C_p versus wind speed curve can be expected to be higher in comparison with the one in which the higher values of C_p are

available only at high wind speeds. However the maximum value of C_p of the novel VAWT, derived from these field test results, is lower than those of other wind turbines currently available on the market as discussed at paragraph 8.2.3.2 of this chapter.

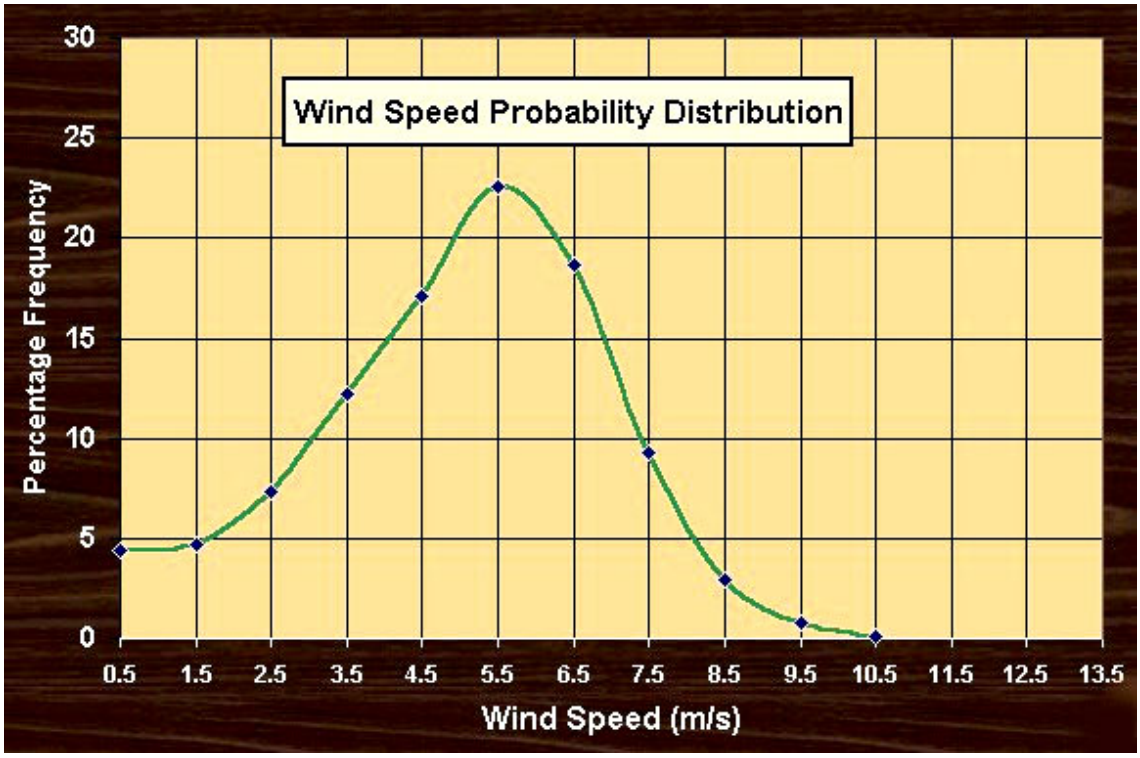

Figure 8.5

8.2.3 Variation of Coefficient of Performance with Tip Speed Ratio:

8.2.3.1 The graph in figure 8.3 shows the variation of coefficient of performance with tip speed ratio. As evident from the graph, C_p gradually increased with the tip speed ratio and reached a peak value of 0.137 at tip speed ratio of 0.41 in case of external load of 56.7 ohms. The subsequent portion of the curve shows a sharp decline in the value of C_p to 0.045 with the tip speed ratio varying in the narrow range of 0.41 to 0.49. The coefficient of performance versus tip speed ratio curve for external load of 104 ohms shows a maximum value of C_p of 0.19 at tip

speed ratio of 0.59 and sharp decline thereafter. In fact the curve is not very smooth with values of Cp varying between .0166 and 0.19 with tip speed ratio in the range of 0.54 to 0.70 as shown by a number of points in the graph. However the best fitting curve has been drawn to bring out a trend.

8.2.3.2 The maximum value of C_P (i.e. 0.19) obtained for the novel VAWT for the wind speed ranging from 0 to 15.5 m/s is much lower than those of horizontal axis wind turbines currently available on the market ($C_{P\ max}$ for HAWTs lies in the range of 0.37 to 0.49). Further, it is also lower than that of Darrieus rotors ($C_{P\ max}$ for Darrieus rotors varies between 0.3 and 0.39).

8.2.4 Variation of Shaft Torque with Rotational Speed:

8.2.4.1 The figure 8.4 plots the variation of shaft torque with rotor speed. As can be seen from the graph, the novel VAWT has low rotational speed and high shaft torque. For wind speeds in the range of 0 to 15.5 m/s, the rotor speed varied between 0 and 199 r.p.m. for external load of 104 ohms. The shaft torque increased sharply with rotor speed as clear from the initial part of curve and reached near saturation at rotor speed of around 165 r.p.m. The maximum shaft torque was 3.66 Nm at rotor speed of 199 r.p.m. Further the shaft torque versus rotor speed curve for load resistance of 56.7 ohms was higher than that for 104 ohms load resistance at any rotor speed. But the plateau of the curve could not be established as the maximum wind speed during the testing period was only 10.14 m/s.

8.2.4.2 The low rotational speed of the rotor is attributable to its high solidity ratio. In the present form, the novel VAWT is unsuitable for generation of electricity due to its low speed although the frequency of the induced e.m.f. in alternator has been increased by using a high number of poles (twelve poles) to compensate

for low speed. The novel VAWT can be more suitably used for mechanical applications such as for pumping of water in remote areas.

Chapter 9: Conclusions and Recommendations

General

This chapter outlines the conclusions drawn from the results of the field tests carried out on the novel VAWT prototype and includes certain recommendations for improving its performance characteristics.

9.1.0 Conclusions:

9.1.1 The test set up, which was planned, calibrated and verified for accuracy of measurements at labs of University of Strathclyde before deployment at the test site, carried out the field testing of the novel VAWT prototype successfully and provided useful data for the development of its performance characteristics. The power performance curves were drawn for two different resistive loads connected across the directly coupled alternator. The power performance characterisation was only for the wind rotor and did not include the performance of the alternator. The following conclusions were drawn from the analysis of the field test results:

a) In case of a variable speed rotor like the novel VAWT, the power output of the rotor at any wind speed is dependent upon the load on the machine as the power extracted by the wind rotor is not only a function of wind speed but also of the rotor speed which will vary depending upon the machine loading. Hence it is not possible to obtain a single power curve showing the variation of power extracted by the wind rotor against the wind speed unless the rotor speed is optimised to vary with the wind speed on a fixed pattern irrespective of the load on the machine. By conducting a series of experiments over a long time period when the wind is available over a

wide spectrum, a family of power curves, each curve corresponding to a fixed rotational speed of the rotor, can be established. From this family of curves, the power maximisation curve can be drawn (see paragraph 8.2.1 of chapter 8 for details).

b) By optimising the rotor speed to follow the wind speed in a pre-determined pattern, it is possible to operate the variable speed rotor at the peak of the coefficient of performance versus tip-speed ratio curve at all times. This will ensure capturing maximum energy from the wind at all wind speeds irrespective of the rotor loading.

c) Two power curves were drawn for two different loads on the novel VAWT, which illustrated the usual trend of steady increase in power output of the wind rotor with the wind speed. The power output of the rotor increased gradually from 0 to 76.27 watts with wind speed ranging from 0 to 15.5 m/s for the external load of 104 ohms. With the external load of 56.7 ohms, the variation in power output was 0 to 40.87 watts for wind speed ranging from 0 to 10.5 m/s. However the peaks or plateaux, if existing in the power curves of the novel VAWT, could not be established conclusively due to the limited wind speed spectrum available during the testing period, although the shaft torque did show saturation beyond rotor speed of 165 r.p.m. in case of external load of 104 ohms on the alternator. The shaft torque versus rotor speed curve reached a peak value of 3.66 Nm at a rotor speed of 199 r.p.m., corresponding to a wind speed of 14.5 m/s and power output of 76.27 watts.

d) The novel VAWT started generating power at an average wind speed of 1.5 m/s which is lower than the cut in speeds of most of the wind turbines currently available on the market (usually varying between 3 to 4 m/s).

e) The power output/weight ratio of the novel VAWT is low.

f) The coefficient of performance, C_P, gradually increased with the tip speed ratio (λ) as expected and reached a maximum value of 0.137 for a tip speed ratio of 0.41 in the case of external load of 56.7 ohms. The curve showed a sharp decline thereafter pointing to possible stalling of rotor in turbulence. Further, the peak value of the coefficient of performance was 0.19 in case of external load resistance of 104 ohms connected across the alternator.

g) The variation of coefficient of performance with wind speed showed a noticeable feature that the C_P of the novel VAWT remained relatively high in the most probable wind speed range. The wind speed varied between 1.5 and 7.5 m/s for over 80% of the testing period with the load of 56.7 ohms. For this wind speed range, the coefficient of performance increased from 0.088 at 1.5 m/s to 0.137 at 3.5 m/s of wind speed and then gradually reduced to 0.055 at 7.5 m/s. The annual energy yield from this pattern of C_p versus wind speed curve can be expected to be higher in comparison with the one in which the higher values of C_p are available only at high wind speeds.

h) The maximum value of coefficient of performance of the novel VAWT determined from the field test results (i.e.0.19) is far lower than those of horizontal axis wind turbines currently available on the market. The peak value of C_P for horizontal axis wind turbines is in the range of 0.37 to 0.49. Further, it appears to be lower than that of Darrieus rotors also ($C_{P\ max}$ for Darrieus rotors lies in the range of 0.3 to 0.39).

i) The novel VAWT is a slow rotating wind turbine with high shaft torque. For wind speeds in the range of 0 to 15.5 m/s, the rotational speed varied

between 0 to 199 r.p.m for an external load of 104 ohms. The low rotational speed of the rotor is attributable to its high solidity ratio.

j) The low rotational speed of the novel VAWT makes it unsuitable for generation of electricity unless it is coupled with a gearbox to convert low rotor speed into high rotational speed required for alternator. Alternately the novel VAWT can be used for mechanical applications such as for pumping of water in remote areas which are commercially nonviable for transmission of electricity or inaccessible due to poor weather conditions.

In nutshell, it appears that the power performance characteristics of the novel VAWT prototype are not challenging to the dominating position of HAWTs in the commercial market.

However, it is prudent to mention here that these field test results proved the existence of a new concept in wind turbine design. Further it was the first prototype of the novel VAWT, which was subjected to full-scale field testing, after successful lab testing of its model at University of Strathclyde in 1998. Like any other experimental work, these field tests pointed out certain clues for improvement in design, which are discussed in the succeeding paragraph. It is, therefore, concluded that the field test results should be viewed as the beginning of a new chapter in wind turbine technology rather than giving an absolute measure of success or failure of the novel VAWT

9.2.0 Recommendations for Design Improvement and Future Work:

The power performance behaviour of the novel VAWT was analysed vis-à-vis its construction and operational features and certain improvement areas were identified. Following is a list of recommendations, which may lead to improvement in its performance characteristics:

9.2.1 Damping of Wind Collection Housing Oscillations:

The moment of inertia of the entire VAWT assembly is very high due to its heavy weight. It is considered that the wind collection housing often misses its equilibrium position and keeps on swivelling around, while following the wind direction. As a result, the wind collection housing is not able to collect and direct as much wind flow as in the ideal situation. This aspect may be verified by mounting a fixed-referencing wind vane (see paragraph 5.2.1 of chapter 5 for explanation of fixed-referencing wind vane) on the top of the housing of the novel VAWT as explained below:

The opening of the housing may first be directed to point towards north direction by using a magnetic compass. The assembly should be locked in this position. The north marking on the wind vane potentiometer may now be aligned with the north direction and the bottom screw of the wind vane may be tightened. In this position, if the tail fin of the wind vane is pointed towards north, the wind vane will record zero degree (or 1.75/358.25 degrees due to electrical gap of 3.5 degree between potentiometer terminals). Now the wind collection housing and the wind vane may be set free to align themselves to the wind direction. If the wind collection housing is aligning to the wind direction as pointed by wind vane, the wind vane reading will remain at zero degree irrespective of the wind direction. Any misalignment in the housing with respect to wind direction pointed by wind vane will be indicated by a shift in reading of wind vane from zero degree.

The data collected over a few days will point out the deficiency of the wind collection housing in aligning with the wind direction.

The oscillations in the wind collection housing may be reduced by using a suitable damping arrangement such as an oil-cup a rocker wheel. Further the

weight of the rotating assembly can be reduced by implementing the recommendation as described at paragraph 9.2.7 of this chapter

9.2.2 Raising Mounting Height of The Turbine:

The novel VAWT prototype is presently mounted very close to the ground (ground clearance from the bottom of the assembly is 0.45 m) due to which it receives a lot of turbulence in wind flow as well as low wind speed. By raising the mounting height by 1.5 meters, it is estimated that the energy production of the turbine can be increased by nearly 40% (considering an exponential factor of 0.2 for shear effects near ground). An opposing factor to this suggestion may be the corresponding increase in visual impacts on the surroundings. However, these are not expected to be very pronounced. There may be further consideration of safety aspects as the entire structure might fall in wind storms This aspect can be taken care of by reducing the overall weight of the assembly as described at paragraph 9.2.7 of this chapter. Guy cables may also be used to enhance the stability.

9.2.3 Review of Blades Profile:

The design of the blades needs to be reviewed to determine whether the blade section is airfoil. The optimal design will lead to improvement in lift forces on the blades and the consequential gain in power extraction by rotor from the wind.

9.2.4 Review of Length of Diffuser:

The purpose of the diffuser at the rear of the turbine is to increase the suction effect so that the overall volumetric flow rate of the wind through the rotor increases. However a small length of the diffuser is equivalent to a wide diffuser

angle which causes sudden expansion in the flow and loss of energy due to development of eddies. The length of diffuser appears to be small in the novel VAWT and needs to be reviewed.

9.2.5 Optimisation of The Rotor Speed:

As the novel VAWT is a variable speed wind turbine, its rotational speed may be optimised with respect to wind speed so that the operating point of the wind turbine always remains at the peak of coefficient of performance versus tip speed ratio curve irrespective of the wind speed and the rotor loading. A number of electrical and mechanical devices are available for this purpose as discussed at paragraph 8.2.1.3 of chapter 8.

9.2.6 Review of Alternator:

The shaft torque versus speed characteristics of the alternator need to be matched with that of the wind rotor otherwise the mismatch problem may lead to either high losses of energy in the alternator or less power extraction by the rotor from the wind. In both cases, the net output is reduced. The novel VAWT prototype has been found to basically a low rotating speed machine. Such rotors, if directly coupled with the generator, are considered unsuitable for generation of electricity. Therefore a gearbox needs to be provided in between the wind rotor and the alternator for converting the low rotational speed of wind rotor to high speed.

Further the internal resistance of the armature winding has been found to be very high (around 19.3 ohms) leading to significant copper losses. The thickness of the wire used needs to be reviewed.

9.2.7 Use of Single Rotor Per Turbine:

Presently, the novel VAWT houses two contra-rotating rotors due to which generators are required to be mounted either on the top or bottom of the housing, making it a very heavy structure. The use of gearbox in between the wind rotor and the alternator, as suggested earlier, will add to the weight of an already heavy assembly. The VAWTs enjoy an advantage over the HAWTs that the generator, gearbox and converter can be positioned at the ground level keeping the rotor free from their weights. This inherent design advantage of the VAWTs can be conveniently adopted in the novel VAWT by keeping one rotor per VAWT. Although this may be considered a major design modification and require thorough reworking, it is considered that it will have significant effect on the turbine performance. Firstly it will reduce the moment of inertia of the wind collection housing reducing its oscillation problems. Secondly the load on the bottom bearing will also reduce increasing its reliability considerably. Thirdly the mounting height of the turbine can also be raised without requiring use of any guy wires. Lastly it will improve the power output/weight ratio of the rotor.

The implementations of the aforesaid suggestions and the repetition of the field tests may constitute an interesting work area for the future.

Appendix-1: Test Results for Verification of Wind Anemometer Calibration

Atmospheric Pressure recorded by mercury barometer = P = 747 mm of Hg
Temperature recorded by thermometer exposed to airflow = T = 16.4 degree C
Air density = d = P * 100000 / (750 * 287.1 * (T + 273.15)) = 1.1981 kg/m^3

Manometer Liquid level	Airflow Static Pressure	Wind Speed as per Pilot tube	Delta logger	Percentage Error
h	P_{st}	V_{act}= 1.9426*(2*P_{st}/d)$^{0.5}$	V	(V_{act} - V) * 100/ V_{act}
(mm)	(N/m^2)	(knots)	(knots)	(%)
0	0	0.0000	0.00	0.00%
7	7	6.6404	6.64	0.01%
12	12	8.6944	8.67	0.28%
19	19	10.9402	10.98	-0.36%
37	37	15.2668	15.34	-0.48%
48	48	17.3887	17.56	-0.98%
59	59	19.2785	19.49	-1.10%
73	73	21.4441	21.32	0.58%
87	87	23.4103	23.57	-0.68%
105	105	25.7183	25.76	-0.16%
134	134	29.0536	29.15	-0.33%
167	167	32.4344	32.27	0.51%
193	193	34.8679	34.93	-0.18%
215	215	36.8016	36.53	0.74%
227	227	37.8146	37.89	-0.20%
233	233	38.3111	38.43	-0.31%
247	247	39.4453	39.39	0.14%
278	278	41.8475	41.73	0.28%
296	296	43.1810	43.01	0.40%
315	315	44.5453	44.97	-0.95%
332	332	45.7316	45.57	0.35%
351	351	47.0220	47.51	-1.04%
369	369	48.2126	47.98	0.48%
387	387	49.3745	49.76	-0.78%
406	406	50.5720	50.53	0.08%
421	421	51.4977	51.54	-0.08%
439	439	52.5871	52.79	-0.39%
451	451	53.3010	53.67	-0.69%
468	468	54.2963	54.36	-0.12%
479	479	54.9307	54.87	0.11%
497	497	55.9532	55.79	0.29%
487	487	55.3875	55.56	-0.31%
479	479	54.9307	54.67	0.47%
461	461	53.8887	53.54	0.65%
449	449	53.1827	52.87	0.59%
437	437	52.4672	52.07	0.76%
411	411	50.8824	51.37	-0.96%
391	391	49.6290	49.29	0.68%
373	373	48.4732	48.71	-0.49%

Manometer Liquid level	Airflow Static Pressure	Wind Speed as per Pilot tube	Delta logger	Percentage Error
h	P_{st}	$V_{act}= 1.9426*(2*P_{st}/d)^{0.5}$	V	$(V_{act} - V) * 100/ V_{act}$
(mm)	(N/m^2)	(knots)	(knots)	(%)
357	357	47.4221	47.43	-0.02%
334	334	45.8691	45.87	0.00%
311	311	44.2616	44.23	0.07%
297	297	43.2539	43.48	-0.52%
278	278	41.8475	42.17	-0.77%
259	259	40.3922	40.19	0.50%
243	243	39.1246	39.31	-0.47%
219	219	37.1423	37.54	-1.07%
198	198	35.3167	35.03	0.81%
177	177	33.3913	33.15	0.72%
165	165	32.2396	32.41	-0.53%
153	153	31.0451	31.31	-0.85%
137	137	29.3770	29.19	0.64%
115	115	26.9151	26.87	0.17%
100	100	25.0985	25.16	-0.25%
91	91	23.9424	23.87	0.30%
79	79	22.3080	22.54	-1.04%
53	53	18.2720	18.21	0.34%
41	41	16.0709	16.19	-0.74%
30	30	13.7470	13.83	-0.60%
19	19	10.9402	11.03	-0.82%
7	7	6.6404	6.67	-0.45%
0	0	0.0000	0.00	0.00%
34	34	14.6348	14.61	0.17%
87	87	23.4103	23.41	0.00%
119	119	27.3792	27.57	-0.70%
61	61	19.6025	19.76	-0.80%
137	137	29.3770	29.21	0.57%
211	211	36.4576	36.27	0.51%
265	265	40.8573	40.69	0.41%
325	325	45.2469	45.76	-1.13%
252	252	39.8426	39.56	0.71%
277	277	41.7722	41.43	0.82%
202	202	35.6716	35.43	0.68%
250	250	39.6842	39.93	-0.62%
315	315	44.5453	44.74	-0.44%
379	379	48.8615	48.74	0.25%
423	423	51.6199	51.53	0.17%
389	389	49.5019	49.21	0.59%
307	307	43.9761	43.75	0.51%
253	253	39.9215	39.74	0.45%
193	193	34.8679	34.59	0.80%
114	114	26.7978	26.69	0.40%
73	73	21.4441	21.32	0.58%

Manometer Liquid level	Airflow Static Pressure	Wind Speed as per Pilot tube	Delta logger	Percentage Error
h	P_{st}	$V_{act}= 1.9426*(2*P_{st}/d)^{0.5}$	V	$(V_{act} - V) * 100/ V_{act}$
(mm)	(N/m^2)	(knots)	(knots)	(%)
23	23	12.0368	12.13	-0.77%

Appendix- 2: Test Results for Verification of Wind Vane Calibration

Angular rotation as per Cardboard marking	Direction reading as per Wind Vane	Percentage Error
Qc	Qwv	(Qc-Qwv)*100/Qc
(Degrees)	(Degrees)	
1.75	1.78	-1.71%
15	15.23	-1.53%
35	34.20	2.29%
60	59.76	0.40%
90	91.10	-1.22%
120	121.70	-1.42%
145	146.11	-0.77%
170	168.99	0.59%
180	181.30	-0.72%
205	203.34	0.81%
220	221.23	-0.56%
235	234.04	0.41%
255	256.56	-0.61%
270	268.03	0.73%
285	282.98	0.71%
300	301.76	-0.59%
320	317.89	0.66%
330	328.23	0.54%
345	343.97	0.30%
355	357.23	-0.63%
358.25	358.90	-0.18%

Appendix- 3: Test Results for Verification of Thermocouple Calibration

Temperature recorded by thermometer	Temperature interpreted by logger from thermocouple output	Difference in temperatures
T'	T	(T'-T)
(Degree C)	(Degree C)	(Degrees C)
100	99.8	0.20
96.7	96.23	0.47
91.9	91.74	0.16
87.1	86.85	0.25
81.5	81.61	-0.11
76.9	76.74	0.16
69.3	69.06	0.24
61.4	61.78	-0.38
55.7	55.98	-0.28
50.1	50.17	-0.07
44.3	44.13	0.17
40.9	40.54	0.36
35.3	35.39	-0.09
30.2	30.47	-0.27
27.3	27.17	0.13
23.2	23.11	0.09
19.2	19.17	0.03
17.1	17.19	-0.09
3.4	3.21	0.19
4.1	4.17	-0.07
5.7	5.96	-0.26
7.6	7.78	-0.18
9.5	9.76	-0.26
11.3	11.39	-0.09
13.5	13.43	0.07
15.2	15.31	-0.11
17	17.11	-0.11

Appendix- 4:Test Results for Verification of Composite CT Filter Circuit

External Load resistance = 26 ohms
Heat dissipation capacity = 400 Watts
Max. permissible current = $(400/26)^{0.5}$ = 3.92 Amperes

Current as per mutimeter	Current as recorded by logger	Error
I'	I	I'-I
(Amperes)	(Amperes)	(Amperes)
0.00	0.00	0.00
0.06	0.06	0.00
0.08	0.08	0.00
0.10	0.10	0.00
0.14	0.14	0.00
0.18	0.18	0.00
0.25	0.25	0.00
0.31	0.31	0.00
0.48	0.48	0.00
1.00	1.00	0.00
1.76	1.75	0.01
1.98	1.98	0.00
2.09	2.08	0.01
0.78	0.78	0.00
3.15	3.15	0.00
3.67	3.66	0.01
3.80	3.80	0.00
2.13	2.13	0.00
0.05	0.05	0.00
0.09	0.09	0.00
0.00	0.00	0.00
0.14	0.14	0.00
1.21	1.21	0.00
1.71	1.71	0.00
2.97	2.97	0.00
1.09	1.09	0.00
0.65	0.65	0.00
0.43	0.43	0.00
0.87	0.87	0.00
1.32	1.32	0.00
0.23	0.23	0.00
0.74	0.74	0.00
2.71	2.71	0.00
3.41	3.41	0.00
1.54	1.54	0.00
0.78	0.78	0.00

Appendix- 5: Test Results for Calibration of Tachometer Coupled with DC Shunt Motor

Voltage Output of DC Generator Techometer	Rotational Speed Measured by Optical Techometer
V_{speed}	N
(Volts)	(r.p.m.)
0	0
0.32	16
0.64	32
1.96	95
2.48	119
3.41	165
4.5	212
5.17	247
6.44	309
8.56	409
10.97	527
12.87	615
15.62	746
17.83	852
21.4	1024
23.98	1146
27.6	1319
29.74	1421
31.8	1520
32.87	1571
33.21	1590
33.42	1597
31.46	1503
29.72	1420
28.65	1367
26.64	1270
24.61	1176
22.92	1095
20.76	994
19.72	942
17.56	839
15.8	757
13.81	657
11.72	560
8.91	427
7.26	344
5.55	265
4.27	201
3.12	149
1.55	72
1.26	58
0.46	21

Appendix-6: Test Results for Calibration of DC Shunt Motor

Outer diameter of Motor casing = 220 mm
Height of chain clip attached to motor casing = 17.145 mm
Diameter of screw fastening the chain to motor clip = 3.429 mm
Arm Length of Dynamometer = (220/2)+17.145+(3.429/2) = 128.86 mm = 0.12886 m

V_f	I_f	V_a	I_a	V_{speed}	N	Load	Torque	P_{input}	P_{output}	Efficiency
					$47.787 \times V_{speed}$		LoadxArmx9.81	$V_f x I_f + V_a x I_a$	TorquexNx2xpie/60	$P_{output} x 100 / P_{input}$
(Volts)	(Amperes)	(Volts)	(Amperes)	(Volts)	(r.p.m.)	(kg)	(Nm)	(watts)	(watts)	(%)
212	0.314	71	1.02	12.590	601.64	0.675	0.8533	138.99	53.73	38.66%
212	0.314	71.5	1.12	12.645	604.27	0.750	0.9481	146.65	59.96	40.89%
210	0.312	72.7	1.44	12.816	612.44	1.025	1.2957	170.21	83.06	48.80%
211	0.312	73.8	1.63	12.970	619.80	1.225	1.5485	186.13	100.46	53.97%
210	0.311	74.8	1.86	13.103	626.15	1.450	1.8330	204.44	120.13	58.76%
211	0.312	75.9	2.07	13.263	633.80	1.650	2.0858	222.95	138.37	62.06%
210	0.311	76.8	2.32	13.460	643.21	1.875	2.3702	243.49	159.57	65.54%
210	0.310	77.5	2.65	13.421	641.35	2.150	2.7179	270.48	182.44	67.45%
210	0.309	77.6	2.69	13.431	641.83	2.200	2.7811	273.63	186.83	68.28%
210	0.309	77.2	2.73	13.353	638.10	2.200	2.7811	275.65	185.74	67.38%
210	0.309	73.8	2.99	12.704	607.09	2.400	3.0339	285.55	192.78	67.51%
212	0.309	80.9	0.92	14.406	688.42	0.650	0.8217	139.94	59.21	42.31%
212	0.308	81.8	1.08	14.600	697.69	0.775	0.9797	153.64	71.54	46.56%
212	0.309	81.9	1.13	14.626	698.93	0.825	1.0429	158.06	76.29	48.27%
212	0.306	82.5	1.24	14.708	702.85	0.900	1.1377	167.17	83.70	50.07%
211	0.307	83.8	1.44	14.908	712.41	1.100	1.3905	185.45	103.69	55.91%
211	0.307	84.5	1.63	14.995	716.57	1.275	1.6117	202.51	120.88	59.69%
212	0.308	84.7	1.74	14.992	716.42	1.400	1.7698	212.67	132.71	62.40%
211	0.307	84.8	1.91	14.985	716.09	1.550	1.9594	226.75	146.86	64.77%
210	0.307	85.8	2.17	15.064	719.86	1.775	2.2438	250.66	169.06	67.45%
210	0.306	86.4	2.4	15.395	735.68	2.000	2.5282	271.62	194.68	71.67%
210	0.306	86.3	2.69	15.090	721.11	2.250	2.8443	296.41	214.67	72.43%
211	0.306	86.2	2.99	14.256	681.25	2.500	3.1603	322.30	225.34	69.92%
209	0.305	75.6	3.16	13.037	623.00	2.600	3.2867	302.64	214.32	70.82%

V_f	I_f	V_a	I_a	V_{speed}	N	Load	Torque	P_{input}	P_{output}	Efficiency
					$47.787xV_{speed}$		LoadxArmx9.81	$V_fxI_f + V_axI_a$	TorquexNx2xpie/60	$P_{output}x100/P_{input}$
(Volts)	(Amperes)	(Volts)	(Amperes)	(Volts)	(r.p.m.)	(kg)	(Nm)	(watts)	(watts)	(%)
209	0.305	57.7	2.88	9.770	466.88	2.475	3.1287	229.92	152.89	66.50%
210	0.306	58.4	2.5	9.981	476.96	2.200	2.7811	210.26	138.84	66.03%
210	0.306	57.7	2.22	9.948	475.39	2.000	2.5282	192.35	125.80	65.40%
211	0.307	56.9	1.99	9.824	469.46	1.850	2.3386	178.01	114.91	64.55%
211	0.307	54.7	1.55	9.529	455.36	1.500	1.8962	149.56	90.37	60.43%
211	0.307	53.3	1.28	9.352	446.90	1.150	1.4537	133.00	68.00	51.13%
211	0.307	53	1.17	9.323	445.52	1.025	1.2957	126.79	60.42	47.66%
211	0.307	52.1	0.88	9.247	441.89	0.800	1.0113	110.63	46.77	42.28%
212	0.308	53.8	0.67	9.597	458.61	0.450	0.5689	101.34	27.31	26.94%
211	0.307	54	0.6	9.711	464.06	0.350	0.4424	97.18	21.49	22.11%
211	0.319	15.2	0.54	2.532	121.00	0.950	1.2009	75.52	15.21	20.14%
211	0.318	14.82	0.43	2.486	118.80	0.655	0.8280	73.47	10.30	14.01%
211	0.318	14.45	0.35	2.454	117.27	0.550	0.6953	72.16	8.53	11.83%
211	0.318	14.35	0.28	2.433	116.27	0.400	0.5056	71.12	6.15	8.65%
210	0.310	34.8	1.13	5.989	286.20	1.100	1.3905	104.42	41.65	39.89%
210	0.310	38.2	0.94	5.943	284.00	0.950	1.2009	101.01	35.70	35.34%
211	0.309	33.3	0.78	5.866	280.32	0.750	0.9481	91.17	27.82	30.51%
211	0.309	33.1	0.63	5.802	277.26	0.620	0.7838	86.05	22.74	26.43%
211	0.309	31.6	0.47	5.610	268.09	0.400	0.5056	80.05	14.19	17.72%
211	0.309	31.8	0.45	5.645	269.76	0.350	0.4424	79.51	12.49	15.71%
212	0.307	97.5	0.84	17.561	839.19	0.500	0.6321	146.98	55.52	37.77%
212	0.306	98.1	0.98	17.655	843.68	0.550	0.6953	161.01	61.40	38.13%
212	0.306	98.1	1.05	17.629	842.44	0.600	0.7585	167.88	66.88	39.84%
212	0.306	98.5	1.14	17.700	845.83	0.650	0.8217	177.16	72.74	41.06%
211	0.305	99	1.38	17.843	852.66	0.875	1.1061	200.98	98.71	49.12%
211	0.305	99.6	1.52	17.826	851.85	1.050	1.3273	215.75	118.34	54.85%
211	0.305	100.4	1.62	17.870	853.95	1.125	1.4221	227.00	127.11	56.00%
210	0.304	100.4	1.74	17.928	856.73	1.225	1.5485	238.54	138.86	58.21%
211	0.304	100.7	1.86	17.967	858.59	1.350	1.7066	251.45	153.36	60.99%
210	0.305	101.2	2	18.026	861.41	1.500	1.8962	266.45	170.96	64.16%

V_f	I_f	V_a	I_a	V_{speed}	N	Load	Torque	P_{input}	P_{output}	Efficiency
					$47.787xV_{speed}$		LoadxArmx9.81	$V_fxI_f + V_axI_a$	TorquexNx2xpie/60	$P_{output}x100/P_{input}$
(Volts)	(Amperes)	(Volts)	(Amperes)	(Volts)	(r.p.m.)	(kg)	(Nm)	(watts)	(watts)	(%)
210	0.304	101.9	2.18	18.115	865.66	1.650	2.0858	285.98	188.99	66.08%
210	0.304	102.7	2.47	18.190	869.25	1.950	2.4650	317.51	224.27	70.63%
210	0.304	102.4	2.67	18.114	865.61	2.100	2.6546	337.25	240.51	71.32%
210	0.303	95.3	3.08	16.717	798.86	2.400	3.0339	357.15	253.67	71.03%

Appendix-7: Test Results for Calibration of Alternator and Rectifier using Calibrated DC Motor

A) Load resistance connected across rectifier = 104 ohms

Calibrated DC Shunt Motor									Alternator and Rectifier			
V_f	I_f	V_a	I_a	V_{speed}	N	P_{input}	Efficiency	P_{output}	P_{in}	Output Current	P_{out}	Efficiency
					$47.787 x V_{speed}$	$V_f x I_f + V_a x I_a$	*	$P_{input} x Eff.$	$=P_{output\ motor}$	I	I^2R	$P_{output} x 100 / P_{input}$
(Volts)	(Amperes)	(Volts)	(Amperes)	(Volts)	(r.p.m.)	(Watts)		(Watts)	(Watts)	(Amperes)	(Watts)	(%)
218.4	0.32	6.01	0.57	1.013	48.41	73.31	0.2275	16.68	16.68	0.12	1.50	8.98
218.3	0.32	8.32	0.69	1.418	67.76	75.60	0.2783	21.04	21.04	0.17	3.01	14.29
218.3	0.32	11.09	0.92	1.859	88.84	80.06	0.3676	29.43	29.43	0.22	5.03	17.11
218.1	0.32	13.75	1.12	2.281	109.00	85.19	0.4365	37.18	37.18	0.27	7.58	20.39
217.7	0.32	18.51	1.35	3.038	145.18	94.65	0.5057	47.87	47.87	0.36	13.48	28.16
217.4	0.32	23.53	1.76	3.701	176.86	110.98	0.6026	66.88	66.88	0.44	20.13	30.11
217.4	0.32	26.47	1.84	4.050	193.54	118.27	0.6175	73.04	73.04	0.48	23.96	32.81
217.6	0.32	28.7	1.97	4.402	210.36	126.17	0.6390	80.63	80.63	0.52	28.12	34.88
217.6	0.32	30.36	2.12	5.075	242.52	134.00	0.6596	88.38	88.38	0.60	37.44	42.36
217.2	0.32	34.5	2.31	5.591	267.18	149.20	0.6791	101.32	101.32	0.66	45.30	44.71
217.4	0.32	37.4	2.49	6.000	286.72	162.69	0.6908	112.40	112.40	0.71	52.43	46.64
217.2	0.32	38.7	2.56	6.256	298.96	168.58	0.6936	116.93	116.93	0.74	56.95	48.70
217.2	0.32	39.9	2.62	6.431	307.32	174.04	0.6952	121.00	121.00	0.76	60.07	49.64
216.9	0.32	42.6	2.8	6.854	327.53	188.69	0.6957	131.27	131.27	0.81	68.23	51.98
216.9	0.32	45.3	2.97	7.285	348.13	203.95	0.6901	140.74	140.74	0.86	76.92	54.65
216.2	0.31	47.4	3.07	7.542	360.41	212.54	0.6841	145.39	145.39	0.89	82.38	56.66
216.2	0.31	49.6	3.19	7.791	372.31	225.25	0.6742	151.85	151.85	0.92	88.03	57.97
216.4	0.31	52.9	3.4	8.123	388.17	246.94	0.6498	160.47	160.47	0.96	95.85	59.73

* Motor Efficiency = $-0.1012 I_a^2 + 0.551 I_a - 0.0537$

Where I_a is the armature current (For details, please refer to DC motor calibration in paragraph 5.6.2 of chapter 5)

B) Load resistance connected across rectifier = 56.7 ohms

Calibrated DC Shunt Motor								Alternator and Rectifier			
V_f	I_f	V_a	I_a	V_{speed}	N	P_{input}	Efficiency	P_{output}	P_{in}	Output Current	P_{out}	Efficiency
					$47.787 \times V_{speed}$	$V_f I_f + V_a I_a$	*	$P_{input} \times$ Eff.	$=P_{output\ motor}$	I	I^2R	$P_{output} \times 100 / P_{input}$
(Volts)	(Amperes)	(Volts)	(Amperes)	(Volts)	(r.p.m.)	(Watts)		(Watts)	(Watts)	(Amperes)	(Watts)	(%)
217.4	0.32	5.38	0.6	0.998	47.69	72.80	0.2405	17.51	17.51	0.20	2.27	12.96
217.4	0.32	6.93	0.75	1.254	59.92	74.77	0.3026	22.63	22.63	0.24	3.27	14.43
217.5	0.32	8.32	0.88	1.481	70.77	76.92	0.3528	27.14	27.14	0.28	4.45	16.38
217.5	0.32	10.92	1.11	1.785	85.30	81.72	0.4332	35.40	35.40	0.34	6.55	18.51
217.3	0.32	12.71	1.29	2.026	96.82	85.93	0.4887	41.99	41.99	0.39	8.62	20.54
216.9	0.32	14.85	1.52	2.385	113.97	91.98	0.5500	50.59	50.59	0.45	11.48	22.70
216.9	0.32	17.58	1.75	2.872	137.24	100.17	0.6006	60.17	60.17	0.53	15.93	26.47
216.5	0.32	19.35	1.92	3.053	145.89	106.43	0.6312	67.18	67.18	0.58	19.07	28.39
216.7	0.32	21.72	2.13	3.418	163.34	115.61	0.6608	76.39	76.39	0.65	23.96	31.36
216.7	0.31	23.82	2.32	3.571	170.65	122.44	0.6799	83.25	83.25	0.68	26.22	31.49
216.7	0.31	24.67	2.41	3.989	190.62	126.63	0.6864	86.92	86.92	0.75	31.89	36.69
216.6	0.31	27.72	2.69	4.446	212.46	141.71	0.6962	98.66	98.66	0.84	40.01	40.55
215.9	0.31	29.98	2.9	4.597	219.68	153.87	0.6931	106.65	106.65	0.87	42.92	40.24
215.7	0.31	31.2	3.01	4.805	229.62	160.78	0.6879	110.60	110.60	0.91	46.95	42.45
215.9	0.31	32.9	3.17	5.011	239.46	171.22	0.6760	115.75	115.75	0.95	51.17	44.21
215.8	0.31	34.3	3.3	5.222	249.54	180.09	0.6625	119.31	119.31	0.99	55.57	46.58
216.2	0.31	35.2	3.38	5.327	254.56	186.00	0.6525	121.37	121.37	1.01	57.84	47.66

* Motor Efficiency = $-0.1012 I_a^2 + 0.551 I_a - 0.0537$

Where I_a is the armature current (For details, please refer to DC motor calibration in paragraph 5.6.2 of chapter 5)

Appendix- 8: Data Obtained from Trial Run

DELTA-T LOGGER
VAWT
28/07/01 16:08
07/08/01 14:38

Channel number	5	1		2	4		6		31
Sensor code	5	TM1		WS	TCK		I-1		WV2
Label	5	cold jn		Wind Speed	Temp		I-Gen-1		Wind Dir
Unit	5	deg C		Knots	deg C		A		deg
Minimum value	5	22.04		0	13.74		0		5.557
Maximum value	5	25.32		18.8	23.08		0.25		353.5
28/07/01 16:08	5	22.8		3.95	19.72		0.05		188.2
28/07/01 16:18	5	22.54		5.56	19.32	$	0.05		187
28/07/01 16:28	5	22.3		5.74	19.1	$	0.05		183.7
28/07/01 16:38	5	22.04		5.45	18.97	$	0.05		183.2
28/07/01 16:48	5	22.05	$	5.21	19.45	$	0.05	#	181.1
28/07/01 16:58	5	22.54		5.37	19.52	$	0.05		179
28/07/01 17:08	5	22.82		5.49	20.02	$	0.05		185.3
28/07/01 17:18	5	22.82		4.83	19.42	$	0.05		189.3
28/07/01 17:28	5	23.09		4.87	19.7	$	0.05		189.6
28/07/01 17:38	5	23.36	$	4.49	19.4	$	0.05		192.3
28/07/01 17:48	5	23.36	$	4.73	19.37	$	0.05		197.9
28/07/01 17:58	5	23.36	#	4.68	19.37	$	0.05	#	183.9
28/07/01 18:08	5	23.64		5.12	18.85	$	0.05		179.5
28/07/01 18:18	5	23.64		5.15	19.05	$	0.05		178.6
28/07/01 18:28	5	23.91		5.3	18.52	$	0.05		179.3
28/07/01 18:38	5	23.91		4.77	18.52	$	0.05		178.4
28/07/01 18:48	5	23.91		5.36	18.52	$	0.05		175.3
28/07/01 18:58	5	23.91		4.87	18.32	$	0.05		180.9
28/07/01 19:08	5	23.91		4.69	18.32	$	0.05		183.5
28/07/01 19:18	5	23.91		4.85	18.32	$	0.05		182.5
28/07/01 19:28	5	23.91		4.91	18.12	$	0.05		177.9
28/07/01 19:38	5	24.18		4.67	18.2	$	0.05		177
28/07/01 19:48	5	24.18		4.65	18	$	0.05		174.2
28/07/01 19:58	5	24.46	$	4.01	18.1	$	0.01		186.7
28/07/01 20:08	5	24.46	$	4.49	17.7	$	0.05		184
28/07/01 20:18	5	24.46		5.05	17.85	$	0.05		175.8
28/07/01 20:28	5	24.18		4.83	17.6	$	0.05		175.1
28/07/01 20:38	5	24.18		5.04	17.38	$	0.05		174.8
28/07/01 20:48	5	24.46		5.14	17.48	$	0.05		172.7
28/07/01 20:58	5	24.46		5.06	17.48	$	0.05		171.3
28/07/01 21:08	5	24.46		4.83	17.28	$	0.05		173.5
28/07/01 21:18	5	24.46		6.01	17.25	$	0.05		167.9
28/07/01 21:28	5	24.46		5.45	17.08	$	0.05		168.1
28/07/01 21:38	5	24.46		5.76	16.85	$	0.05		171.1
28/07/01 21:48	5	24.46		6.46	16.88	$	0.05		167
28/07/01 21:58	5	24.73		5.49	16.93	$	0.05		169.8
28/07/01 22:08	5	24.73		5.5	16.75	$	0.05		171.6
28/07/01 22:18	5	24.73		6.26	16.55	$	0.05		164.8
28/07/01 22:28	5	24.73		6.03	16.55	$	0.05		165.6

Channel number	5	1		2	4		6		31
Sensor code	5	TM1		WS	TCK		I-1		WV2
Label	5	cold jn		Wind Speed	Temp		I-Gen-1		Wind Dir
Unit	5	deg C		Knots	deg C		A		deg
28/07/01 22:38	5	24.73		6.03	16.35	$	0.05		170.4
28/07/01 22:48	5	24.73		6.4	16.35	$	0.09		169.1
28/07/01 22:58	5	24.73		6.56	16.55	$	0.05		166.3
28/07/01 23:08	5	24.73		7.1	16.53	$	0.05		167.6
28/07/01 23:18	5	24.73		6.93	16.35	$	0.05		166.3
28/07/01 23:28	5	24.73		6.86	16.15	$	0.09		167.4
28/07/01 23:38	5	25		7.04	16.23	$	0.05		166.5
28/07/01 23:48	5	25		7.2	16.23	$	0.09		167.6
28/07/01 23:58	5	25		7.18	16.2	$	0.09		168.4
29/07/01 00:08	5	25		7.79	16.2	$	0.09		169.1
29/07/01 00:18	5	25		7.28	16.4	$	0.09		169.1
29/07/01 00:28	5	25		7.01	16.2	$	0.09		167.6
29/07/01 00:38	5	25		6.81	16.43	$	0.09		171.4
29/07/01 00:48	5	25		7.51	16.4	$	0.09		170.2
29/07/01 00:58	5	25		6.32	16.43	$	0.09		175.1
29/07/01 01:08	5	25		6.14	16.2	$	0.05		179.3
29/07/01 01:18	5	25		6.2	16.23	$	0.09		174.4
29/07/01 01:28	5	25		6.66	16.43	$	0.09		175.1
29/07/01 01:38	5	25		6	16.43	$	0.05		181.8
29/07/01 01:48	5	25	$	5.53	16.43	$	0.05		183.5
29/07/01 01:58	5	25	$	5.49	16.4	$	0.05		181.1
29/07/01 02:08	5	25		6.14	16.4	$	0.05		181.4
29/07/01 02:18	5	25		5.47	16.4	$	0.05		180.2
29/07/01 02:28	5	25		5.61	16.4	$	0.05		179.1
29/07/01 02:38	5	25		6.15	16.43	$	0.05		179.3
29/07/01 02:48	5	25	$	5.13	16.4	$	0.05		182.8
29/07/01 02:58	5	24.73		4.92	16.13	$	0.05		185.6
29/07/01 03:08	5	24.73		5.45	16.33	$	0.05		186.3
29/07/01 03:18	5	24.73		6.09	16.53	$	0.05		188.6
29/07/01 03:28	5	24.73		5.71	16.55	$	0.05		187.5
29/07/01 03:38	5	24.73	#	6.36	16.75	$	0.05	#	199.3
29/07/01 03:48	5	24.73		6.42	16.75	$	0.05		203.8
29/07/01 03:58	5	24.73		6.89	16.75	$	0.09		199.1
29/07/01 04:08	5	24.73	#	7.68	16.53	$	0.09	#	203.5
29/07/01 04:18	5	24.73		7.19	16.35	$	0.09		205.6
29/07/01 04:28	5	24.73		7.3	16.15	$	0.05		205.6
29/07/01 04:38	5	24.73		6.56	16.15	$	0.05		204.3
29/07/01 04:48	5	24.46		6.42	15.88	$	0.09		206.8
29/07/01 04:58	5	24.46		7.07	16.08	$	0.09		203.5
29/07/01 05:08	5	24.46		7.36	16.08	$	0.09		208.4
29/07/01 05:18	5	24.46		7.28	15.88	$	0.09		214
29/07/01 05:28	5	24.46		8.62	15.88	$	0.09		218
29/07/01 05:38	5	24.46		6.59	15.86	$	0.05		207
29/07/01 05:48	5	24.46	#	6	15.68	$	0.05	#	206.3
29/07/01 05:58	5	24.46		5.6	15.66	$	0.05		210.6
29/07/01 06:08	5	24.46		5.81	15.46	$	0.05		207.7

Channel number	5	1		2	4		6		31
Sensor code	5	TM1		WS	TCK		I-1		WV2
Label	5	cold jn		Wind Speed	Temp		I-Gen-1		Wind Dir
Unit	5	deg C		Knots	deg C		A		deg
29/07/01 06:18	5	24.46		5.16	15.48	$	0.05		208.4
29/07/01 06:28	5	24.46		5.06	15.46	$	0.05		211
29/07/01 06:38	5	24.46		5.9	15.68	$	0.05		212
29/07/01 06:48	5	24.46		5.79	15.46	$	0.05		216.1
29/07/01 06:58	5	24.46		6.48	15.68	$	0.05		216.8
29/07/01 07:08	5	24.46		7.13	15.68	$	0.09		218.5
29/07/01 07:18	5	24.46		6.47	15.86	$	0.05		218.4
29/07/01 07:28	5	24.46		5.4	15.66	$	0.05		215.6
29/07/01 07:38	5	24.46		5.2	15.66	$	0.05		214.2
29/07/01 07:48	5	24.46		5.79	15.88	$	0.05		218
29/07/01 07:58	5	24.46		5.83	16.05	$	0.05		221.5
29/07/01 08:08	5	24.46		5.61	16.05	$	0.05		224
29/07/01 08:18	5	24.46		5.23	16.08	$	0.05		232.2
29/07/01 08:28	5	24.46		6.82	16.05	$	0.05		241.1
29/07/01 08:38	5	24.73		6.87	16.33	$	0.01		253.2
29/07/01 08:48	5	24.73		6.38	16.53	$	0.01		256.5
29/07/01 08:58	5	24.73		5.76	16.93	$	0.01		250.2
29/07/01 09:08	5	24.73		6.25	16.93	$	0.01		251.1
29/07/01 09:18	5	24.73		6.41	16.53	$	0.01		247.9
29/07/01 09:28	5	24.73		7.55	16.73	$	0.05		249.3
29/07/01 09:38	5	24.73		7.77	16.93	$	0.05		250.9
29/07/01 09:48	5	24.73		7.75	17.13	$	0.05		254.1
29/07/01 09:58	5	24.73		7.49	17.13	$	0.05		254.9
29/07/01 10:08	5	24.73		6.87	16.73	$	0.01		248.3
29/07/01 10:18	5	24.73		6.43	17.53	$	0.05		243.4
29/07/01 10:28	5	24.73		8.25	17.73	$	0.05		252
29/07/01 10:38	5	24.73	#	8.32	17.53	$	0.05	#	260.9
29/07/01 10:48	5	24.73		10.06	17.33	$	0.09		261.4
29/07/01 10:58	5	25		9.06	17.8	$	0.05		257.9
29/07/01 11:08	5	25		8.31	17.8	$	0.05		257.4
29/07/01 11:18	5	25		8.36	17.8	$	0.05		256
29/07/01 11:28	5	25		7.89	17.6	$	0.05		248.3
29/07/01 11:38	5	25		7.05	17.43	$	0.05		250.2
29/07/01 11:48	5	25		9.03	17.4	$	0.05		253.9
29/07/01 11:58	5	25		9.59	18.22	$	0.09		257.8
29/07/01 12:08	5	25		8.1	18.22	$	0.05		255.1
29/07/01 12:18	5	25		7.68	17.2	$	0.05		246.9
29/07/01 12:28	5	25		7.04	17.8	$	0.05		248.3
29/07/01 12:38	5	25		6.96	17.2	$	0.05		237.6
29/07/01 12:48	5	24.73		8.95	17.73	$	0.05		253.9
29/07/01 12:58	5	25		9.94	17.4	$	0.09		254.6
29/07/01 13:08	5	24.73		9.97	17.53	$	0.09		258.1
29/07/01 13:18	5	24.73	#	10.28	17.35	$	0.09	#	259.5
29/07/01 13:28	5	24.73		10.61	17.53	$	0.09		263
29/07/01 13:38	5	24.73		9.74	17.73	$	0.09		259.3
29/07/01 13:48	5	24.73		10.51	17.73	$	0.09		257.6

Channel number	5	1		2	4		6		31
Sensor code	5	TM1		WS	TCK		I-1		WV2
Label	5	cold jn		Wind Speed	Temp		I-Gen-1		Wind Dir
Unit	5	deg C		Knots	deg C		A		deg
29/07/01 13:58	5	24.73		9.61	18.12	$	0.09		259.3
29/07/01 14:08	5	24.46		11.18	17.88	$	0.09		257.8
29/07/01 14:18	5	24.46		10.56	17.65	$	0.09		256.2
29/07/01 14:28	5	24.46		11.46	17.68	$	0.13		258.6
29/07/01 14:38	5	24.46		11.25	17.65	$	0.13		260.6
29/07/01 14:48	5	24.46		10.82	18.27	$	0.09		258.5
29/07/01 14:58	5	24.46		9.85	17.85	$	0.09		260.2
29/07/01 15:08	5	24.46		9.38	18.07	$	0.05		252.3
29/07/01 15:18	5	24.46		8.72	18.05	$	0.05		251.6
29/07/01 15:28	5	24.46		8.31	17.88	$	0.05		250.4
29/07/01 15:38	5	24.46		8.06	17.65	$	0.05		251.1
29/07/01 15:48	5	24.46		7.26	17.88	$	0.05		240.4
29/07/01 15:58	5	24.73		7.76	18.12	$	0.05		242.9
29/07/01 16:08	5	24.73		7.63	18.15	$	0.05		241.5
29/07/01 16:18	5	24.73		7.91	18.32	$	0.09		236.4
29/07/01 16:28	5	24.73		7.35	17.93	$	0.05		238.1
29/07/01 16:38	5	24.73		7.54	17.93	$	0.05		242
29/07/01 16:48	5	24.73		7.97	18.15	$	0.05		246.2
29/07/01 16:58	5	24.73		7.81	18.52	$	0.05		247.6
29/07/01 17:08	5	24.73		7.35	18.32	$	0.05		238.7
29/07/01 17:18	5	24.46		7.62	18.05	$	0.05		236
29/07/01 17:28	5	24.46		8.37	18.25	$	0.05		247.9
29/07/01 17:38	5	24.73		9.16	19.12	$	0.05		253.5
29/07/01 17:48	5	24.73		9.29	21.11	$	0.05		250.2
29/07/01 17:58	5	24.73		8.92	23.08	$	0.05		249
29/07/01 18:08	5	24.73	#	9.04	22.09	$	0.05	#	250.4
29/07/01 18:18	5	24.73		8.95	22.69	$	0.05		249.9
29/07/01 18:28	5	24.73		8.24	22.91	$	0.05		243.7
29/07/01 18:38	5	24.73		7.97	22.32	$	0.05		240.8
29/07/01 18:48	5	24.73		9.02	20.71	$	0.05		242.9
29/07/01 18:58	5	24.73		8.25	20.32	$	0.05		243.7
29/07/01 19:08	5	24.73		9.04	20.14	$	0.05		242.9
29/07/01 19:18	5	24.73		6.98	20.12	$	0.05		243.9
29/07/01 19:28	5	24.73		6.18	20.12	$	0.05		237.6
29/07/01 19:38	5	24.46		7.53	18.45	$	0.05		243.4
29/07/01 19:48	5	24.46		7.76	18.25	$	0.05		243.2
29/07/01 19:58	5	24.18		7.6	18.37	$	0.05		242
29/07/01 20:08	5	24.18		6.66	17.78	$	0.05		239.5
29/07/01 20:18	5	23.91		5.82	17.3	$	0.01		241.3
29/07/01 20:28	5	23.91		5.02	16.93	$	0.01		239.7
29/07/01 20:38	5	23.91	$	4.41	17.3	$	0.01		228.7
29/07/01 20:48	5	23.91		3.75	16.9	$	0.01		222.9
29/07/01 20:58	5	23.91	$	3.69	17.1	$	0.01		225
29/07/01 21:08	5	24.18		4.35	16.78	$	0.01		229.7
29/07/01 21:18	5	24.18		4.88	16.78	$	0.05		233.2
29/07/01 21:28	5	24.46		4.77	16.68	$	0.05		231.1

Channel number	5	1		2	4		6	31
Sensor code	5	TM1		WS	TCK		I-1	WV2
Label	5	cold jn		Wind Speed	Temp		I-Gen-1	Wind Dir
Unit	5	deg C		Knots	deg C		A	deg
29/07/01 21:38	5	24.46		4.93	16.08	$	0.05	231.8
29/07/01 21:48	5	24.46		4.52	15.66	$	0.01	235.2
29/07/01 21:58	5	24.46		5.17	15.66	$	0.05	237.3
29/07/01 22:08	5	24.46		5.15	15.66	$	0.05	237.8
29/07/01 22:18	5	24.46	$	5.89	15.71	$	0.05	239
29/07/01 22:28	5	24.46		4.49	15.71	$	0.01	232.9
29/07/01 22:38	5	24.46		4.4	16.08	$	0.01	227.3
29/07/01 22:48	5	24.73		4.85	16.13	$	0.05	232.4
29/07/01 22:58	5	24.73		6.91	15.93	$	0.05	242
29/07/01 23:08	5	24.73		8.64	15.53	$	0.05	245
29/07/01 23:18	5	24.73		7.85	15.73	$	0.01	245.7
29/07/01 23:28	5	24.73		7.64	15.53	$	0.05	242.9
29/07/01 23:38	5	25		8.39	15.81	$	0.05	244.8
29/07/01 23:48	5	25		7.98	15.81	$	0.05	245.3
29/07/01 23:58	5	25		7.72	15.61	$	0.05	243.9
30/07/01 00:08	5	25		8.1	15.41	$	0.05	246.5
30/07/01 00:18	5	25.32		8.45	15.53	$	0.05	250
30/07/01 00:28	5	25.32		8.02	15.33	$	0.05	249.5
30/07/01 00:38	5	25.31		6.7	15.13	$	0.01	251.6
30/07/01 00:48	5	25.32		7.8	14.93	$	0.05	258.3
30/07/01 00:58	5	25.32		6.31	14.76	$	0.05	264.8
30/07/01 01:08	5	25.32		4.94	14.76	$	0.01	260.7
30/07/01 01:18	5	25.31		5.49	14.93	$	0.01	250.6
30/07/01 01:28	5	25.32		5.93	14.93	$	0.05	238.5
30/07/01 01:38	5	25.32		6.19	14.76	$	0.05	239.4
30/07/01 01:48	5	25.32		7.99	14.53	$	0.05	252.5
30/07/01 01:58	5	25.32		6.38	14.53	$	0.01	259.9
30/07/01 02:08	5	25.31		7.85	14.16	$	0.05	270.7
30/07/01 02:18	5	25.32		6.35	14.13	$	0.01	262
30/07/01 02:28	5	25.32		4.29	13.76	$	0.01	269.7
30/07/01 02:38	5	25.32		3.62	13.74	$	0.01	254.1
30/07/01 02:48	5	25.31		5.06	13.74	$	0.01	247.2
30/07/01 02:58	5	25.31		5.49	14.13	$	0.01	246.4
30/07/01 03:08	5	25.32		5.27	14.36	$	0.01	253.7
30/07/01 03:18	5	25.32		5.19	14.13	$	0.01	251.1
30/07/01 03:28	5	25.32		4.5	13.96	$	0.01	254.2
30/07/01 03:38	5	25.31	$	3.57	14.16	$	0.01	252
30/07/01 03:48	5	25.32		4.45	14.36	$	0.01	246.5
30/07/01 03:58	5	25	$	4.33	14.21	$	0.01	248.5
30/07/01 04:08	5	25		4.03	14.21	$	0.01	249.9
30/07/01 04:18	5	25		3.91	14.21	$	0.01	246.7
30/07/01 04:28	5	25		4.85	14.43	$	0.01	246
30/07/01 04:38	5	25	$	4.69	14.41	$	0.01	249.9
30/07/01 04:48	5	25		4.08	14.41	$	0.01	246.4
30/07/01 04:58	5	25		4.02	14.41	$	0.01	244.3
30/07/01 05:08	5	24.73		3.94	14.13	$	0.01	239.5

Channel number	5	1		2	4		6		31
Sensor code	5	TM1		WS	TCK		I-1		WV2
Label	5	cold jn		Wind Speed	Temp		I-Gen-1		Wind Dir
Unit	5	deg C		Knots	deg C		A		deg
30/07/01 05:18	5	24.73		3.86	13.94	$	0.01		237.6
30/07/01 05:28	5	24.73	#	3.72	13.74	$	0.01	#	239.2
30/07/01 05:38	5	24.73	$	2.77	13.96	$	0.01		231.1
30/07/01 05:48	5	24.73	$	3.01	14.13	$	0.01		237.1
30/07/01 05:58	5	24.73		4.82	14.33	$	0.01		243.6
30/07/01 06:08	5	24.73		5.58	14.33	$	0.01		246.4
30/07/01 06:18	5	24.73		6.11	14.33	$	0.01		249
30/07/01 06:28	5	24.73	#	6.52	14.33	$	0.01	#	250.4
30/07/01 06:38	5	24.73		6.41	14.53	$	0.01		248.8
30/07/01 06:48	5	24.73		6.35	14.56	$	0.01		245.8
30/07/01 06:58	5	24.73		6.14	14.56	$	0.01		245.1
30/07/01 07:08	5	24.73		5.49	14.73	$	0.01		246.7
30/07/01 07:18	5	24.73		5.52	14.76	$	0.01		243.2
30/07/01 07:28	5	24.73		5.48	15.33	$	0.01		243
30/07/01 07:38	5	24.73	$	4.13	15.33	$	0.01		233.6
30/07/01 07:48	5	24.73		3.85	15.73	$	0.01		236.7
30/07/01 07:58	5	24.46		4.24	15.28	$	0.01		227.6
30/07/01 08:08	5	24.46		4.06	15.26	$	0.01		235.3
30/07/01 08:18	5	24.73	$	4.37	16.13	$	0.01		226.8
30/07/01 08:28	5	24.46		5.36	15.66	$	0.05		222.2
30/07/01 08:38	5	24.18		4.58	15.78	$	0.01		225.7
30/07/01 08:48	5	24.18		4.67	16.03	$	0.01		221.7
30/07/01 08:58	5	24.46	$	4.01	16.48	$	0.01		234.5
30/07/01 09:08	5	24.46	$	4.93	16.48	$	0.01	#	225.9
30/07/01 09:18	5	24.46		4.22	16.65	$	0.01		223.3
30/07/01 09:28	5	24.46		4.61	16.65	$	0.05		214.7
30/07/01 09:38	5	24.18	$	4.81	16.78	$	0.01		220.6
30/07/01 09:48	5	24.18	#	5.24	16.78	$	0.05	#	217.5
30/07/01 09:58	5	24.18		5.19	17.38	$	0.01		218.7
30/07/01 10:08	5	24.18		5.21	17.98	$	0.05		217
30/07/01 10:18	5	23.91		4.99	17.3	$	0.05		214
30/07/01 10:28	5	23.91		5.17	17.13	$	0.05		215.6
30/07/01 10:38	5	23.91		5	16.9	$	0.05		210.6
30/07/01 10:48	5	23.91		5.2	17.5	$	0.05		219.1
30/07/01 10:58	5	23.91		5.92	17.5	$	0.05		230.3
30/07/01 11:08	5	23.91		5.57	17.7	$	0.05		231.3
30/07/01 11:18	5	23.91		6.29	17.7	$	0.05		236.4
30/07/01 11:28	5	23.91		6.92	18.12	$	0.05		243.9
30/07/01 11:38	5	23.91		7.02	17.9	$	0.05		236.4
30/07/01 11:48	5	23.91		6.33	17.73	$	0.05		236.6
30/07/01 11:58	5	24.18		6.03	17.8	$	0.05		231.7
30/07/01 12:08	5	24.18		5.77	17.6	$	0.05		235.5
30/07/01 12:18	5	24.18		5.23	17.78	$	0.05		235.2
30/07/01 12:28	5	24.18		5.24	18.2	$	0.05		232.9
30/07/01 12:38	5	24.46		5.47	17.85	$	0.01		239.9
30/07/01 12:48	5	24.46		6.13	17.88	$	0.01		242

Channel number	5	1		2		4		6	31
Sensor code	5	TM1		WS		TCK		I-1	WV2
Label	5	cold jn		Wind Speed		Temp		I-Gen-1	Wind Dir
Unit	5	deg C		Knots		deg C		A	deg
30/07/01 12:58	5	24.18		5.58		17.6	$	0.01	243.2
30/07/01 13:08	5	24.46		5.64		17.65	$	0.01	240.4
30/07/01 13:18	5	24.46		5.26		17.85	$	0.01	241.1
30/07/01 13:28	5	24.46	$	4.85		18.07	$	0.01	239.7
30/07/01 13:38	5	24.46		5.26		18.05	$	0.01	254.9
30/07/01 13:48	5	24.46		5.78		17.45	$	0.01	265.6
30/07/01 13:58	5	24.46		5.7		16.85	$	0.01	265.3
30/07/01 14:08	5	24.46		4.72		16.88	$	0.01	262.3
30/07/01 14:18	5	24.46	$	4.05		16.88	$	0.01	268.1
30/07/01 14:28	5	24.18		4.01		16.2	$	0.01	267.7
30/07/01 14:38	5	24.18		4.28		16.2	$	0.01	266
30/07/01 14:48	5	24.18		4.91		16.2	$	0.01	272.5
30/07/01 14:58	5	24.46		4.46		16.25	$	0.01	269.8
30/07/01 15:08	5	24.46		4.31		16.28	$	0.01	280.3
30/07/01 15:18	5	24.46		5.46		15.48	$	0.01	283.8
30/07/01 15:28	5	24.46		4.77		14.86	$	0.01	287.3
30/07/01 15:38	5	24.46		4.28		14.46	$	0.01	295.4
30/07/01 15:48	5	24.46		4.24		14.06	$	0.01	289.8
30/07/01 15:58	5	24.46	$	2.97		14.08		0	281.2
30/07/01 16:08	5	24.46		1.77		14.26		0	278.4
30/07/01 16:18	5	24.46		2.94		14.28		0	283.3
30/07/01 16:28	5	24.46	$	3.45		14.26		0	284.2
30/07/01 16:38	5	24.46	$	3.17		14.46		0	284
30/07/01 16:48	5	24.46	$	3.05		14.26		0	277
30/07/01 16:58	5	24.73	$	2.09		14.76		0	262.7
30/07/01 17:08	5	24.73	$	1.45		14.93		0	276.5
30/07/01 17:18	5	24.46	$	1.57		14.48		0	261.1
30/07/01 17:28	5	24.73	$	0.61		14.93		0	224
30/07/01 17:38	5	24.73	$	0.81		14.93		0	222.4
30/07/01 17:48	5	24.73	$	1.13		15.13		0	215.2
30/07/01 17:58	5	24.73	$	1.29		14.93		0	219.1
30/07/01 18:08	5	24.73	$	1.77		14.93		0	208.7
30/07/01 18:18	5	24.46	$	1.65		14.86		0	194.4
30/07/01 18:28	5	24.46	$	1.49		15.08		0	181.4

Appendix-9: Sample Data Processing Sheet

Swept Area of Rotor = 1.8767 m2

Load Resistance = 104 ohms

Dry air density at sea level at 15 deg C = 1.2250 kg/m3

Error Flag	Date and time of Observation	Atm. Pressure	Temp.	Air Density	Wind Speed		Current thr. Load	Electrical Power	Com. Efficiency of Gen. & Rect.	Turbine Power	Turbine Power at std. air density	Wind Dir
		P_{Hg}	T	d	WS	V	I	P_{el}	Eff.	$P_{turbine}$	$P_{std\text{-}turbine}$	
	Unit	mm of Hg	deg C	kg/m3	Knots	m/s	A	W	%	W	W	deg
A	B	C	D	E	F	G	H	I	J	K	L	M
	12/08/01 09:01	754.00	16.33	1.2096	2.33	1.20	0.01	0.0104	0.71	1.4555	1.4740	183.30
	12/08/01 09:11	754.00	16.33	1.2096	2.97	1.53	0.01	0.0104	0.71	1.4555	1.4740	188.10
#	12/08/01 09:21	754.00	16.13		3.73		0.05					187.40
	12/08/01 09:31	754.00	16.35	1.2096	4.02	2.07	0.05	0.2600	3.53	7.3569	7.4508	189.50
	12/08/01 09:41	754.00	16.73	1.2080	4.03	2.07	0.05	0.2600	3.53	7.3569	7.4606	179.50
	12/08/01 09:51	754.00	16.53	1.2088	4.12	2.12	0.05	0.2600	3.53	7.3569	7.4554	189.10
	12/08/01 10:01	754.00	16.73	1.2080	4.70	2.42	0.05	0.2600	3.53	7.3569	7.4606	187.50
	12/08/01 10:11	754.00	16.53	1.2088	4.40	2.27	0.05	0.2600	3.53	7.3569	7.4554	179.00
	12/08/01 10:21	754.00	16.73	1.2080	4.75	2.45	0.05	0.2600	3.53	7.3569	7.4606	173.40
	12/08/01 10:31	754.00	16.93	1.2071	4.51	2.32	0.05	0.2600	3.53	7.3569	7.4657	175.60
	12/08/01 10:41	754.00	17.20	1.2060	4.13	2.13	0.01	0.0104	0.71	1.4555	1.4784	198.40
	12/08/01 10:51	754.00	16.73	1.2080	4.49	2.31	0.05	0.2600	3.53	7.3569	7.4606	189.60
	12/08/01 11:01	754.00	16.53	1.2088	4.09	2.11	0.05	0.2600	3.53	7.3569	7.4554	187.90
	12/08/01 11:11	754.00	16.73	1.2080	4.20	2.16	0.05	0.2600	3.53	7.3569	7.4606	200.70
	12/08/01 11:21	754.00	16.33	1.2096	4.25	2.19	0.05	0.2600	3.53	7.3569	7.4503	193.30
	12/08/01 11:31	754.00	16.33	1.2096	4.81	2.48	0.05	0.2600	3.53	7.3569	7.4503	190.00
	12/08/01 11:41	754.00	16.33	1.2096	5.03	2.59	0.05	0.2600	3.53	7.3569	7.4503	189.50
	12/08/01 11:51	754.00	16.53	1.2088	4.73	2.43	0.05	0.2600	3.53	7.3569	7.4554	199.60
	12/08/01 12:01	754.00	16.13	1.2105	6.24	3.21	0.05	0.2600	3.53	7.3569	7.4451	209.10
	12/08/01 12:11	754.00	16.55	1.2087	5.00	2.57	0.05	0.2600	3.53	7.3569	7.4559	205.20
	14/08/01 13:32	761.40	17.65	1.2160	4.93	2.54	0.00	0.0000	0.00	0.0000	0.0000	156.00

Error Flag	Date and time of Observation	Atm. Pressure	Temp.	Air Density	Wind Speed		Current thr. Load	Electrical Power	Com. Efficiency of Gen. & Rect.	Turbine Power	Turbine Power at std. air density	Wind Dir
		P_{Hg}	T	d	WS	V	I	P_{el}	Eff.	$P_{turbine}$	$P_{std\text{-}turbine}$	
	Unit	mm of Hg	deg C	kg/m3	Knots	m/s	A	W	%	W	W	deg
A	B	C	D	E	F	G	H	I	J	K	L	M
	14/08/01 13:37	761.40	17.98	1.2146	8.26	4.25	0.12	1.4976	8.32	17.9999	18.1541	191.90
	14/08/01 13:42	761.40	17.50	1.2166	8.91	4.59	0.13	1.7576	8.99	19.5542	19.6892	181.80
	14/08/01 13:47	761.40	18.12	1.2140	9.61	4.95	0.13	1.7576	8.99	19.5542	19.7312	175.60
	14/08/01 13:52	761.40	18.62	1.2119	9.42	4.85	0.14	2.0384	9.65	21.1172	21.3449	171.40
	14/08/01 13:57	761.40	18.02	1.2144	8.63	4.44	0.15	2.3400	10.31	22.6889	22.8864	177.90
	14/08/01 14:02	761.40	18.42	1.2128	9.87	5.08	0.18	3.3696	12.27	27.4575	27.7345	191.90
	14/08/01 14:07	761.40	18.22	1.2136	10.43	5.37	0.17	3.0056	11.62	25.8590	26.1020	186.10
	14/08/01 14:12	761.40	18.25	1.2135	10.28	5.29	0.16	2.6624	10.97	24.2695	24.5001	190.50
	14/08/01 14:17	761.40	18.45	1.2126	11.44	5.89	0.13	1.7576	8.99	19.5542	19.7535	181.40
	14/08/01 14:22	761.40	18.25	1.2135	9.26	4.77	0.15	2.3400	10.31	22.6889	22.9045	178.60
	14/08/01 14:27	761.40	18.25	1.2135	10.09	5.19	0.16	2.6624	10.97	24.2695	24.5001	194.50
	14/08/01 14:32	761.40	18.45	1.2126	10.25	5.28	0.19	3.7544	12.92	29.0650	29.3613	172.50
	14/08/01 14:37	761.40	18.25	1.2135	9.93	5.11	0.19	3.7544	12.92	29.0650	29.3412	174.90
	14/08/01 14:42	761.40	18.50	1.2124	11.75	6.05	0.18	3.3696	12.27	27.4575	27.7421	160.60
	14/08/01 14:47	761.40	18.10	1.2141	10.19	5.25	0.16	2.6624	10.97	24.2695	24.4875	149.00
	14/08/01 14:52	761.40	17.90	1.2149	8.82	4.54	0.14	2.0384	9.65	21.1172	21.2922	172.80
	14/08/01 14:57	761.40	18.30	1.2133	10.07	5.18	0.14	2.0384	9.65	21.1172	21.3215	192.10
	14/08/01 15:02	761.40	18.27	1.2134	10.29	5.30	0.15	2.3400	10.31	22.6889	22.9061	181.80
	14/08/01 15:07	761.40	18.17	1.2138	9.09	4.68	0.17	3.0056	11.62	25.8590	26.0975	182.10
	14/08/01 15:12	761.40	18.55	1.2122	9.05	4.66	0.14	2.0384	9.65	21.1172	21.3398	175.60
	14/08/01 15:17	761.40	18.37	1.2130	9.64	4.96	0.15	2.3400	10.31	22.6889	22.9140	168.40
	14/08/01 15:22	761.40	18.75	1.2114	9.75	5.02	0.15	2.3400	10.31	22.6889	22.9438	177.70
	14/08/01 15:27	761.40	18.82	1.2111	9.42	4.85	0.16	2.6624	10.97	24.2695	24.5480	183.30
	14/08/01 15:32	761.40	17.98	1.2146	10.47	5.39	0.16	2.6624	10.97	24.2695	24.4774	184.20
	14/08/01 15:37	761.40	17.75	1.2156	8.38	4.31	0.12	1.4976	8.32	17.9999	18.1397	170.20
	14/08/01 15:42	761.40	17.98	1.2146	10.05	5.17	0.12	1.4976	8.32	17.9999	18.1541	175.30
	14/08/01 15:47	761.40	17.75	1.2156	8.21	4.23	0.13	1.7576	8.99	19.5542	19.7061	193.30
	14/08/01 15:52	761.40	17.75	1.2156	8.82	4.54	0.12	1.4976	8.32	17.9999	18.1397	167.40
	14/08/01 15:57	761.40	17.95	1.2147	8.21	4.23	0.13	1.7576	8.99	19.5542	19.7197	182.50

Error Flag	Date and time of Observation	Atm. Pressure	Temp.	Air Density	Wind Speed		Current thr. Load	Electrical Power	Com. Efficiency of Gen. & Rect.	Turbine Power	Turbine Power at std. air density	Wind Dir
		P_{Hg}	T	d	WS	V	I	P_{el}	Eff.	$P_{turbine}$	$P_{std\text{-}turbine}$	
	Unit	mm of Hg	deg C	kg/m3	Knots	m/s	A	W	%	W	W	deg
A	B	C	D	E	F	G	H	I	J	K	L	M
*	14/08/01 16:02	761.40	18.37		8.74		0.11					220.80
	14/08/01 16:07	761.40	17.58	1.2163	8.84	4.55	0.11	1.2584	7.65	16.4542	16.5723	179.10
	14/08/01 16:12	761.40	17.85	1.2151	8.49	4.37	0.13	1.7576	8.99	19.5542	19.7129	158.80
	14/08/01 16:17	761.40	18.25	1.2135	8.29	4.27	0.12	1.4976	8.32	17.9999	18.1709	166.50
	14/08/01 16:22	761.40	18.25	1.2135	8.43	4.34	0.09	0.8424	6.29	13.3883	13.5156	168.10
	14/08/01 16:27	761.40	18.02	1.2144	9.90	5.10	0.11	1.2584	7.65	16.4542	16.5974	176.00
	14/08/01 16:32	761.40	17.83	1.2152	10.75	5.53	0.13	1.7576	8.99	19.5542	19.7115	186.80
	14/08/01 16:37	761.40	17.85	1.2151	10.17	5.24	0.13	1.7576	8.99	19.5542	19.7129	187.50
	14/08/01 16:42	761.40	17.63	1.2161	9.10	4.68	0.14	2.0384	9.65	21.1172	21.2725	134.70
	14/08/01 16:47	761.40	17.45	1.2168	8.06	4.15	0.12	1.4976	8.32	17.9999	18.1210	199.10
	14/08/01 16:52	761.40	17.63	1.2161	9.14	4.71	0.13	1.7576	8.99	19.5542	19.6980	212.90
	14/08/01 16:57	761.40	17.45	1.2168	9.53	4.91	0.10	1.0400	6.97	14.9170	15.0174	186.30
	14/08/01 17:02	761.40	17.03	1.2186	8.14	4.19	0.11	1.2584	7.65	16.4542	16.5410	188.40
	14/08/01 17:07	761.40	16.83	1.2194	8.25	4.25	0.09	0.8424	6.29	13.3883	13.4497	181.40
	14/08/01 17:12	761.40	16.83	1.2194	7.30	3.76	0.09	0.8424	6.29	13.3883	13.4497	178.60
	14/08/01 17:17	761.40	16.83	1.2194	7.06	3.63	0.08	0.6656	5.61	11.8680	11.9224	164.40
	14/08/01 17:22	761.40	16.85	1.2193	9.46	4.87	0.12	1.4976	8.32	17.9999	18.0836	194.00
	14/08/01 17:27	761.40	16.65	1.2202	7.91	4.07	0.11	1.2584	7.65	16.4542	16.5193	193.30
	14/08/01 17:32	761.40	16.63	1.2203	8.74	4.50	0.12	1.4976	8.32	17.9999	18.0699	190.50
	14/08/01 17:37	761.40	16.45	1.2210	8.33	4.29	0.16	2.6624	10.97	24.2695	24.3488	176.00
	14/08/01 17:42	761.40	16.23	1.2219	9.12	4.69	0.13	1.7576	8.99	19.5542	19.6032	162.70
	14/08/01 17:47	761.40	16.45	1.2210	7.66	3.94	0.13	1.7576	8.99	19.5542	19.6181	134.30
	14/08/01 17:52	761.40	16.05	1.2227	6.59	3.39	0.10	1.0400	6.97	14.9170	14.9451	178.80
	14/08/01 17:57	761.40	16.03	1.2228	6.89	3.55	0.07	0.5096	4.92	10.3561	10.3748	188.80
	14/08/01 18:02	761.40	16.05	1.2227	7.30	3.76	0.10	1.0400	6.97	14.9170	14.9451	168.60

Appendix-10: Sample Calculations for Determination of Power Output of Wind Turbine

The following calculations illustrate the computation of power output of wind turbine for the data contained in the highlighted row in Appendix-9.

Column A: No error flag. Hence data was processed for evaluating power performance

Column B: Date and time of recording observation: 14.08.2001 at 13:42

Column C: Atmospheric pressure = P = 761.40 mm of mercury column

Column D: Temperature of freely flowing wind = T = 17.50 degrees C

Column E: Air density is determined by inputting the values of pressure and temperature in the following equation derived from Perfect gas equation

$$\rho = (P_{Hg} \times 10^5) / (750 \times 287.1 \times (T + 273.15))$$
$$= (761.4 \times 10^5) / (750 \times 287.1 \times (17.5 + 273.15))$$
$$= 1.2166 \text{ kg/m}^3$$

Column F: Wind speed = 8.91 knots

Column G: Wind speed = 8.91/1.9426 m/s = 4.59 m/s

Column H: Current flowing through external resistance of 104 ohms = I = 0.13 A

Column I: Electrical power = $P_{el} = I^2R$

$$= 0.13^2 \times 104$$
$$= 1.7576 \text{ W}$$

Column J: Combined efficiency of generator and rectifier is determined by inputting the value of stator current in the following expression established experimentally for the alternator:

$$\eta_{com} = -19.26\ I^2 + 71.645\ I$$
$$= -19.26 \times 0.13^2 + 71.645 \times 0.13$$
$$= 8.98836\ \% \cong 8.99\%$$

Column K: Power extracted by wind turbine from freely flowing wind is computed by using the following relation:

$$P_{turbine} = 100\ P_{el} / \text{Efficiency}$$
$$= 100 \times 1.7576 / 8.98836$$
$$= 19.5542\ W$$

Column L: Power at standard air density of 1.225 kg/m3 (air density at 750 mm Hg pressure and 15 degrees C temperature) is computed as follows:

$$P_{std\text{-}turbine} = P_{turbine} \times 1.225 / \rho$$
$$= 19.5542 \times 1.225 / 1.2166$$
$$= 19.6892\ W$$